



Volume II

## Appendix A1

- i -

Table A1.1

## Drill Hole Material Tested

Reference Fig. A2.1	Drill Hole Name	Location		Length (feet)	Material	Location of Material	Formations <sup>+</sup> Penetrated	Test		Mineralogy Sample No.
		Lat.	Long.					k	p	
1	White Lead DDH-DLY5	30°14'	138°35'	540	Core	SADM corestore	TPLY/YUD	x		
2	Paull Consolidated DDH-PC2	30°23'	138°40'	573	Split core	"	"	x		
3	Southern Cross Mine 368E/389N	30°32'	138°33'	470	Cuttings	At drill site	TPLY	x		(CO63)
4	Baratta DDH3	31°56'	139°11'	234	Core	SADM corestore	"	x		
5	Prince Alfred Mine DDH2	32°07'	138°46'	450	"	"	"	x		
6	Waukaringa Hole 8	32°17'	139°26'	160	Cuttings	R.M.C. Minerals	TCIE/TPLY	x		(OR61)
	" Hole 9	"	"	140	"	"	"	x		
7	Ajax Hole 1	32°33'	139°23'	50	"	"	APLA	x		(OR62)
	" Hole 2	"	"	72	"	"	"	x		
	" Hole 3	"	"	50	"	"	"	x		
	" Hole 4	"	"	50	"	"	"	x		
	" Hole 5	"	"	36	"	"	"	x		
	" Hole 6	"	"	26	"	"	"	x		
	" Hole 7	"	"	72	"	"	"	x		(OR60)
8	Walloway Hole 1	32°29'	138°40'	74	"	Mining, Minerals & Metallurgy Ltd.	Quaternary sediments	x		
	" Hole 3	"	"	81	"	(Adelaide)	"	x		
	" Hole 5	"	"	69	"	"	"	x		(OR58 & OR59)
	" Hole 6	"	"	110	"	"	"	x		
9	Spring Creek Mine DDH1/29	32°44'	138°08'		Core	R.M.C. Minerals	TPLY/YUD	x		
10	Anabama Hill DDH-AN1	32°43'	140°13'	469	"	SADM corestore	Granite	x		
	" DDH-AN2	"	"	594	"	"	"	x		
	" DDH-AN3	"	"	514	"	"	"	x		

<sup>+</sup> APLA = Appila Tillite

TCIE = Tarcowie Siltstone

TPLY = Tapley Hill Formation (includes Tindelpina Shale Member) - shales & siltstone

YUD = Yudnamutana Subgroup (includes Appila Tillite) - siltstones & quartzites

Appendix A2

MAGNETIC PROPERTIES OF ROCK SAMPLES

A2.1 Volume magnetic susceptibility

Measurements of volume magnetic susceptibility were made on drill cores, drill hole cuttings and crushed surface samples using variously two MS-3 Magnetic Susceptibility Bridges manufactured by Soiltest Inc., Evanston, U.S.A. The bridge used for the work on all but one of the cores belonged to the SADM, and that used for all other measurements belonged to the Department of Economic Geology, University of Adelaide.

The MS-3 is an A.C. bridge instrument (1,000 cycles per second) which measures the change of inductive coupling between coils when a magnetic substance is placed between them. The change is registered on a potentiometer graduated in ohms and is determined by obtaining a 'null' with an earphone attachment. The ohm reading can be converted to susceptibility by standard charts provided with the instrument. Maximum field intensity at the sample position is about two Oersteds. Test samples should be cylindrical and about 9 cm long. If they have the maximum diameter possible for the test coils provided (3-6.3 cm), then susceptibilities or changes of susceptibility as low as  $5 \times 10^{-6}$  c.g.s. units can be measured. With ten or more independent repeat readings lower measurements can be made (e.g.  $1 \times 10^{-6}$  c.g.s. units). Susceptibilities as low as this are not of interest in magnetic interpretation.

If samples are of smaller diameter than the test coils a simple correction for volume is required to bring the measured 'apparent susceptibility' to a true value. If samples are crushed, then an additional volume correction, sometimes referred to as a 'porosity correction', is necessary if the susceptibility of solid rock is required.

At the SADM corestore, where the readings on all but one of the cores were made, strong electrical interference (thought to be due to motors in an adjacent factory) prevented measurements of susceptibilities or differences in susceptibilities below  $100 \times 10^{-6}$  c.g.s. units. It is suggested to any further workers that core held by the SADM be examined at some location remote from the corestore, if susceptibilities below  $100 \times 10^{-6}$  c.g.s. units are of interest.

The calibration of the two instruments was checked and adjustments were made accordingly to the measured values.

#### A2.1.1 Calibration corrections

Two known susceptibilities were used to provide fixed comparisons of MS-3 readings and true values. One came from a ferric chloride solution, the other from a core sample tested with an Astatic magnetometer and the University MS-3 by Mr. J. Wolfensberger (pers. comm.).

The susceptibility of an aqueous ferric chloride solution can be calculated with the following formula (Forsythe, 1959, p.462).

$$k_{\text{mass}} = \frac{p}{100} \times k_1 + \left(1 - \frac{p}{100}\right) k_2$$

where  $k_{\text{mass}}$  = mass susceptibility of the solution,

$p$  = percentage by weight of anhydrous  $\text{FeCl}_3$  in solution,

$k_1$  = mass magnetic susceptibility of anhydrous  $\text{FeCl}_3$  -  
=  $90 \times 10^{-6}$  c.g.s. units at room temperature,

$k_2$  = mass magnetic susceptibility of pure water  
=  $-.079 \times 10^{-6}$  c.g.s. units at room temperature.

then  $k$  =  $k_{\text{mass}} \times$  density of the solution

where  $k$  = volume magnetic susceptibility.

The solution used by the author had a measured density of  $1.435 \text{ g/cm}^3$

and thus contained 41.3% by weight of anhydrous  $\text{FeCl}_3$  (density converted to percentage from Weast (1964, table D-181). The calculated volume susceptibility was  $52.7 \times 10^{-6}$  c.g.s. units.

Besides the tests with  $\text{FeCl}_3$  and Wolfensberger's sample (J.W. Sample 2) two of the author's ground rock samples (D.H.T. Samples 1 & 2) were used to compare the two MS-3's. The results are summarised on Table A2.1.

Table A2.1

Calibration Tests on MS-3 Bridges

Instrument Sample	Coils**	University MS-3		SADM MS-3			Astatic Magnetometer	Calculated
		A	B	A	B	C		
$\text{FeCl}_3$		70*	42	67	59	37	-	52.7
D.H.T. Sample 1		1140	850	915	1040	715	-	-
J.W. Sample 2		-	5100	-	-	-	5100	-
D.H.T. Sample 3		7140	6150	5800	7550	6830	-	-

\* Susceptibilities from MS-3 bridges were calculated with the calibration curves supplied with the instruments. All values should be multiplied by  $10^{-6}$  to give c.g.s. units.

\*\* Test coils:

- A. Internal diameter 3.02 cm ( $1\frac{3}{16}$  in)
- B. " " 4.13 cm ( $1\frac{5}{8}$  in)
- C. " " 6.35 cm ( $2\frac{1}{2}$  in)

It is believed that a susceptibility measured with either of the instruments is within 30% of the actual susceptibility. Work with

the SADM bridge was too inaccurate to warrant application of calibration corrections. Calibration corrections applied to measurements made with the University MS-3 are shown on Table A2.2. Most susceptibility measurements were made with coil A.

Table A2.2

Calibration Corrections for University MS-3

Measured Susceptibility Range (c.g.s. units)	Factor*	
	Coil A	Coil B
0- 500 x 10 <sup>-6</sup>	0.75	1.25
500- 3,000 x 10 <sup>-6</sup>	0.85	1.15
3,000-50,000 x 10 <sup>-6</sup>	0.90	1.00

\* Factor by which susceptibility measured using manufacturer's specification should be multiplied to give a true value.

A2.1.2 Porosity correction

Most of the author's susceptibility measurements were for crushed rocks. All samples were shaken down into a 2.35 cm diameter flat bottomed glass tube until few air spaces were visible. A comparison of density of 58 solid and crushed rock samples indicated that for samples consisting of unsorted chips ranging from about pea size to fine powder, the ratio

$$\frac{\text{density of solid rock}}{\text{density of cuttings}}$$

fell in the range 1.7-2.5. The mean of the 58 tests was 1.95.

A porosity correction factor of two was adopted for all crushed drill hole samples, whether they were drill hole cuttings or powder from a seed mill (density of solid samples was unknown). For measurements on crushed samples of surface rocks collected by the author, the appropriate volume factor for each sample was applied because both the solid and crushed rock densities were known.

## A2.2 Susceptibilities measured

### A2.2.1 Drill core

#### A2.2.1.1 The base of the Tapley Hill Formation

Five drill cores were tested. In the area of most of the drill holes, mapping by the SADM indicated that the Tindelpina Shale Member occurs at the base of the Tapley Hill Formation. All of the cores contain pyrite and red iron oxides, usually as thin bands less than 0.1 cm thick, and parallel to the sedimentary layering. Often the fine bands are only 0.2-0.5 cm apart.

Spring Creek Mine - DDH 1/29

Core samples were tested with the University MS-3 at the corestore of R.M.C. Minerals, Adelaide. The sampling interval was approximately 4.5 m over sufficient length of core to pass from the Tindelpina Shale into the Yudnamutana Subgroup (Appila Tillite). The results are shown on Figure A2.1. Most values lie in the range  $25-100 \times 10^{-6}$  c.g.s. units, and the average is about  $75 \times 10^{-6}$  c.g.s. units. Two values lie close to  $300 \times 10^{-6}$  c.g.s. units. There appears to be no significant difference between values for the Tindelpina Shale and the Yudnamutana Subgroup. Thin bands of pyrite (less than 0.1 cm thick) occur within 15 m of the top of the core.

Paull Consolidated - DDH PC2

Split core samples were tested with the SADM MS-3 at the SADM corestore. The sampling interval was approximately 0.6 m over the entire length of core (573 ft, 175 m). The core extends from the Tindelpina Shale Member into the Yudnamutana Subgroup (Fig. A2.1). Occasional pyrite bands (0.1-0.2 cm thick) occur below 40 m; the core is stained by iron oxides over its entire length.

No measured values were obtained due to the influence of strong electrical noise. The susceptibility of all tested samples was less than  $100 \times 10^{-6}$  c.g.s. units.

White Lead - DDH DLY5

Core samples were tested with the SADM MS-3 at the SADM corestore. The sampling interval was approximately 1.5 m over the entire length of core (358 ft, 109 m). A cross section for the drill hole is shown on Figure A2.1. Pyrite bands occur below 65 m. No measured values were obtained due to the electrical noise. The susceptibility of all but one sample tested was less than  $100 \times 10^{-6}$  c.g.s. units. One sample at 45 m containing a 0.2 cm thick pyrite layer produced a barely detectable response in the earphones probably corresponding to a susceptibility of about  $100 \times 10^{-6}$  c.g.s. units. There was no significant difference between different rock units.

Prince Alfred Mine - DDH 2

Core samples were tested with the SADM MS-3 at the SADM corestore. The sampling interval was approximately 1.5 m over the length 12-137 m. The core consists of shale and siltstone similar in appearance to Tindelpina Shale. Fine disseminated pyrite occurs throughout the core.



Electrical noise prevented useful measurements. The susceptibility of all samples tested was less than  $100 \times 10^{-6}$  c.g.s. units.

Baratta - DDH 3

Core samples were tested with the SADM MS-3 at the SADM corestore. The sampling interval was approximately 0.6 m over the length 43-71 m. The core consists of shales and siltstones similar in appearance to Tindelpina Shale. It is heavily iron oxide stained above 50 m and contains occasional bands of oxides 2-5 mm thick over its entire length. Occasional bands of pyrite (up to 0.2 cm thick) occur below 50 m. Electrical noise prevented useful recordings. The susceptibility of all samples tested was less than  $100 \times 10^{-6}$  c.g.s. units.

A2.2.1.2 Discussion

Despite equipment problems it appears that the lower part of the Tapley Hill Formation (Tindelpina Shale), at the tested localities is only very weakly magnetic. All of the cores contain pyrite below about 50 m. Near the surface the core is stained by layers of iron oxides. There are no aeromagnetic anomalies recorded at the locality of any of the drill holes and it therefore appears that in these areas the Lower Tapley Hill Formation either contains no strongly magnetic beds or else they are extremely thin. The latter possibility does not seem very likely, although in the Spring Creek Mine core (DDH 1/29) two susceptibilities were recorded which are approximately four times the general background level of about  $75 \times 10^{-6}$  c.g.s. units. On the basis that the depth at which fresh pyrite occurs is the depth of oxidation and the depth of magnetic weathering, it appears that in the absence of strongly magnetic beds the susceptibility of both the fresh and weathered rock is about  $75 \times 10^{-6}$  c.g.s. units. From tests of random samples from

each drill hole, with a magnetometer, it appears that the rock does not possess a strong component of remanent magnetism.

#### A2.2.2 Percussion drill cuttings

##### A2.2.2.1 The top of the Yudnamutana Subgroup

Seven shallow percussion holes were drilled by R.M.C. Minerals at a locality suggested by the author 12 km south-west of Waukaringa (2 km south of the Ajax Mine). At the locality the upper part of the Yudnamutana Subgroup mainly consists of quartzites, dolomites and boulder tillite of the Appila Tillite. The drill holes were positioned by ground magnetometer work which recorded anomalies attributable to small sources within 5 m of the surface at the locality of Hole 6 and Hole 1 and within 10 m of the surface at the locality of Holes 3, 4 and 5 (Fig. A2.2). The magnetic interpretation indicated that the sources are strongly remanently magnetized.

##### Ajax - Holes 1 to 7

Seed mill samples of percussion hole cuttings collected over 0.6 m intervals were tested with the University MS-3. The results are shown on Figure A2.2. Most values lie in the range  $50-100 \times 10^{-6}$  c.g.s. units. In most holes there is a drop in susceptibility over the first 2-3 m, followed by a rise over the next 2-5 m, followed by a general levelling off beyond 10 m. Mineragraphic studies (see Appendix A4, Samples OR62 & OR60) showed the presence of about 1.5% pyrrhotite (by weight) in two samples tested (Hole 1 (1.5-2.5 m), and Hole 7 (17-17.5 m)). This quantity is probably sufficient to cause the observed susceptibility.

##### A2.2.2.2 The top of the Tapley Hill Formation

Two shallow percussion holes (Waukaringa, Holes 8 & 9) were drilled by R.M.C. Minerals at a locality suggested by the author,

1 km north of Waukaringa. In this area the ORROROO geological map shows an unnamed felspathic sandstone bed at the top of the Tapley Hill Formation. Gold bearing sulphide ore has been mined from the 15 m thick sandstone bed. Aeromagnetic and ground work indicate that a magnetic bed interpreted to be 50-60 m below the surface, may be associated with the sandstone.

#### Waukaringa - Holes 8 & 9

The two holes were drilled by R.M.C. Minerals to test the geochemistry of the sandstone bed. The drill did not have the capacity to reach the predicted magnetic material. Therefore the work was confined to the near surface part of the sandstone member. Seed mill samples of percussion hole cuttings collected over 3.5 m intervals were tested with the University MS-3; the results are shown on Figure A2.3. Except for one value of  $400 \times 10^{-6}$  c.g.s. units near the top of Hole 8, and  $170 \times 10^{-6}$  c.g.s. units near the top of Hole 9, all susceptibilities lie below  $100 \times 10^{-6}$  c.g.s. units. Pyrrhotite was identified in the high susceptibility sample (OR61, see Appendix A4).

#### A2.2.2.3 Quaternary sediments of the Walloway Plain

Six shallow percussion holes were drilled by Minerals, Mining and Metallurgy Ltd. at a site suggested by the author, 12 km north-east of Eurelia Railway Station. The holes were drilled to make a preliminary test of the source of a linear aeromagnetic anomaly along the west side of the Walloway Plain. Geological mapping (Binks, 1968, 1971) indicates that the partly consolidated strata of the Walloway Plain are of Quaternary age. Susceptibility measurements on material from four of the drill holes are discussed below.

## Walloway Plain - Holes 1, 3, 5 & 6

Percussion hole cuttings were tested with the University MS-3. Material from the holes consisted mainly of heavily iron oxide stained clay and sand, with occasional pebbles of quartzite.

Susceptibility measurements are shown on Figure A2.4. The Quaternary sediments at the locality have a surprisingly high susceptibility. For samples from Hole 6 the average over 30 m of section is about  $1,090 \times 10^{-6}$  c.g.s. units. Magnetite was identified in two samples (Appendix A4, Samples OR58 & OR59). It is considered that the high susceptibility of the sediments is probably caused by this mineral. In Hole 6 susceptibilities below 30 m are significantly lower than those above. The low susceptibilities recorded for samples near the bottom of Holes 3 and 6 are close to the background level recorded elsewhere for Adelaidean strata ( $75 \times 10^{-6}$  c.g.s. units). On this basis it is probable that magnetically weathered Adelaide System sediments were penetrated at 30 m in Hole 6. Two small chips of shale were found in the cuttings below 30 m. This is weak supporting evidence that Adelaidean strata were penetrated by the drill hole below 30 m.

### A2.2.3 Surface samples

Approximately 100 surface rock samples associated with magnetic bodies were collected and tested for susceptibility. Most were from ORROROO. Each rock sample collected was one to four fists in size. A small piece 50-100 cm<sup>3</sup> in volume was cut from each sample and crushed in a press. Thus test specimens contained a range of particle sizes ranging from dust up to pea size.

The 72 samples for which frequency histograms of susceptibility are shown on Figure A2.5 were collected from Adelaide System sedimentary beds, which interpretation of the magnetic anomalies indicates are magnetic below the surface. Results of tests on the other samples are not included here. The samples were from a variety of sedimentary formations, small intrusive bodies and mine dumps. Some of the measurements are mentioned in the text of the thesis.

#### A2.2.3.1 Ulupa Siltstone

31 samples of Ulupa Siltstone were collected along ground magnetometer traverses 14A, 15 and 18 over total distances less than 300 m, where interpretation of the anomalies indicates that near surface rocks are magnetic. The histogram (Fig. A2.5(a)) shows two weak groupings of values, one less than  $100 \times 10^{-6}$  c.g.s. units, and the other centred near  $1,000 \times 10^{-6}$  c.g.s. units (range approximately  $500-5,000 \times 10^{-6}$ ). The most strongly magnetic sample which has a susceptibility of  $15,000 \times 10^{-6}$  c.g.s. units, contains about 20% magnetite (Appendix A4, Sample OR17).

#### A2.2.3.2 Lower Tapley Hill Formation (Tindelpina Shale)

Measurements on 26 samples collected by the author and Mr. J. Sumartojo from different localities, are summarised on Figure A2.5(b). Most of these samples came from outcrops which the magnetometer profile interpretation indicates were the surface outcrop of deep magnetic beds. The values lie in the range  $10-80 \times 10^{-6}$  c.g.s. units and are grouped near  $30 \times 10^{-6}$  c.g.s. units.

#### A2.2.3.3 Appila Tillite and Holowilena Ironstone

Measurements on 11 samples of Appila Tillite from different

localities and four specimens of Holowilena Ironstone from two localities 10 km north-north-east of Waykaringa are summarised on Figure A2.5(c). Values for the Appila Tillite lie below  $180 \times 10^{-6}$  c.g.s. units and are grouped around  $70 \times 10^{-6}$  c.g.s. units.

Values for the four Holowilena Ironstone samples show a wide range ( $150-58,000 \times 10^{-6}$  c.g.s. units). The most strongly magnetic specimen contains about 25% magnetite (Appendix A4, Sample AAH1).

#### A2.2.3.4 Discussion

Susceptibilities of surface samples show a significant grouping below  $100 \times 10^{-6}$  c.g.s. units. These values are presumably those of the magnetically weathered material. Even in the most strongly magnetic rocks there is mineragraphic evidence of weathering. An average susceptibility of a fresh magnetic bed cannot be derived from the available surface data.

#### A2.2.4 Soil samples

The susceptibilities of two residual soil samples over the Ulupa Siltstone were 40 and  $120 \times 10^{-6}$  c.g.s. units. Three red drift sand samples had susceptibilities in the range  $80-1,200 \times 10^{-6}$  c.g.s. units. Magnetite was identified in a drift sand sample.

#### A2.3 Susceptibility anisotropy

Approximate estimates of susceptibility anisotropy were made on a surface sample of Ulupa Siltstone, Tindelpina Shale and Holowilena Ironstone in the following manner. A 10 cm long specimen with square cross section (1.8 cm/side) was cut from the rock such that the bedding plane was parallel to the long axis of the specimen. This was cut into five cubes. Measurements were then made with the University MS-3 on the

five cubes taped together so that bedding planes were first parallel to the long axis of the sample (giving  $R_p$ ) and then normal to it (giving  $R_t$ ); the measurements  $R_p$  and  $R_t$  were scale units of the MS-3, and were not converted to susceptibilities. With this arrangement the axial magnetic field of the test coil was first parallel to the bedding planes and then normal to them. After each pair of measurements the cube at the bottom was placed at the top and the measuring procedure repeated. Thus a total of five pairs of readings were obtained. These were averaged. Within each group of five readings the difference between the highest and lowest values obtained was less than 28% of the highest value.

The measurements and calculated percentage anisotropy are shown on Table A2.3.

Table A2.3

Susceptibility Anisotropy

Sample	Lithology	$R_p$	$R_t$	% Anisotropy
OR25	Ulupa Siltstone	79	81	2.5
OR50	Tindelpina Shale	3.4	3.4	0
AAH1	Holowilena Ironstone	3664	3463	5.5

Two of the samples appear to be slightly anisotropic with regard to susceptibility. For the Ulupa Siltstone sample the easy direction of magnetization is transverse to the sedimentary layering, while for the Holowilena Ironstone the opposite is the case. For the Holowilena Ironstone it was noted that magnetite grains are elongated parallel to

the sedimentary layering. The measurement method was too insensitive to give a meaningful estimate for the Tindelpina Shale sample.

#### A2.4 Measurements of remanent magnetic properties

The main factors of interest to interpreters of magnetic anomalies, apart from susceptibility, are (1) the direction of the remanent magnetism in a rock and (2) the Koenigsberger ratio  $Q_n$ ,

where  $Q_n = \frac{\text{intensity of natural remanent magnetism}}{\text{intensity of magnetization induced by the earth's field}}$

(cf. Irving, 1964, p.11)

While there are various elaborate methods which can be applied to find these properties (see Collinson, Creer & Runcorn, 1967), the author devised a very simple technique based on approximate methods described by Fromm (1967), and Doell and Cox (1967). The technique devised to find these factors for small cubic rock samples is rapid to apply and gives useful approximate results for strongly magnetic samples. Once a sample has been cut, measurements and computations take about 20 minutes. The method may be of appeal to others working on strongly magnetic rocks (such as the Banded Iron Formations in Western Australia) and is therefore described fully below.

The remote head of the University's fluxgate magnetometer was firmly fixed inside a flat topped glass tube such that the centre of the sensing element was 3.0 cm below the top face of the tube. On the top face of the glass tube a square of cardboard with a 1.8 cm square hole in it was glued so that samples could be relocated in exactly the same position. This arrangement was taped to a block of wood such that the sensor was aligned parallel to the earth's field (inclination  $-65^\circ$ , intensity 59,000 gammas at Adelaide). Thus the instrument was set up



as a total field magnetometer. The deflection on the magnetometer (gammas) was noted as each of the six faces of cubes of rock (with side length of 1.8 cm) were located in the cardboard square.

Fromm (op. cit.) stated that the error in assuming the magnetic effect of a cube could be approximated by a point dipole at its centre of gravity, is less than 1.5% if the angle between the centre of the fluxgate sensing element and the nearest edges of the cube is less than  $34^{\circ}$ . To conform with this, for the author's specimens the distance between the sample and the centre of the sensing head was 3.0 cm. Thus the results of the six measurements on each cube can be treated as being due to a point dipole. Each measurement recorded the combined influence of inductive magnetism and the component of remanent magnetism in the direction parallel to the long axis of the system. Each face of the cubes was marked with a letter corresponding to a right handed orthogonal coordinate system, e.g. Z' for the face normal to OZ' axis, Y normal to OY, Z normal to OZ, Y' normal to OY', X' normal to OX', and X normal to OX. In the table of results (Table A2.4) reading corresponds with the face Z' being nearest to the sensing head and normal to the earth's field; reading Y corresponds with face Y in the above arrangement etc. The formulae used to derive the inclination of remanent magnetism with respect to the bedding planes, and the Koenigsberger ratio are shown below the table. To simplify the mathematics, the faces X' and X were cut parallel to bedding planes and the edge defined by the join of faces X and Z was cut approximately parallel to the horizontal (marked in the field). Thus Y'OY defined the horizontal.

Table A2.4

Remanence tests on Holowilena Ironstone, Sample AAH1

Results \ Specimen No.	1	2	3
Reading Z' (gammas)	-130	-55	-65
" Y "	-330	-160	-200
" Z "	-60	-45	-50
" Y' "	170	70	95
" X' "	-60	-30	-35
" X "	-90	-55	-70
Y-Y'	-500	-230	-295
Z-Z'	70	10	15
X-X'	-30	-25	-35
R	506	232	297
Y+Y'	-160	-90	-110
Z+Z'	-190	-100	-115
X+X'	-150	-85	-105
I	-167	-92	-110
$\theta_R^0$	4°6'	6°42'	5°12'
$Q_n$	3.20	2.52	2.68

All of the above readings have units of gammas, except for  $Q_n$  which is unitless, and  $\theta$  which is a measure in degrees. Gamma readings are accurate to within  $\pm 5$  gammas.

$R = ((B - D)^2 + (C - A)^2 + (E - F)^2)^{\frac{1}{2}}$  is a measure of remanent intensity.

$I = ((B + D) + (C + A) + (E + F))/3$  is a measure of induced intensity.

$$\theta_r^0 = \arccos \left\{ \frac{R^2 + (B - D)^2 + (C - A)^2 - (F - E)^2}{2R \left( (D - B)^2 + (C + A)^2 \right)^{\frac{1}{2}}} \right\}$$
 is the angle

which the remanent vector makes with the bedding plane.

$Q_n$  = is the Koenigsberger ratio.

---

The results indicate that the inclination of remanent magnetism in the samples lies at an angle of about  $5^\circ$  to the bedding planes, and that the ratio of remanent to induced intensity is quite high (2.8 for average of the three specimens). Other elementary calculations indicated that the direction of remanent magnetism is within  $10^\circ$  of the horizontal reference of the sample.

The method was tried unsuccessfully on specimens of Ulupa Siltstone; the reading errors with the magnetometer were too high to warrant a quantitative analysis.

The main problem with the simple apparatus was man-made noise (motor cars). This caused readings to wander by  $\pm 30$  gammas at times. However, the readings Z' to X shown on Table A2.4 are accurate to  $\pm 5$  gammas.

Appendix A3

GROUND MAGNETOMETER LINES

Magnetometers used in the field were as follows:

1. Vertical Field

Ruska Balance - manufactured by Ruska Instrument Corp.

Fluxgate - McPhar M700

2. Total Field

Elsec Proton Precession Magnetometer

Sander Proton Precession Magnetometer

Most ground magnetometer traversing was with reconnaissance lines, one or two being put in at each favourable location. The length was normally in the range 1-4 km; four lines were slightly more than 8 km long. Usually one or two specific anomalies recorded by the aeromagnetic survey were of interest; the main traverses were made sufficiently long to record the background, and extend between points easily identified on 1:63,360 stereo air photos. Traverses were usually normal to geological (and geophysical) strike.

Particular attention was paid to photo location and positioning during the course of ground traversing. On the main traverses distance along the ground was measured by an offsider with a road measurer (graduated in feet). Usually this gave a length 1-2% above the distance scaled from maps, probably due to undulations in the ground surface. This size of error is unimportant in interpretation of anomalies. Magnetometer stations (usually 25-100 ft apart (7.5-30 m)) were marked on the ground, or with a 15 cm long piece of aluminium wire with short lengths of plastic flagging attached. The wire markers were placed at regular intervals

along the line (e.g. 500 ft (150 m)) and left until geological work had been carried out. When working across open country it was found an advantage to drive along the proposed traverse and then walk along the vehicle wheel tracks while reading the magnetometer.

Diurnal variation was recorded by a base station reoccupation method. Usually a base station was reoccupied at intervals of no more than 90 minutes. In this time drift was usually less than 40 gammas. With the fluxgate magnetometer it was found an advantage to use a cement brick or block of wood for a base station. They were placed at a position where a small error in repositioning the magnetometer on the block produced no observable change of reading. On long traverses (4 km or more) three or four blocks were laid in advance along the traverse, and readings were made on the blocks on the outward and return trip.

Particular care was taken to ensure that no magnetic material was carried while reading the magnetometers.

It was found that man-made magnetic sources are often associated with roads and tracks. Where possible traversing on roads was avoided. Various traverses were put in parallel to roads 20-30 m into the adjacent paddocks.

It was found that a considerable amount of time could be saved if magnetometer data were recorded directly on IBM coding forms ready for punching rather than on a note pad (40 hours traversing required 23 hours of transcription to IBM forms for one of the early surveys). Therefore nearly all of the original field data were directly recorded on coding forms. Information on the coding forms used for computing and profile plotting included

1. magnetic anomaly values,
2. distance of each station from the first base station (if a traverse extended both sides of the first base station distances in one direction were positive, and in the other were negative),
3. corrections to compensate for diurnal variations, and
4. corrections to compensate for significant deviations of the traverse from normal to geological strike.

Other information recorded on the coding forms included the traverse number, topographic reference points (e.g. creeks, fences, roads, hilltops etc.) and various geological features (e.g. major outcrops and geological dips and formation boundaries where recognizable).

Figure 2.1 shows the locations of magnetometer surveys. The various areas surveyed are given a reference letter for easy reference on Table A3.1. The main magnetometer traverses are listed on the table. Most of the work was carried out on ORROROO; the locations of the main traverses on this sheet are shown on Figure 1.5.

At various localities one or more short traverses or small grids were made close to the main traverses to check the linear continuity of magnetic features. Distances were usually measured by pacing and the end points of the lines were not usually photo located. A summary of these data is not included on Table A3.1.

The most important original ground magnetometer data are lodged with the Department of Economic Geology, University of Adelaide. This includes

1. Aerial photographs and sketch maps showing the locality of ground traverses,

2. A computer listing of original and corrected data,
3. A microfilm copy of anomaly profiles, and
4. IBM card decks of original data for treatment with program  
MAGLINE (see Appendix A5).

Table A3.1

Ground Magnetometer Traverses

Reference Letter on Fig. 2.1	Locality Name	Traverse Number <sup>1</sup>	Photos <sup>2</sup>	Magnetometer <sup>3</sup>	Formations Crossed <sup>4</sup>
A	Mt. Coffin Diapir	123-134	Angepena (sketch map)	ΔZ	UMB, dolerite dykes
B	Eucolo	6,7	Eucolo	ΔZ	Eyre Peninsula dyke swarm
C	Neuroodla	86,87,88	Hawker	ΔZ	Possible buried intrusive
D	Berrimans Well	136	Siccus (sketch map)	ΔT	UMB
E	Hesso	1,4,5	Yudnapinna	ΔZ	Eyre Peninsula dyke swarm (? dolerite)
F	Yudnapinna	100,101	Yudnapinna	ΔZ	Eyre Peninsula dyke swarm (? dolerite)
G	Corunna	98,99	Corunna	ΔZ	Gawler Range Volcanics basic dyke
H	Cooey Dam	97	Corunna	ΔZ	Dolerite dyke
I	Waukaringa	26-38,44-49,60-72, 76,121,124-127	Koonamore Waukaringa	ΔZ	UMB, top of BRA
J	Walloway Plain	77,78,137-140	Carrieton Orroroo	ΔZ	Quaternary sediments, UMB
K	Walloway Diapir	144 (grid)	Orroroo (sketch map)	ΔZ	Carbonatite dykes & plugs
L	Spring Creek Mine	25	Wilmington	ΔZ	UMB
M	Paratoo Diapir	73,74,123	Paratoo	ΔZ	WNA,UMB
N	Peterborough	8,8A,9,14,14A,15,15A,15C 16A,18,79,89-95,115-120	Peterborough, Melrose, Nackara	ΔZ, ΔT	WNA,UMB,BRA; possible intrusive (94,95)
O	Steelton	84	Riverton	ΔZ	UMB
P	Point Pass	85	Eudunda	ΔZ	UMB
Q	Kapunda	83	Kapunda	ΔZ	UMB
R	Sturt Gorge	75,81,82	Echunga	ΔZ, ΔT	UMB
S	Willunga	80	Echunga	ΔZ	UMB

Notes

- Where traverses cross the same formation twice (e.g. across anticlines), in the text of the thesis they are sometimes referred to in parts, e.g. 65N (north) and 65S (south).
- Aerial photos are indexed according to the official name of 1:63,360 areas. These areas are 15' of latitude high and 30' of longitude wide, e.g. Eucolo.
- ΔZ = vertical field magnetometer; ΔT = total field magnetometer: a few lines were read with both types of instrument, viz. 80, 94 & 115.
- WNA = Wilpena Group; UMB = Umberatana Group; BRA = Burra Group; in most cases any particular traverse crossed only a part of the rock group.



Appendix A4

MAGNETIC MINERAL ANALYSES

The strongly magnetic minerals present in various rock samples were tentatively identified by microscope and/or X-ray analysis. The results of this preliminary work are summarised below. Magnetic susceptibilities indicated in the appendix have been corrected as discussed in Appendix A2.

A4.1 Solid rocks

Polished sections of four surface rock samples collected from localities where detailed ground surveys indicated surface rocks are magnetic, were examined (Table A4.1). The two samples of Ulupa Siltstone came from one locality 17 km north-east of Peterborough. The two samples of Holowilena Ironstone came from one locality 10 km north-north-east of Waukaringa.

Table A4.1

Sample	Source rock	k c.g.s. units	% Iron oxides (by volume)	Composition of average iron oxide grain
AAH1	Holowilena Ironstone	0.058	45-50	50% magnetite 50% martite
AGC1	"	0.011	50	30% magnetite 70% martite
OR17	Ulupa Siltstone	0.015	5-50*	70% magnetite 30% martite
OR13	"	0.005	7	90% magnetite 10% martite

\* Variation across the samples (2 cm wide).

In these samples, magnetite euhedra and aggregates of euhedra were seen to be altering to martite. The diameter of individual grains and aggregates lay in the range 20-80 microns. There was a marked tendency for grains to lie along the sedimentary bedding planes of the sediments. In sample AAH1 grains had an elongation biased parallel to the sedimentary layering.

#### Sample OR55

Collected from: Waukaringa Mine dump.

Source rock: sulphide ore, probably from within the felspathic sandstone member between the Tapley Hill Formation and the Tarcowie Siltstone.

Test material: polished section of the rock and a polished section of the strongly magnetic fraction (separated from a crushed sample with a hand magnet).

Magnetic susceptibility:  $1,000 \times 10^{-6}$  c.g.s. units.

Discussion: the rock mainly consisted of pyrite. It contained approximately 0.5% pyrrhotite and 0.05% magnetite (by volume). These quantities are probably sufficient to produce the observed magnetic susceptibility of the rock.

#### A4.2 Percussion drill cuttings

##### Samples OR58 and OR59

Collected from: Hole 6 - Walloway Plain.

Location: 2 km south-east of Oladdie Mine (12 km north-east of Eurelia Railway Station).

Source rock: sediments of Quaternary age.

Test material: polished sections of the strongly magnetic fraction.

Each 100 g sample of cuttings was sieved to the diameter range 0.0099" - 0.0139" (250-350 microns) and washed. The strongly magnetic fraction was separated from the washed material with a hand magnet (Table A4.2).

Discussion: iron oxides present in the magnetic fraction of both samples included earthy clay limonite, colloform limonite and micro-crystalline goethite. Approximately 10% of the magnetic grains consisted of maghemite (X-ray and reflectance tests). No magnetite was observed. The sample contained a trace of pyrrhotite (20-30 micron diameter grains).

Table A4.2

Magnetic mineral separation of cuttings from Hole 6, Walloway Plain

Sample	Depth Range	k for unwashed material*	<u>Weight of magnetics</u> Sample weight	Maghemite present in washed sample (by weight)
OR58	2.5-5.5 m	0.0006 (cgs)	1.04%	0.1%
OR59	20-22 m	0.0035 (cgs)	10.47%	1.0%

\* Insufficient washed material was available to make susceptibility measurements.

Maghemite has a saturation magnetization close to that for magnetite. On this basis it is probable that the observed susceptibility of the samples is due almost entirely to the presence of maghemite. The reason why grains of other iron oxides present in the samples are strongly magnetic is not known. It is probable that they are strongly remanently magnetized, but contribute little to the susceptibility.

Samples OR60 and OR62

Collected from: Ajax, Hole 7 (OR60), Ajax, Hole 1 (OR62).

Location: 12 km south-west of Waukaringa.

Source rock: dolomite within the Yudnamutana Subgroup (Appila Tillite).

Test materials: polished sections of the magnetic fraction. The strongly magnetic fraction was separated from washed, sieved cuttings with a hand magnet (Table A4.3).

Discussion: the magnetic mineral was identified as pyrrhotite.

Table A4.3

Magnetic mineral separation for samples OR60 & OR62

Sample	Depth Range	k for unwashed material (c.g.s. units)	<u>Weight of magnetics</u> Sample weight
OR60	17-17.5 m	$100 \times 10^{-6}$	1.4%
OR62	1.5-2.5 m	$110 \times 10^{-6}$	1.6%

Sample OR61

Collected from: Waukaringa Hole 8.

Depth range: 1-3 m.

Location: 1 km north of Waukaringa.

Source rock: felspathic sandstone between the Tapley Hill Formation and the Tarcowie Siltstone.

Test material: polished sections of the magnetic fraction (separated from washed cuttings with a hand magnet). The magnetic fraction

was 2.8% by weight of the sample.

Discussion: the only mineral positively identified was pyrrhotite (5-10%). The other 90-95% of the magnetic fraction was tentatively identified as lepidocrocite. Four of these mineral grains had a hardness in the range 295-367 (Vickers Hardness tester). The grains had red internal reflections but did not appear to be anisotropic. The quantity of pyrrhotite detected in the sample is probably too small to cause the observed magnetic susceptibility.

#### Sample C063

Collected from: Southern Cross Mine, Hole 368E/389N.

Depth range: 84-85 m.

Location: Mt. Coffin Diapir (COPLEY).

Source rock: Tindelpina Shale Member.

Magnetic susceptibility:  $35 \times 10^{-6}$  c.g.s. units.

Test material: polished section of the strongly magnetic fraction.

The magnetic minerals (2% by weight) were separated with a Frantz magnetic separator from a crushed and washed percussion drill sample.

Discussion: the magnetic material contained the following:

- (a) rounded grains of magnetite (300 microns diameter)
- (b) flakes of magnetite (350 microns long, 35 microns thick)
- (c) quartz-magnetite composite grains (300 microns diameter)
- (d) quartz grains in a goethite matrix.

#### A4.3 Soil samples

##### Samples OR56 and OR57

Sample OR56 was collected with a hand magnet from a sand drift near

Waukaringa. Sample OR58 was collected with a hand magnet from a dry creek bed 10 km south of Waukaringa. X-ray analysis of the two samples indicated that magnetite was the main magnetic mineral present. Hematite was also detected.

Appendix A5

COMPUTER PROGRAMS

To assist with interpretation of the geophysics, various computer programs were written in Fortran for the University's CDC 6400 machine. None of the programs offer any new innovation to geophysics.

Card decks and listings of the programs used for the thesis, together with source data, are held in the Department of Economic Geology, University of Adelaide. The programs and their functions are listed below.

A5.1 PROGRAM MAGLINE

For: Treatment of field data from individual ground magnetometer traverses.

Functions:

- (1) Ground magnetometer data are corrected for diurnal variation.
- (2) If the traverse is oblique to strike or contains bends along its length (for example, if it follows a road), the station spacings can be adjusted so that the profile is effectively normal to geological strike.
- (3) A linear regional can be removed.
- (4) The data can be gridded to some chosen interval by linear interpolation.
- (5) The data can be linearly filtered using an operator which acts on nine gridded values. Coefficients of the operator can be altered as desired.

- (6) The gridded data can be upward or downward continued up to five times the grid spacing (following the method of Henderson, 1960).

Output:

At any or all of the six stages, printouts and/or plots can be obtained. Plot scales can be altered as desired.

A5.2 PROGRAM COMPS2P

For: Computing theoretical magnetic anomalies across dipping tabular bodies of infinite length and depth extent.

Function:

The program computes the theoretical anomaly on a horizontal surface above one or more (up to nine) dipping flat topped tabular bodies of finite thickness. The equation used for the anomalies is that of Gay (1963) for the case where demagnetization is neglected. The direction of magnetization in the bodies, and their depth, thickness and magnetization can be different. The dip of all bodies must be the same but can be varied as necessary.

Output:

Printout and/or plot.

A5.3 PROGRAM MAGHIL3

Written by Mr. John Trethewie (Austral Exploration Services, Adelaide, S.A.).

For: Computing the theoretical magnetic anomaly of an arbitrarily shaped solid three dimensional body.



Function:

The program computes the theoretical anomaly on a horizontal square grid above a magnetic body for any chosen direction of magnetization. If desired a single north/south or east/west profile can be computed. The program is based on the method of Talwani (1965).

Output:

Printout.

A5.4 PROGRAM GRBOTT2

For: Computing the shape of a basin of infinite length to account for a Bouguer anomaly.

Function:

The program iteratively computes the depth to the bottom of a chosen number of infinitely long rectangular blocks until the resulting theoretical anomaly of the arrangement differs from the input anomaly by less than some chosen criterion. The method follows that of Bott (1960).

Output:

Printout.

A5.5 PROGRAM DENSPR2

For: Computing Bouguer anomalies along a line of gravity stations for six Bouguer densities (2.0, 2.2, 2.4, 2.6, 2.8 & 3.0 g/cm<sup>3</sup>).

Function:

The program was designed to treat Bouguer anomalies originally computed by the BMR for a Bouguer density of 2.67 g/cm<sup>3</sup>. The

value at each station is reduced to the condition where the Bouguer density is zero and then the Bouguer anomaly is recomputed for the six values shown above.

Output:

Printout and/or plot with the six profiles in juxtaposition.

A5.6 PROGRAM MOMENT3

For: Calculating the excess mass (or mass deficiency) associated with a Bouguer anomaly.

Function:

The program integrates over a square or rectangular grid of Bouguer anomalies by the method suggested by Grant and West (1965, pp.269-271), and from the resulting volume of the anomaly calculates the excess mass. As suggested by Grant and West (op. cit.) tail corrections are applied to account for extension of the anomaly outside the grid.

Output:

Printout.

A5.7 PROGRAM GRAVIL3

Written by Mr. John Trethewie (Austral Exploration Services, Adelaide, S.A.).

For: Computing the theoretical Bouguer anomaly of an arbitrarily shaped three dimensional body.

Function:

The program computes the theoretical anomaly on a horizontal grid above a gravitating body. If desired a single profile

across the body can be computed. The program is based on the method of Talwani (1965).

**Output:**

Printout.

Appendix A6

INTERPRETATION OF TABULAR BODY ANOMALIES

The methods for interpreting magnetic anomalies due to dipping tabular bodies of considerable strike length and depth extent are discussed in the literature. Readers of the thesis unfamiliar with interpretation techniques are referred to the following papers (Peters, 1949; Gay, 1963; Bruckshaw & Kunaratnam, 1963; Powell, 1965; Grant & West, 1965; Koulomzine et. al., 1970).

A6.1 Parameters of interest in magnetic interpretation

The parameters usually sought in interpretation of magnetic anomalies over inductively magnetized dipping tabular bodies are

- (a) depth to the top surface and apical width,
- (b) geological dip,
- (c) thickness of the body, and
- (d) magnetic susceptibility.

If the body possesses a strong component of remanent magnetism as well as inductive magnetism, the parameters which can be directly found are

- (1) depth to the top surface and
- (2) apical width.

If the geological dip is known, then the interpretation can find

- (3) thickness,
- (4) strength of the effective magnetization (the effective magnetization is the component of the total magnetization in the dip plane, i.e. the plane normal to the trace of outcrop of the body), and
- (5) the attitude of the effective magnetization in the dip plane.

If the magnetic susceptibility of the beds is also known, then from the anomalies, interpretation can find

- (6) the strength and direction of the effective remanent magnetization.

For magnetic beds in the Adelaide Geosyncline it appears that in most cases, remanent magnetism is an important contributor to the anomalies. Thus the parameters 1-6 are of interest. In general, while the geological dip is known, the susceptibility of the beds is unknown; thus, only parameters 1-5 can be found. With an anomaly similar in shape to the theoretical anomaly of a tabular body, estimation of the parameters 1-3 is straightforward and the various available methods give closely similar results (e.g. Peters, 1949; Koulomzine et al., 1970; Gay, 1963). Gay's standard curve method (Gay, op. cit.) was found most useful for estimating the five parameters.

In the following section the methods used by the author to find parameters 1-5 are outlined.

#### A6.2 Interpretation of magnetic anomalies

The method used to find these parameters is based on the method of Gay (op. cit.) for interpretation of anomalies due to tabular bodies of finite thickness, with demagnetization neglected. The reader is referred to this paper as a preliminary to the following notes.

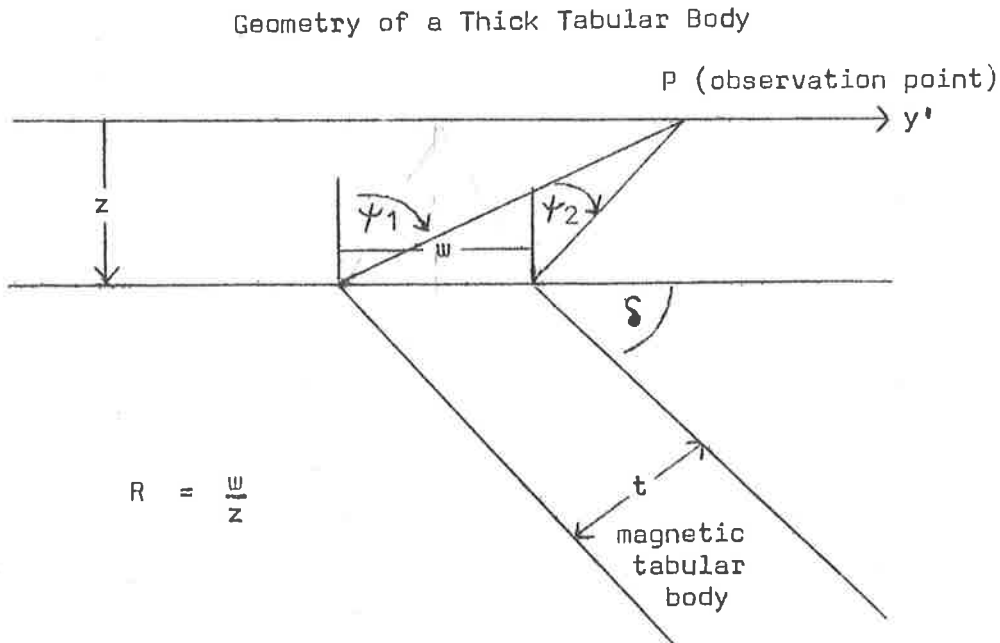
Gay's paper contains a standard **family** of curves (Charts 7 through 16) each of which has a particular index parameter,  $\theta_f$ . The curves were computed with the following formula.

$$\Delta F = C_F \left[ \left( \frac{\psi_1 - \psi_2}{R} \right) \cos \theta_F + \left( \frac{1}{R} \ln \frac{\cos \psi_2}{\cos \psi_1} \right) \sin \theta_F \right]$$

where  $\Delta F$  can be either the vertical field anomaly ( $\Delta Z$ ), the horizontal field anomaly ( $\Delta H$ ) in the direction normal to the strike of outcrop, or the total field anomaly ( $\Delta T_{IO}$ ) in the direction of the earth's magnetic field.

$C_F$  is a coefficient term which in the case of vertical field anomalies (of interest in this discussion) is as follows:

$C_F = 2 J' \frac{t}{z}$ . Here  $J'$  is the intensity of magnetization in the dip plane,  $t$  is the thickness of the tabular body and  $z$  is the depth of the body below the plane of observation. The geometrical relationships of the body which determine  $\psi_1$ ,  $\psi_2$ , and  $R$  are shown below.



Although Gay's method was designed to treat the case of induced magnetism, it also has application in the case of remanently magnetized bodies. He pointed out that the effect of an element of remanent magnetism

is to change the anomaly shape to a new member of the standard family of curves. If the geological dip is known this property can be used to find the actual inclination  $I_0''$  of the effective magnetization. The author's method for finding  $I_0''$  from vertical field anomalies is outlined below.

The field profile is drawn so that the north side of the dipping body corresponds with the right hand part of the profile.

For interpretation of anomalies the method is to successively adjust the scales (distance and amplitude) of the field profile until it matches one of the standard family of curves (computed for various values of the thickness factor  $R$ ). Then the depth ( $z$ ) is derived by comparison of the horizontal scale of the standard curve with the adjusted horizontal side of the field profile. The apical width ( $w$ ) is computed from the factors  $R$  and  $z$ . If geological dip is known, then the thickness  $t$  can be estimated. Then the magnetization  $J'$  in the dip plane is given by

$$J' = \frac{A z}{a t} \times 10^{-5} \text{ c.g.s. units}$$

where  $A$  is the peak-to-peak amplitude of the vertical field anomaly in gammas,  $a$  is an amplitude scale factor which depends on the thickness factor ( $R$ ), and  $z$  and  $t$  are as defined before.

We let  $J'$  have a direction  $I_0''$  which is measured in the dip plane, clockwise from the horizontal on the north side of the body.  $I_0''$  is determined from the standard curves by use of the index parameter  $\theta_F$  which is in the top right hand corner of the standard anomaly curve selected as most similar to the field profile.

$$I_0'' = -(\theta_F - \delta)$$

where  $\delta$  = the north component of dip of the body.

Examples illustrating the relationship of the profile shape to the dip ( $\delta$ ) and  $I_0'''$  are shown on Figure A6.1. On the figure, the anomaly curves are shown for  $\theta_F$  in the range  $-360^\circ-0^\circ$ . Two configurations of tabular bodies and corresponding directions of magnetization are shown which can produce the theoretical anomalies. The direction of magnetization is shown as an arrow: a solid arrow for Body 1 (solid line); a dashed arrow for Body 2 (dashed line). The corresponding values of  $I_0'''$  are shown alongside each profile;  $I_0'''(1)$  corresponds to Body 1,  $I_0'''(2)$  corresponds to Body 2. Thus where  $I_0'''(1)$  is  $420^\circ$ , the effective magnetization of Body 1 is in the direction  $60^\circ$  above the horizontal in the north direction.



Appendix A7

ADDITIONAL MATTERS ARISING FROM COMMENTS

In a thesis of this kind which covers a large area and is the first major attempt to find answers to some of the many complex problems of the area, it is almost inevitable that many questions will remain unanswered and that various points will need clarification. It is the purpose of this appendix to list the main comments made during examination of the thesis and provide answers to some of the questions raised.

A7.1 It was pointed out that the gravity and magnetic sections could have been more closely connected through a more detailed interpretation of the anomalies associated with granites.

This problem was recognised at the time of writing the thesis, but the information for the necessary detailed interpretation was not available and due to local conditions, poor outcrop, deep weathering and only widely spaced gravity data (and no gravity meter in the Department to get more closely spaced data), could not be obtained.

The problem was heightened by this work being the first attempt to draw available information together and extract new answers. Because there was so little known it was difficult to see which directions of work would be the most rewarding and mutually supporting so that in the thesis there are a number of weak links, particularly regarding problems recognised in areas where the geology is poorly exposed or not investigated.

In a similar granite problem at Rum Jungle in the Northern Territory (B.M.R. report in prep.) the problem can be resolved more satisfactorily because fresh samples from drill core are available to define

the density of the different rock groups used in the models which form the basis for calculating expected response. The problem solved at Rum Jungle is similar to the ones encountered in South Australia and the method used to interpret comes as a development of those used in this thesis.

A7.2 A wider discussion of the discoveries set out in Chapter 5, without first obtaining fresh rock samples from the lower Tapley Hill magnetic bed, could only give rise to theories developed from inadequate facts. It had been hoped that such a development of the research work would form a considerable part of the thesis but after spending several months without success, searching for fresh material in the most promising parts of several thousand square kilometers of the area, it became obvious that this study could not be completed within the scope of this Ph.D. thesis. In the course of this search, the Department of Mines and thirty five active exploration companies were approached. Only two companies were able to provide fresh rock and this was not from the areas of magnetic rocks. The difficulties in finding fresh rocks for study, outlined above and on page 4 of the thesis, have been experienced in the area by others (Mumme, 1964; Briden, 1967). Thus interpretation fell to the airborne and ground magnetic data. In view of the difficulties and errors in interpreting anomalies for other than the simplest of magnetic problems, it seemed that speculation regarding the significance of the results should be taken only as far as justified by the data available.

A7.3 Refinements of the gravity model using associated magnetic data, was limited by the spacing of the gravity observations and by the absence of the original magnetic records; the available contour maps are of relatively low information content as the contour intervals are drawn at 100 gammas and are the results of a very early survey flown by the

Bureau of Mineral Resources. The gravity survey was of a regional nature, the observations being made on a 7 kilometer grid. To provide further details for modelling the Anabama Granite would have required extensive field work in an area which was inaccessible and has very poor outcrop. A comparison of this problem with a similar one from an area of Proterozoic rocks at Rum Jungle in the Northern Territory, where fresh rock from drill core provides an adequate number of samples and an indication of the probable proportion of different rock types, has demonstrated the limitations of gravity interpretation with inadequate geological control. In this case, even with the large quantity of drill core available, it is extremely difficult to establish reliable density contrasts.

To discuss a relationship between the presence of the granite and development of magnetic anomalies would probably have called for a further section to the thesis. This was considered during the research project but, as the granites lie outside the ORROROO area and there are no granites known on ORROROO, it was not considered a high priority problem.

The "Burra Granite" cannot be studied because neither the granite nor adjacent contact rocks are exposed. Moreover, the airborne magnetic data, contoured at 50 gammas, was of low quality.

It was suggested that additional magnetic horizons might easily be analysed in relation to the pattern shown on Figs. 5.1 and 5.2.

Other horizons were analysed (pages 81 and 82) and support was found for the interpretation made for the character of the Lower Tapley Hill magnetic bed. In contrast to the Tapley Hill it was found to be impractical to fully analyse other magnetic beds. The amplitude of anomalies was usually not sufficiently high to give enough well defined anomalies over a long strike length, and especially around suitable struc-

tures. Lithologic and stratigraphic changes often made it difficult to be sure the same magnetic bed was under study. In some of the more promising beds the problem of establishing the character of remanent magnetization is compounded by the presence of strong induced magnetization (viz. Holowilena Ironstone and Ulupa Siltstone).

A7.4 It was suggested that an investigation should be made of the influence of susceptibility anisotropy and other mechanisms on the production of the observed remanent magnetism.

Susceptibility anisotropy tested on rock samples of Ulupa Siltstone, Holowilena Ironstone and Tindelpina Shale Member was found to be small (Appendix 2, Table A2.3), and appears to be too low to confine J2 to the bedding. While the presence of J2 was deduced, its explanation must remain open to speculation until fresh rock samples are available. Grain sizes will be found to be important (page 83) as has been suggested by Evans (1972).

Support for the derived direction and suggested time of acquisition for J1 has recently appeared in another source. Embleton (1973) has given Palaeolatitudes for Australia in the Phanerozoic; his picture for the Ordovician fits well with J1 being acquired in low latitudes. Perhaps J2 is a soft component acquired recently by a larger grain size than that which gives the harder J1.

A7.5 It was suggested that it might be possible to determine more about the boundary between areas A and B, especially its attitude.

During the study regional magnetic anomalies were examined with this in mind, but nothing at all was found. Further work in other fields has given support for the location of the boundary (McKirdy, Sumartojo, Tucker and Gostin, 1975).

A7.6 A possible horizontal extension of the Anabama Granite was suggested. There is nothing in the magnetics to indicate extension of the body to the northwest. The depth of 23 kilometers is consistent with the observed gravity anomalies as indicated by the modelling. It could be reinterpreted to use smaller depths by making various uncheckable geological assumptions, but with the present data there is little to be gained by going further in the analysis.

#### REFERENCES

- BRIDEN, J. C., 1967 : Preliminary palaeomagnetic results from the Adelaide System and Cambrian of South Australia. Trans. Roy. Soc. S. Aust., Vol.91, pp.17-25.
- EMBLETON, B. J. J., 1973 : The Palaeolatitude of Australia through Phanerozoic Time. J. Geol. Soc. Aust., Vol.19, pp.475-482.
- EVANS, M. E., 1972 : Single-domain Particles and TRM in Rocks. Comments on Earth Sciences: Geophysics, Vol.2, pp.139-148.
- MUMME, W. G., 1964 : The palaeomagnetism of South Australian and Victorian rocks. Ph.D. Thesis, Univ. Adelaide (unpubl.).
- McKIRDY, D. M., SUMARTOJO, J., TUCKER, D. H. & GOSTIN, V., 1975 : Organic, mineralogic, and magnetic indications of metamorphism in the Late Precambrian Tapley Hill Formation of the Adelaide Geosyncline, South Australia. Prec. Res., Vol.2, pp.345-373.



Plate 1 (pocket) : Locality map of places referred to in the text  
of the thesis.

Figure 1.1 : Distribution of Adelaidean strata in Australia.

Source of data - tectonic map of Australia and New  
Guinea, 1971.

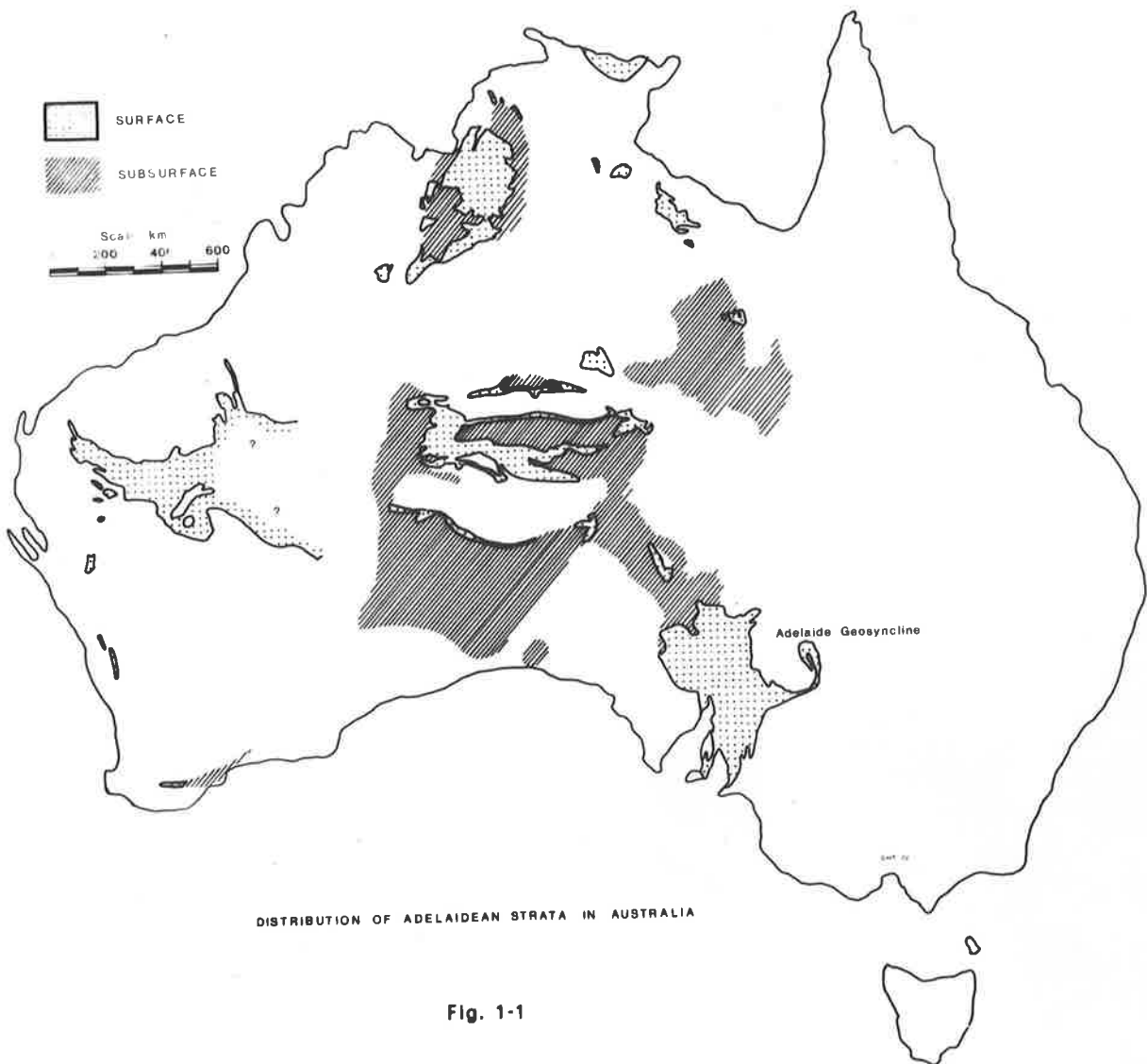


Fig. 1-1



Figure 1.2 : Geology of the Adelaide Geosyncline.

Legend

1. Mainly Cainozoic and Mesozoic sediments
2. Palaeozoic granites
3. Cambrian sediments
4. Adelaidean sediments
5. Lower Proterozoic volcanics (Gawler Range  
Volcanics)
6. Lower Proterozoic metasediments
7. Lower Proterozoic granites and granitization  
complexes
8. Fold axis
9. Fault
10. Little deformed Adelaidean and Cambrian rocks  
essentially unmetamorphosed
11. Mildly folded Adelaidean to Cambrian rocks meta-  
morphosed to chlorite grade
12. Moderately folded Adelaidean to Cambrian rocks  
metamorphosed to biotite grade
13. Strongly folded Adelaidean to Cambrian rocks  
metamorphosed to amphibolite facies

Source of data - geology base from Parkin (1969) and  
SADM geology maps; metamorphic zones from Preiss  
(1971), Offler and Fleming (1968) and Binks (1971).

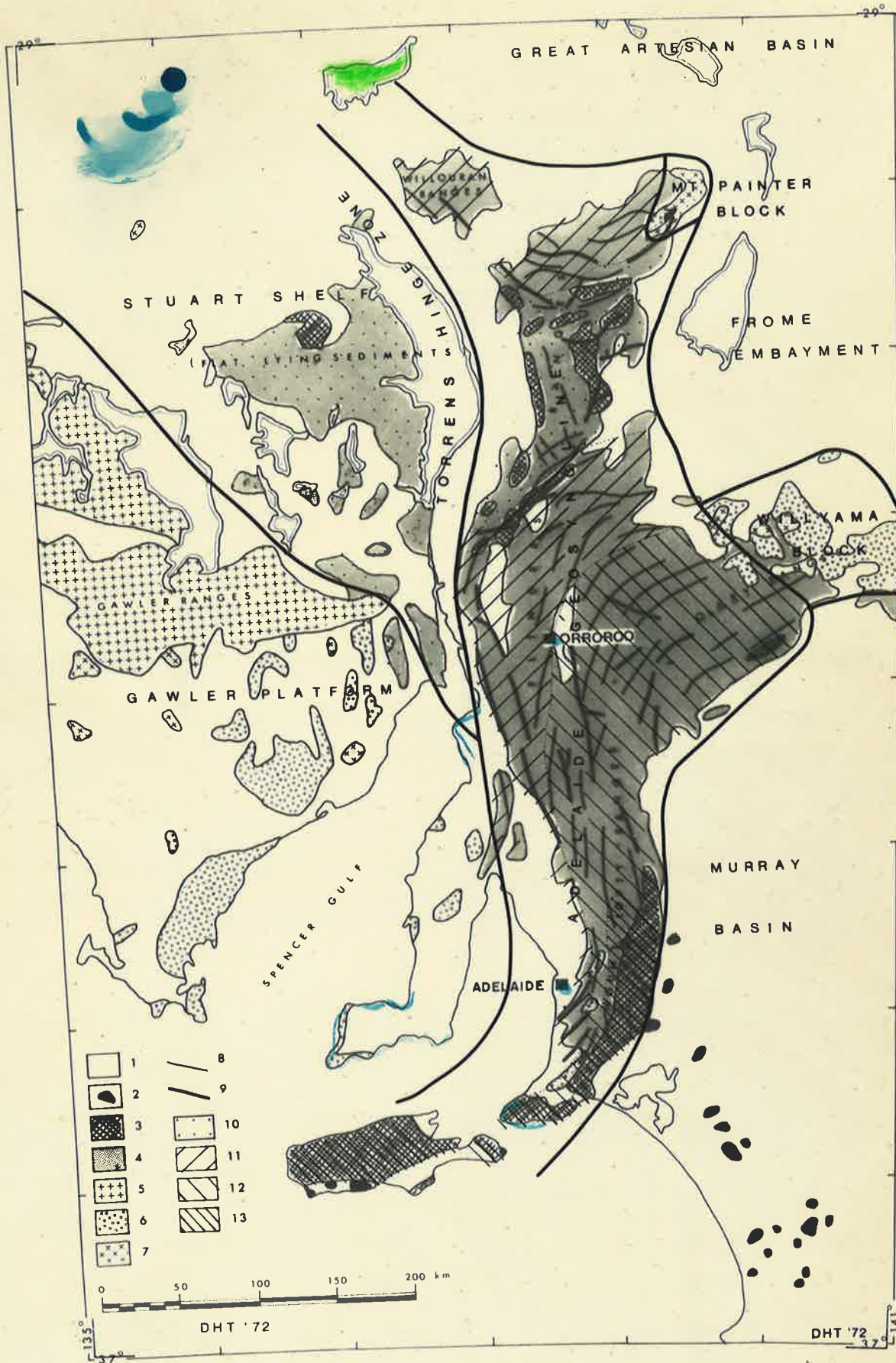


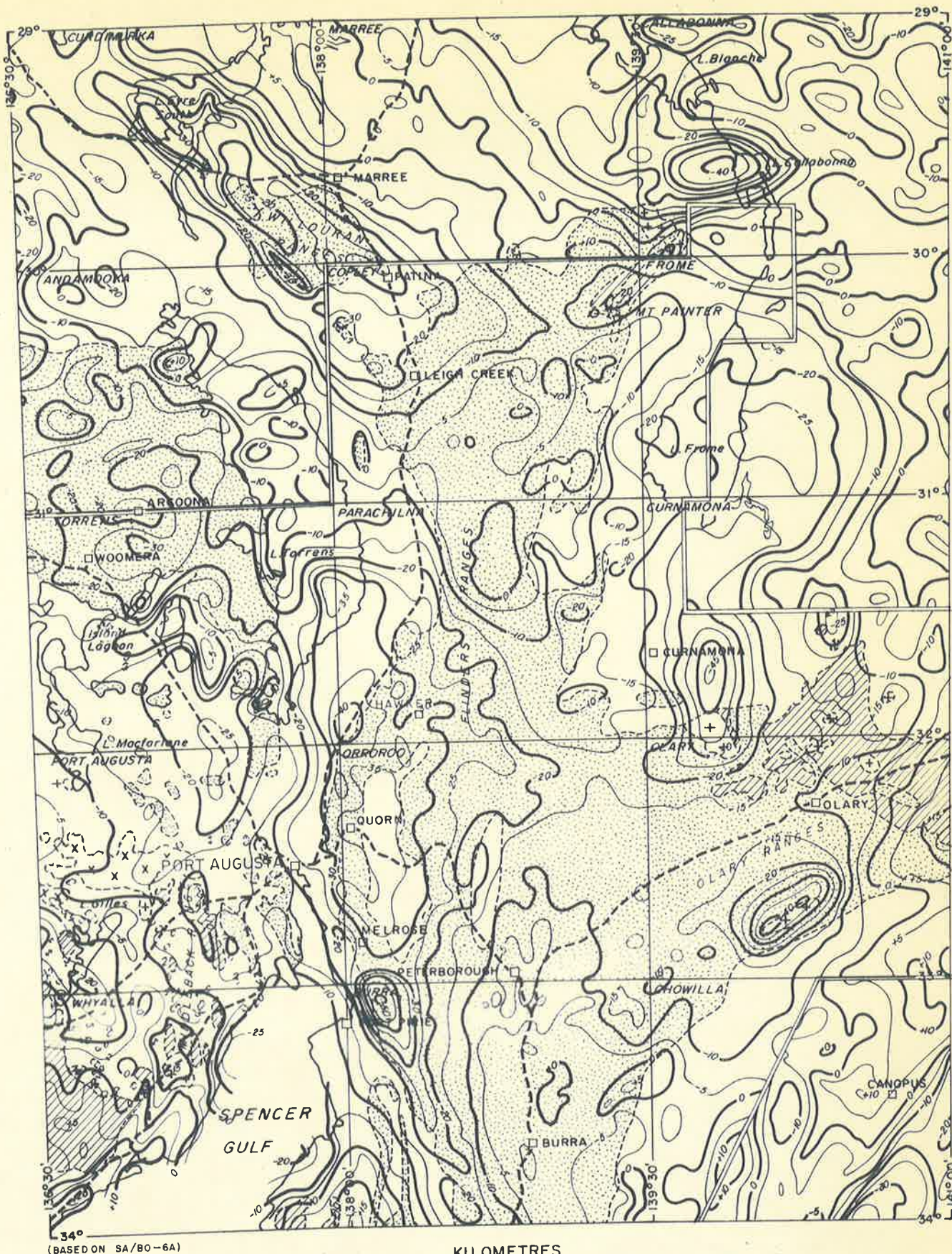
Fig. 1-2

Figure 1.3 : Geology and Bouguer anomalies of the northern part of the Adelaide Geosyncline.

The contour interval is 5 milligals. Over the area inside the double lines the Bouguer density for reduction was  $2.67 \text{ g/cm}^3$ . North and south-east of the double lines the reduction density was  $1.9 \text{ g/cm}^3$  and  $2.2 \text{ g/cm}^3$ .

Source of data - geology generalized after Sprigg (1953); the Bouguer anomaly contours are from unpublished maps by the BMR.





(BASED ON SA/80-6A)



DHT '72

- SEDIMENTS
- CAMBRIAN AND ADELAIDEAN SEDIMENTS
- METAMORPHIC COMPLEXES OF THE MT PAINTER AREA, WILLYAMA BLOCK AND GAWLER CRATON
- + +  
+ + ACID INTRUSIVE AND GRANITOID ROCKS
- x x  
x x FELDSPAR QUARTZ PORPHYRIES OF THE GAWLER RANGES
- 10 BOUGUER ANOMALY CONTOURS

GEOLOGY GENERALIZED AFTER SPRIGG, 1953  
(GEOLOGICAL MAP OF S.A. 32M = 1")

Fig 1-3

**GEOLOGY AND BOUGUER ANOMALIES**



Figure 1.4 : Aeromagnetic map, geology (overlay 1) and interpretation (overlay 2) of the northern part of the Adelaide Geosyncline.

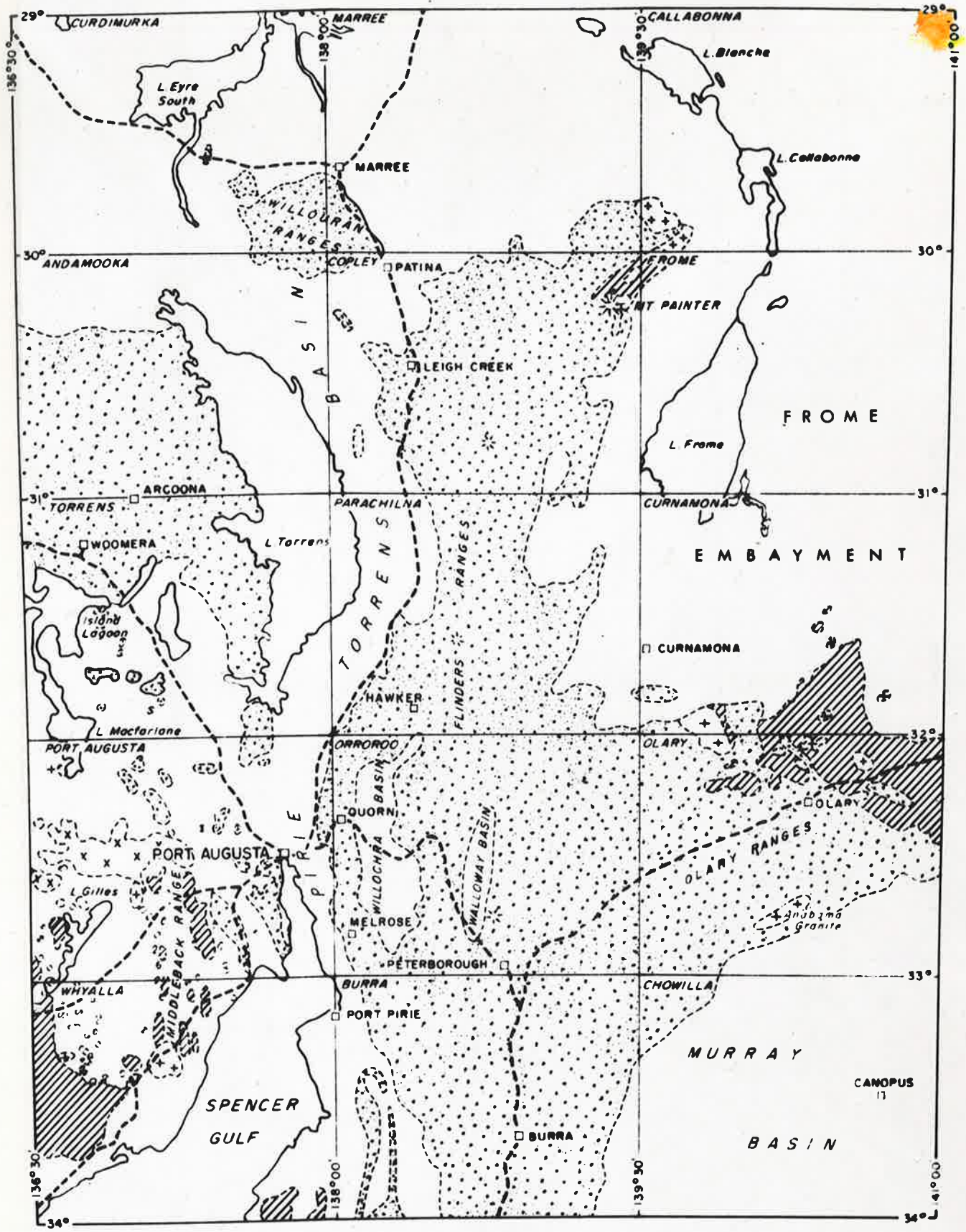
Magnetic sources at or near the surface

1. Magnetic Adelaidean strata
2. (?) dolerite dykes on the Eyre Peninsula
3. Iron Formations of the Middleback Ranges
4. Metasediments (schists, phyllites and acid intrusives)
5. Metasediments and intrusives

Zones of magnetic anomalies

- A Magnetic Gawler Platform strata at or near the surface (depth range 0-1 km)
- B Strong broad anomalies due to unknown sources, possibly intrusive bodies (depth range 2-5 km)
- C Very weak, very broad anomalies probably due to sources in the depth range 5-15 km. Superimposed linear anomalies are due to magnetic Adelaidean strata
- D Magnetic Mt. Painter Block strata at or near the surface (depth range 0-1 km)
- E Strong broad anomalies due to unknown sources, possibly of the kind on the Willyama Block (depth range 1-6 km). The feature circled with a dashed line is referred to in Chapter 7
- F Magnetic Willyama Block strata at or near the surface (depth range 0-1 km)
- G Strong circular anomalies due to unknown sources in the depth range 1-2 km. Anomalies in this zone are similar to zone F. The source rocks in the two zones are probably similar

Source of data - geology after Sprigg (1953). Aeromagnetic contour map from SADM 1:1,000,000 map of S.A. (unpublished). The contour interval is 100 gammas.



DHT '72

LEGEND

- |                           |  |  |                           |  |   |
|---------------------------|--|--|---------------------------|--|---|
| CENOZOIC AND MESOZOIC     |  | SEDIMENTS  | IGNEOUS AND RELATED ROCKS |  | ACID INTRUSIVE AND GRANITOID ROCKS              |
| PALEOZOIC AND PROTEROZOIC |  | CAMBRIAN AND ADELAIDEAN SEDIMENTS  |                           |  | FELDSPAR QUARTZ PORPHYRIES OF THE GAWLER RANGES |
| LOWER PROTEROZOIC         |  | METAMORPHIC COMPLEXES OF THE MT PAINTER AREA, WILLYAMA BLOCK AND GAWLER CRATON |                           |  |   |

Overlay 1, Fig. 1-4

GENERALIZED GEOLOGY



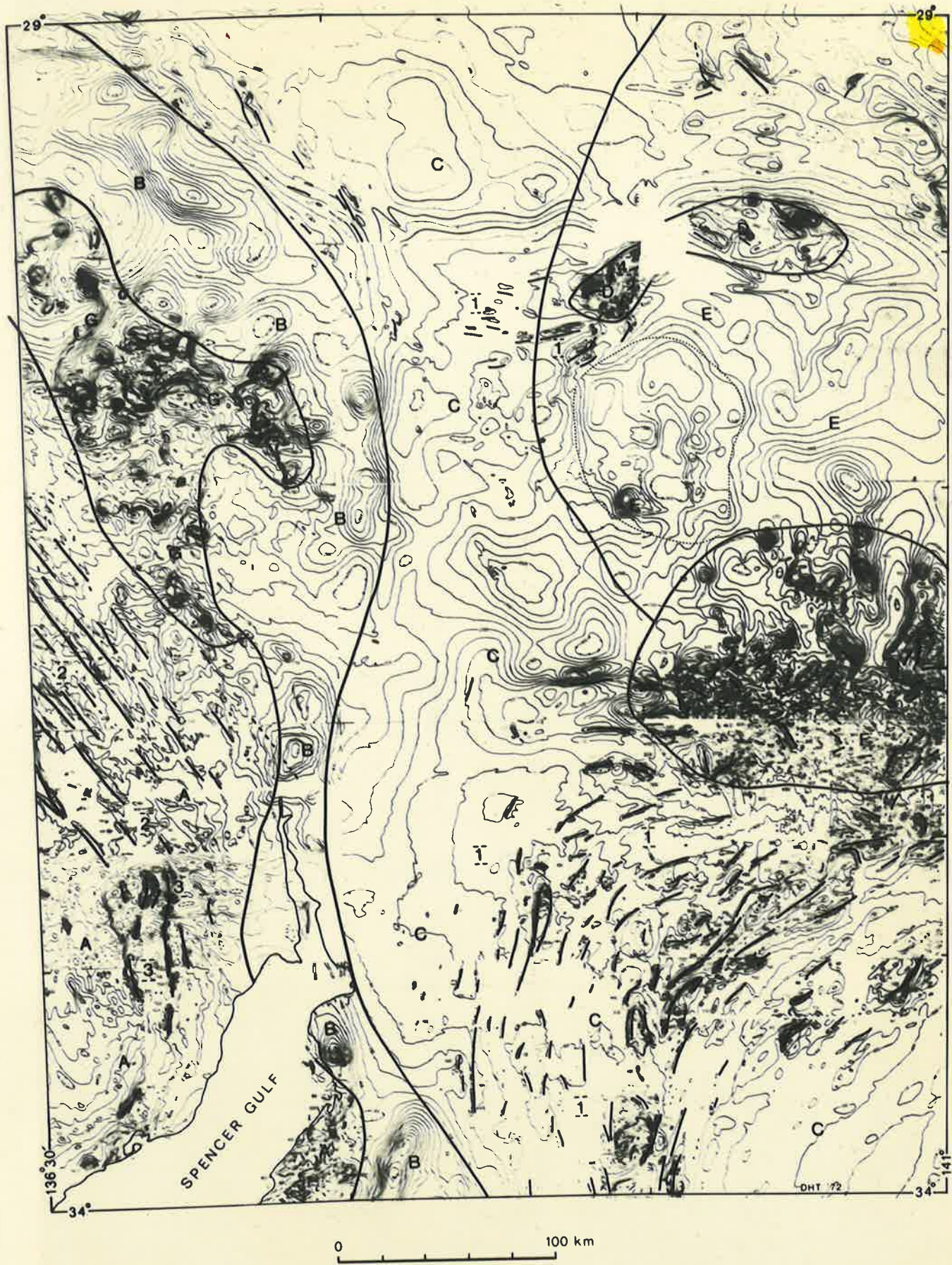


Fig. 1-4

F

Figure 1.5 : ORROROO geological map showing the localities of  
(pocket) ground magnetometer lines.

Magnetometer lines are numbered.



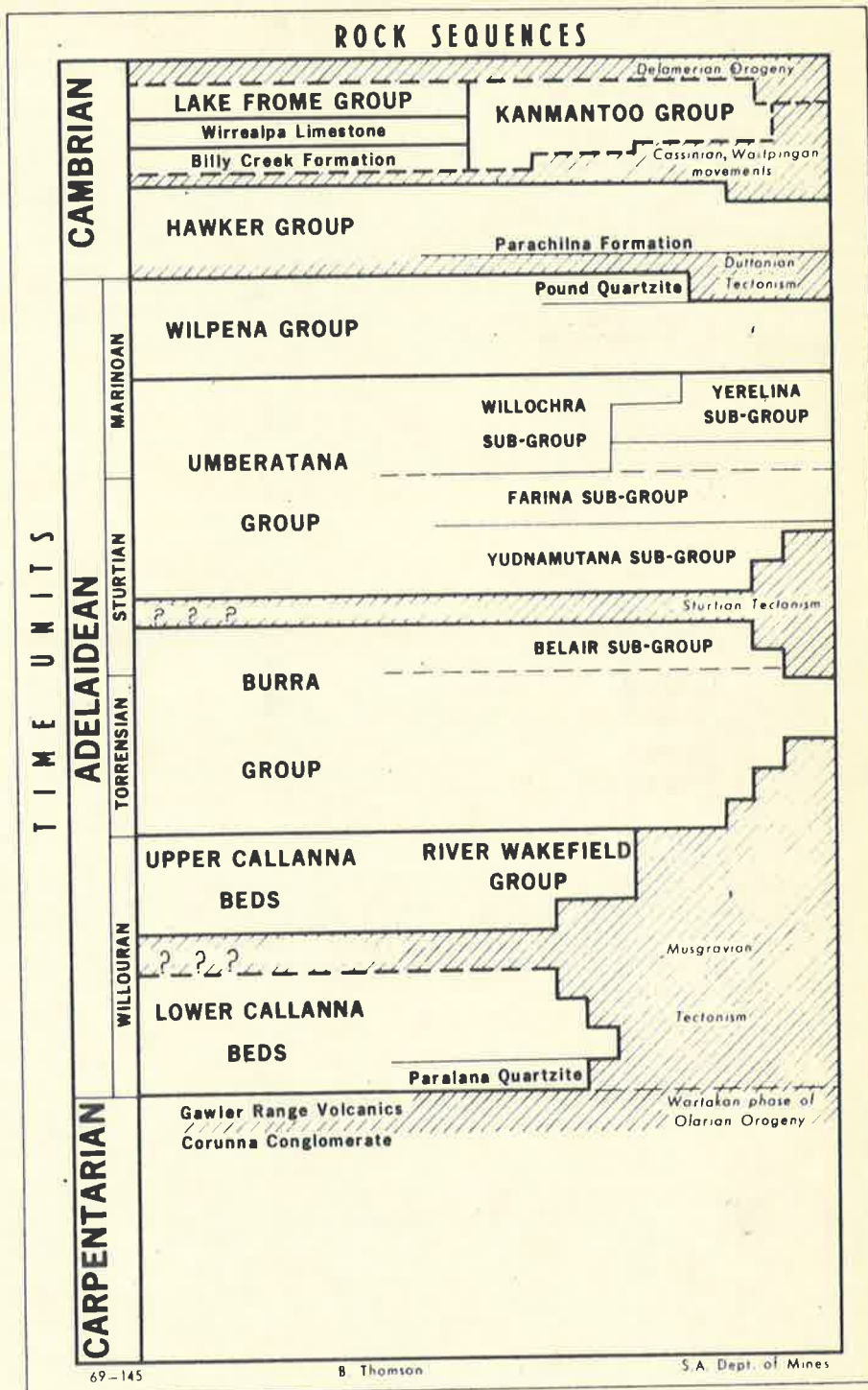
Figure 1.6 : ORROROO aeromagnetic map of total intensity.  
(pocket)

The contour interval is 10 gammas. The data were recorded with an airborne magnetometer at a continuous ground clearance of 150 m.

Figure 1.7 : Time and rock terms used in the Adelaide Geosyncline.

In the study of magnetic anomalies most attention was given to the Wilpena, Umberatana and Burra Groups.

Source of data - Parkin (1969, p.51).

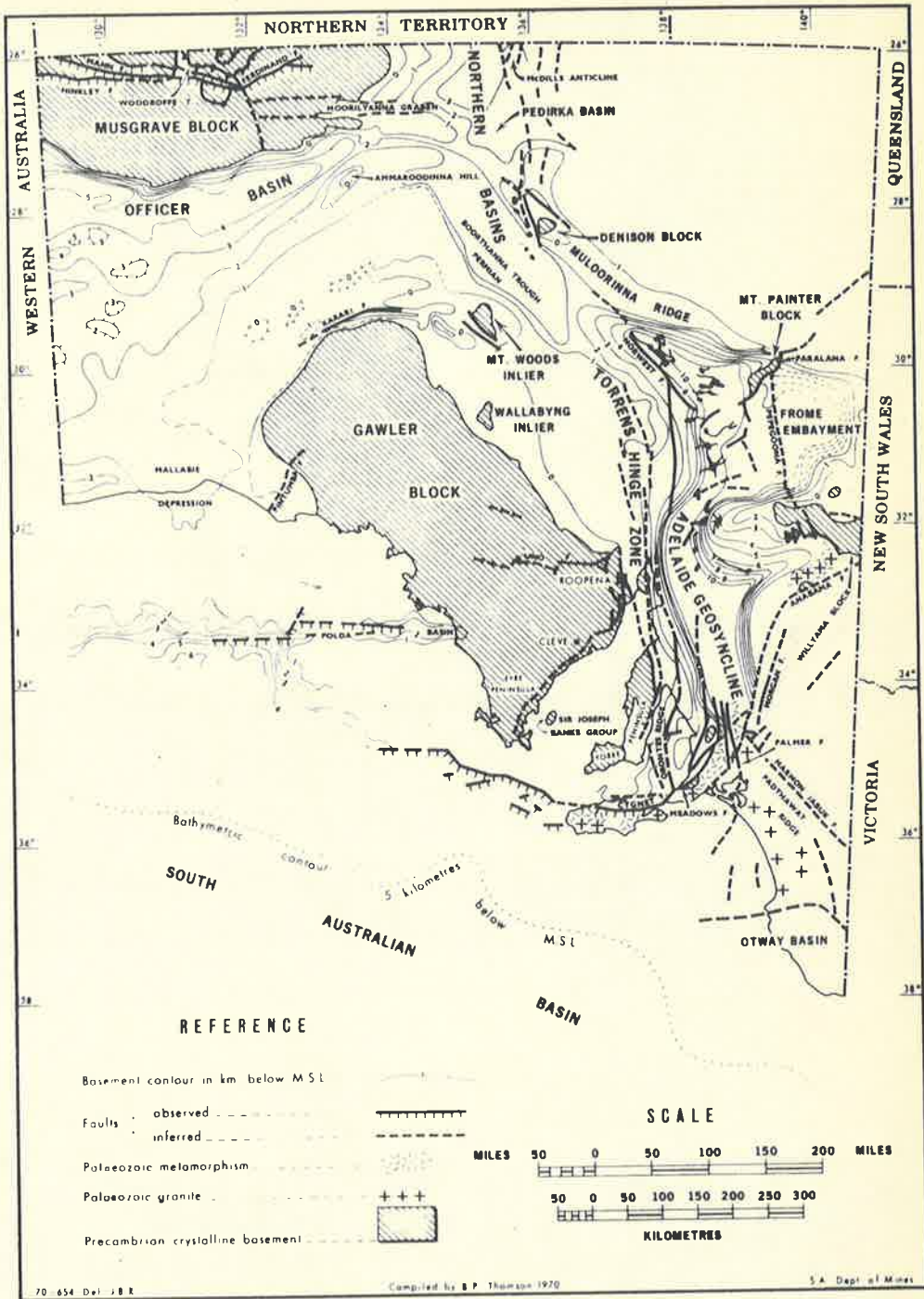


**Time and rock terms used in the Adelaide Geosyncline and adjoining areas.**

Fig. 1-7

Figure 1.8 : Precambrian basement contours, ~~form~~ lines and other structural features in South Australia.

Source of map - Thomson (1970).



Precambrian basement contours, form lines and other structural features in South Australia.

Fig. 1-8

Figure 2.1 : Index map showing 1:250,000 sheet names; the localities of drill holes from which material was tested for magnetic susceptibility, density or mineralogy; and the localities of ground magnetometer surveys.

A table of drill hole names and tests carried out is included in Appendix A1; a table of magnetometer surveys is included in Appendix A3.

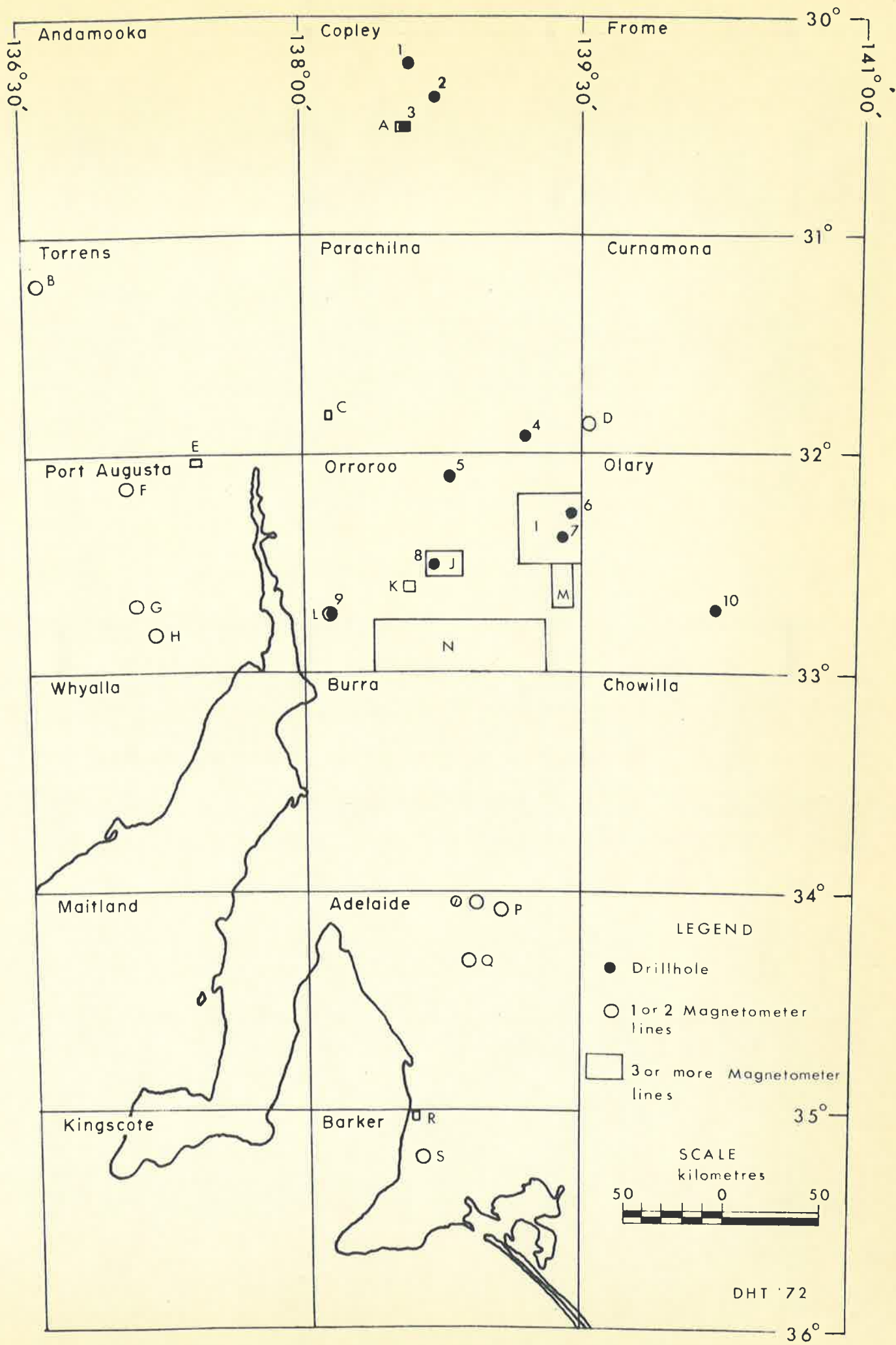


Fig. 2-1

Figure 3.1 : (a) and (b) show total field aeromagnetic flight charts and the interpreted anomalies from near surface sources. (b) illustrates how ambiguity in selected anomalies can occur if there are two reasonable base levels which can be chosen. (c) illustrates the interpretation given to magnetic anomalies on part of the Peterborough 1:63,360 map area. Arrows show the position and sign of peaks of anomalies; dots show the location of photo centres along flight lines. The original scale of the geology base maps and magnetic anomaly compilation sheets was 1:47,520. The horizontal scales of the three diagrams are shown below (c).



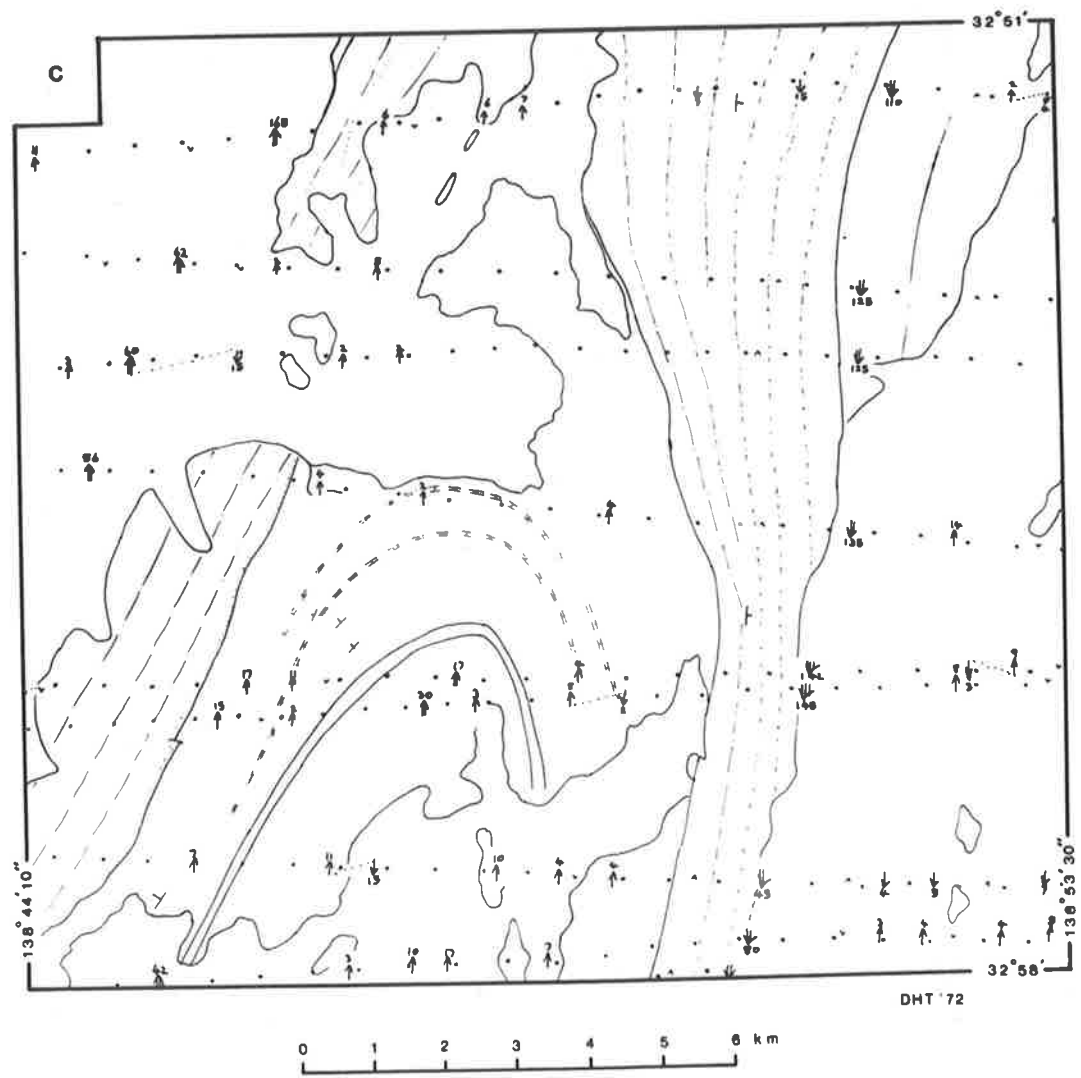
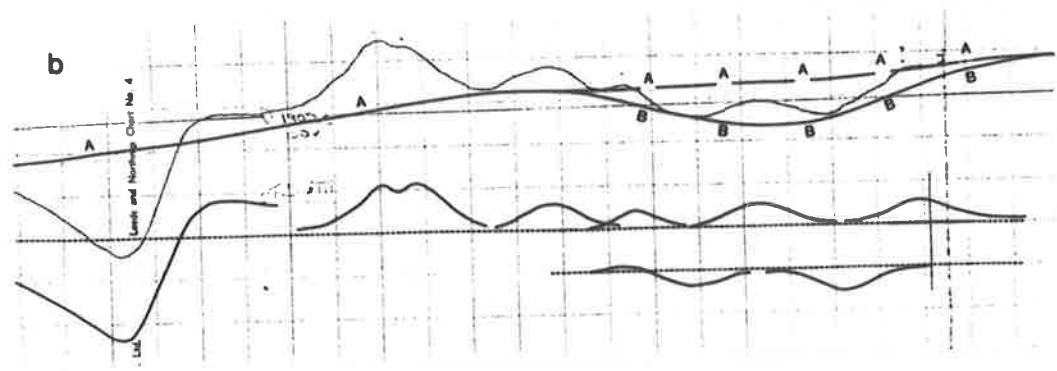
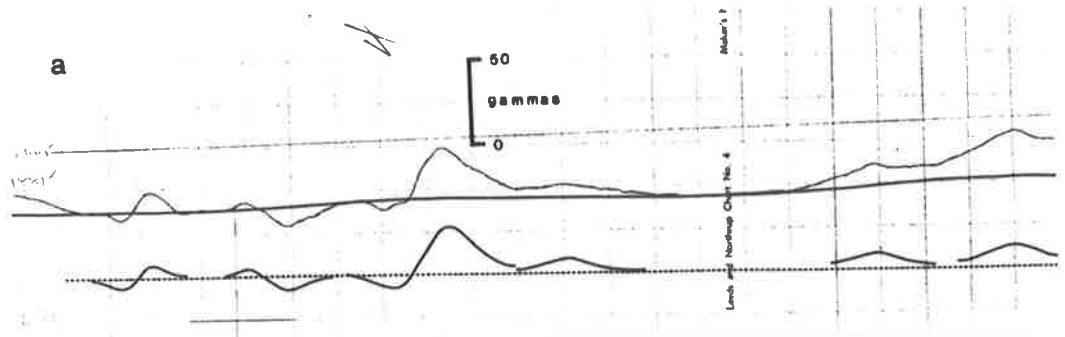


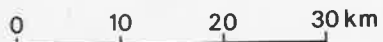
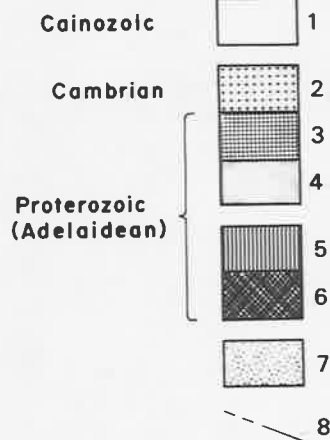
Fig. 3-1

Figure 3.2 : Overlay of interpreted locations of shallow magnetic sources on a simplified geological map of ORROROO.

	<u>Legend - geology</u>	<u>Legend - magnetics (overlay)</u>
Cainozoic	1 Sediments	The amplitude of aeromagnetic anomalies at each source position fall in the following ranges
Palaeozoic	2 Hawker Group sediments	
	3 Wilpena Group sediments	
Proterozoic (Adelaidean)	4 Umberatana Group sediments	
	5 Burra Group sediments	
	6 River Wakefield Group (Callanna Beds)	
	7 Diapiric breccia	
	8 Geological boundary	
		2. 21-100 "
		3. 101-400 "
		4. 401+ "

In Area B (western part) the amplitudes of anomalies usually lie in Range 1; in Area A, amplitudes often lie in Range 2 or higher.

Source of data - geology simplified after Binks (1968); magnetics compiled from a study of original aeromagnetic flight charts.



Orroroo ..... ● O  
 Peterborough ..... ● P  
 Waukaringa ..... ● W



DHT 72

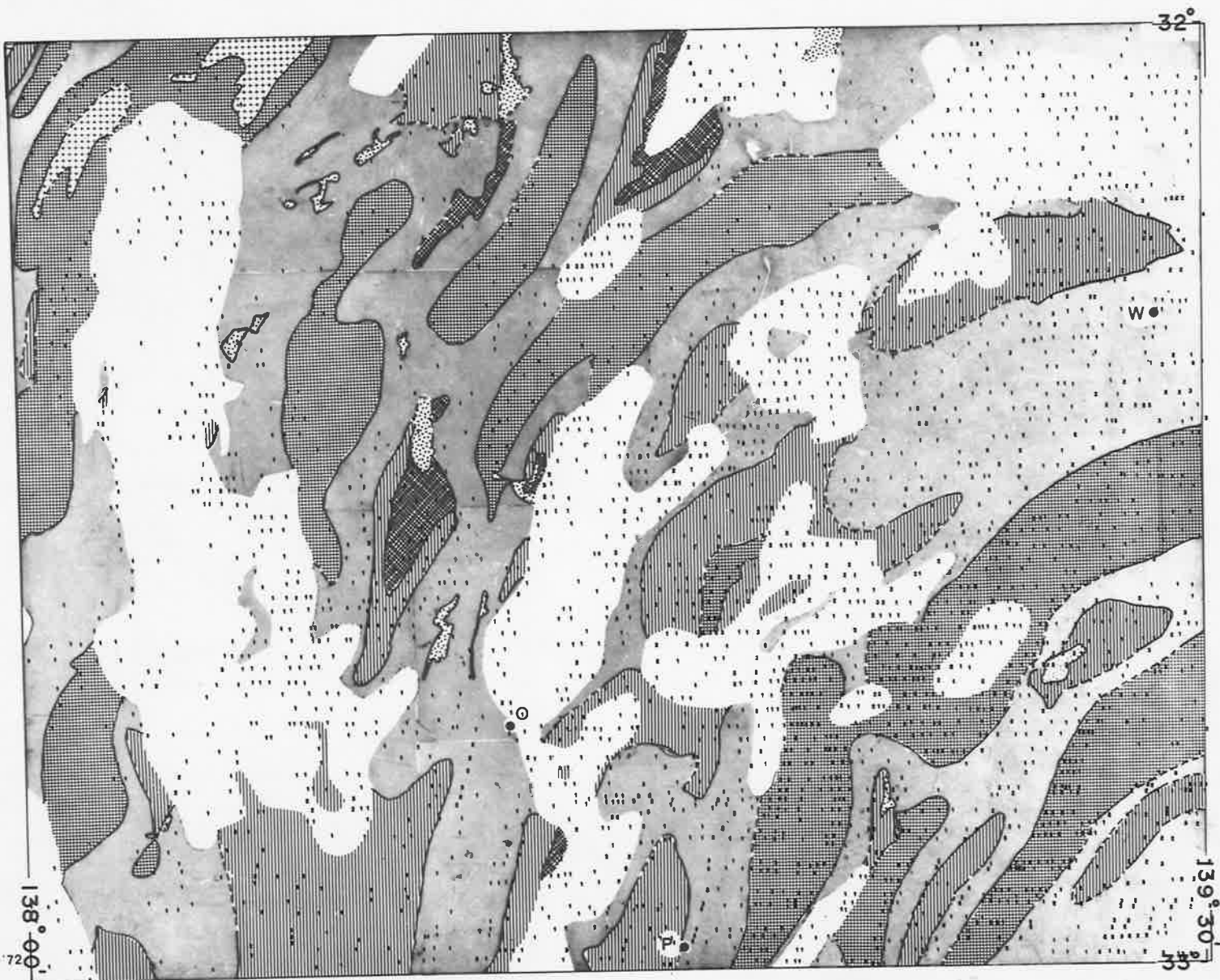


Figure 3.3 : Geophysical interpretation given to two adjacent flight profiles across a synclinal structure near Peterborough.

The heavy black lines on the geological section are interpreted magnetic beds. On the flanks of the high amplitude anomaly the selection of partly resolved low amplitude anomalies possibly caused by weakly magnetic beds is very difficult. The key to whether a particular low amplitude bump indicates the position of a magnetic bed comes from the study of adjacent profiles or profiles from another locality. For example, on the upper section, a magnetic bed is shown just above the contact between units E (Ulupa Siltstone) and D. The amplitude of the anomaly is about 5 gammas. On the lower section, the corresponding anomaly is better resolved and has an amplitude of about 15 gammas.

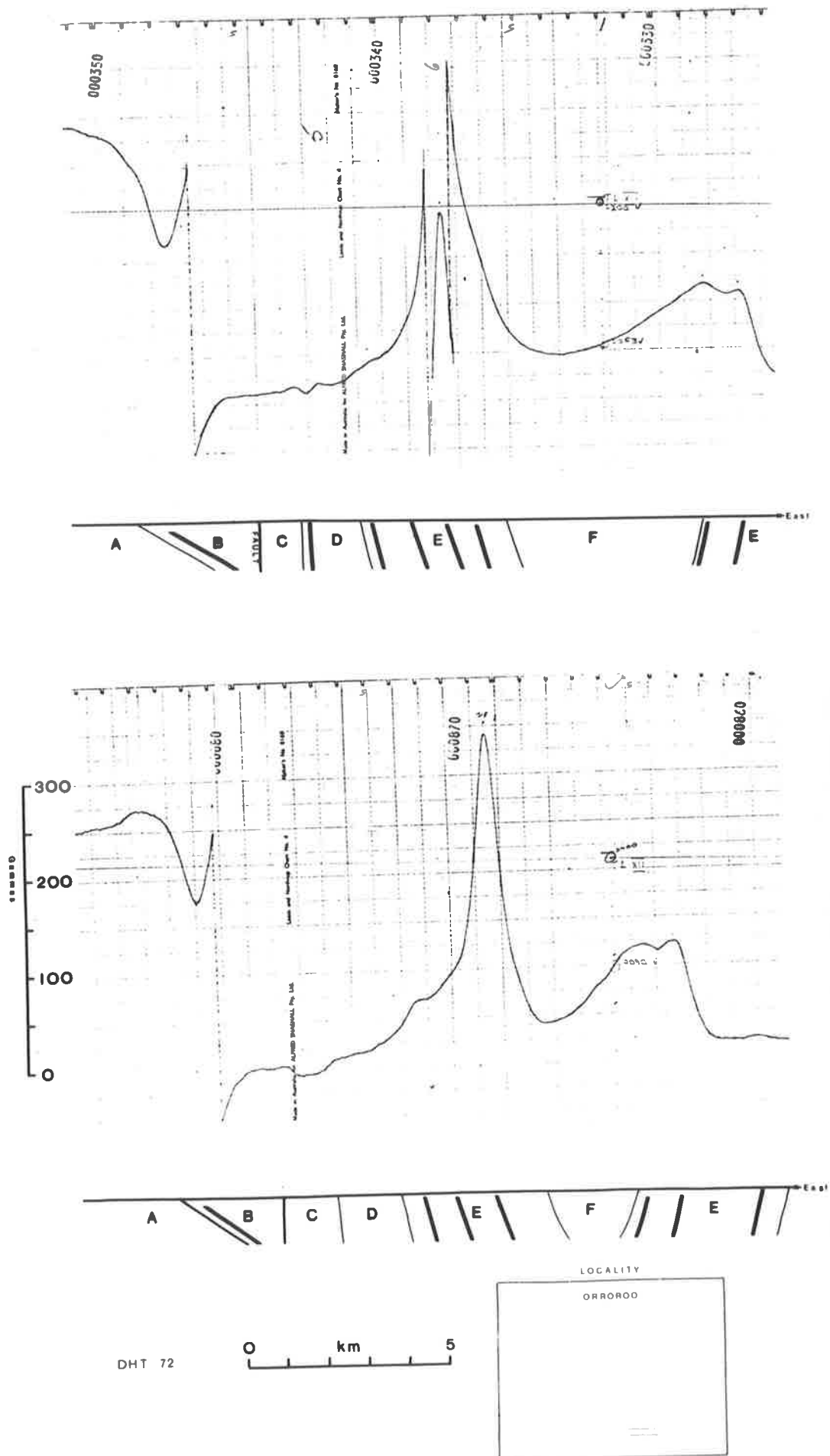


Fig. 3-3

Figure 3.4 : Positions of magnetic beds (black lines) within Adelaide System sediments on ORROROO

Legend - geology

- |                             |   |                                       |
|-----------------------------|---|---------------------------------------|
| Cainozoic                   | 1 | Sediments                             |
| Palaeozoic                  | 2 | Hawker Group sediments                |
| Proterozoic<br>(Adelaidean) | 3 | Wilpena Group sediments               |
|                             | 4 | Umberatana Group sediments            |
|                             | 5 | Burra Group sediments                 |
|                             | 6 | River Wakefield Group (Callanna Beds) |
|                             | 7 | Diapiric breccia                      |
|                             | 8 | Geological boundary                   |

Legend - magnetics

- 9 Magnetic bed

Source of data - geology simplified after Binks (1968); magnetics compiled from a study of original flight charts and 1:47,520 scale geological maps.

Fig. 3-4

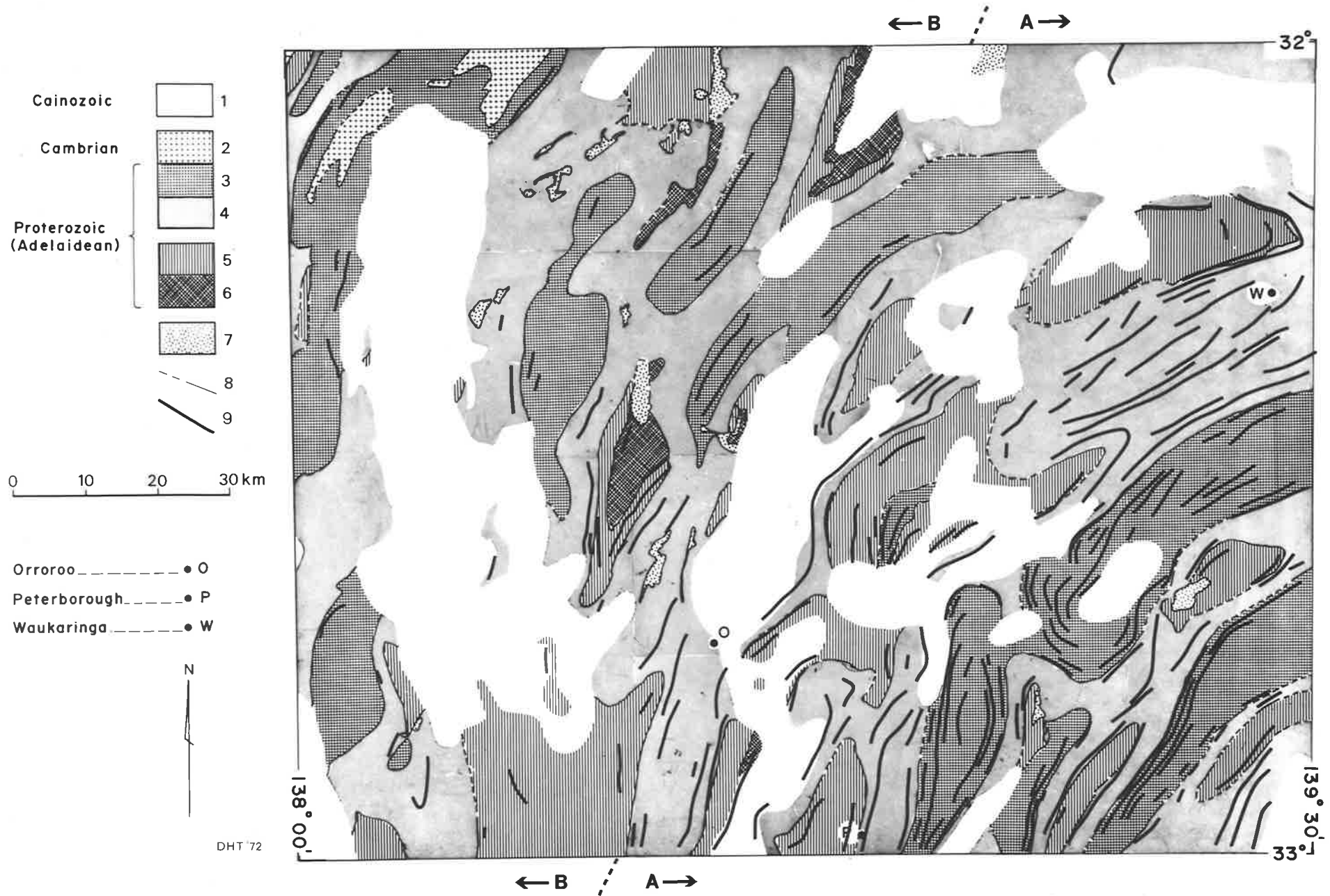


Figure 3.5 : Interpreted position of magnetic beds in the stratigraphic succession for ORROROO.

The maximum amplitudes of aeromagnetic anomalies recorded over the various magnetic beds are indicated in gammas.

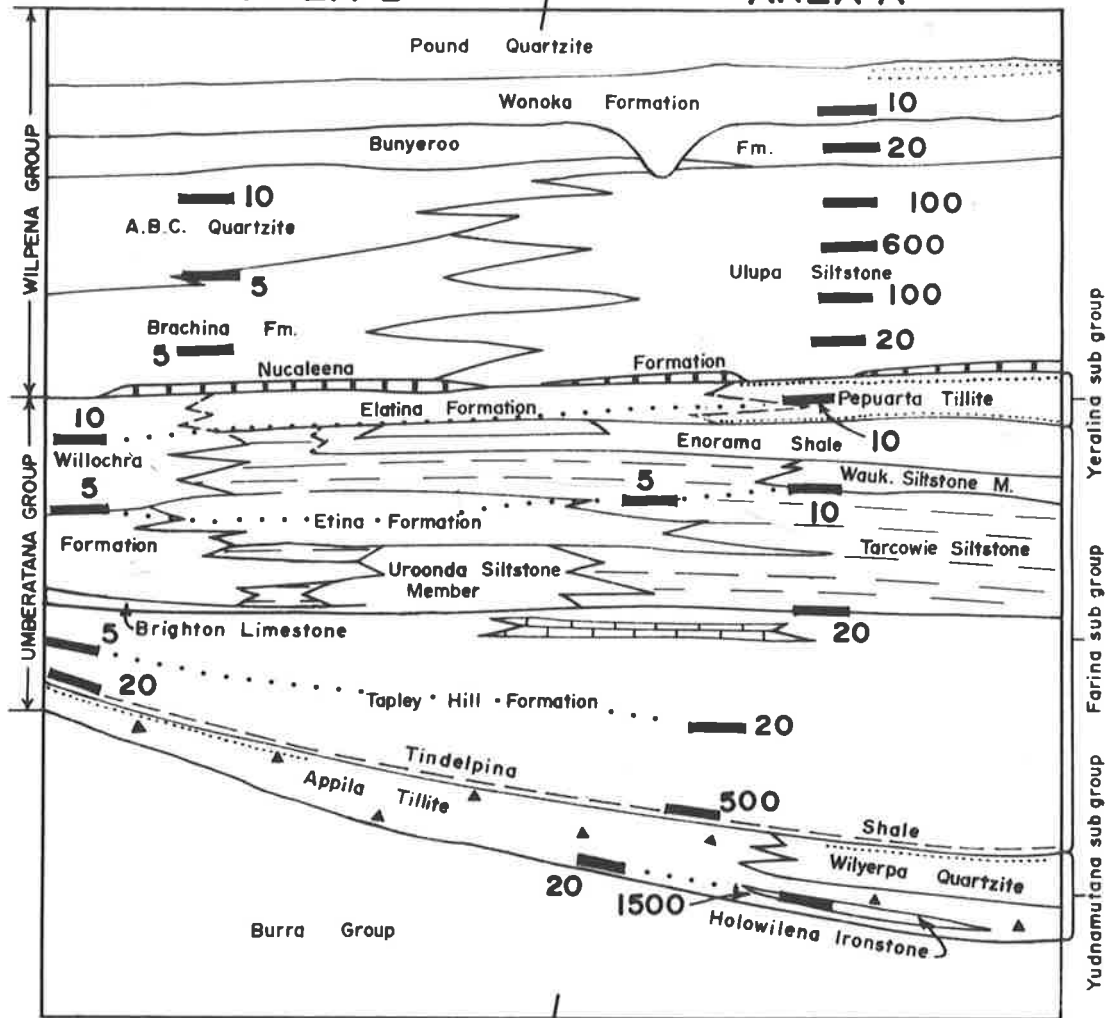
Source of data - rock relation diagram from Binks (1968); magnetics compiled from a study of original flight charts and 1:47,520 scale geological maps



# MAGNETIC BEDS

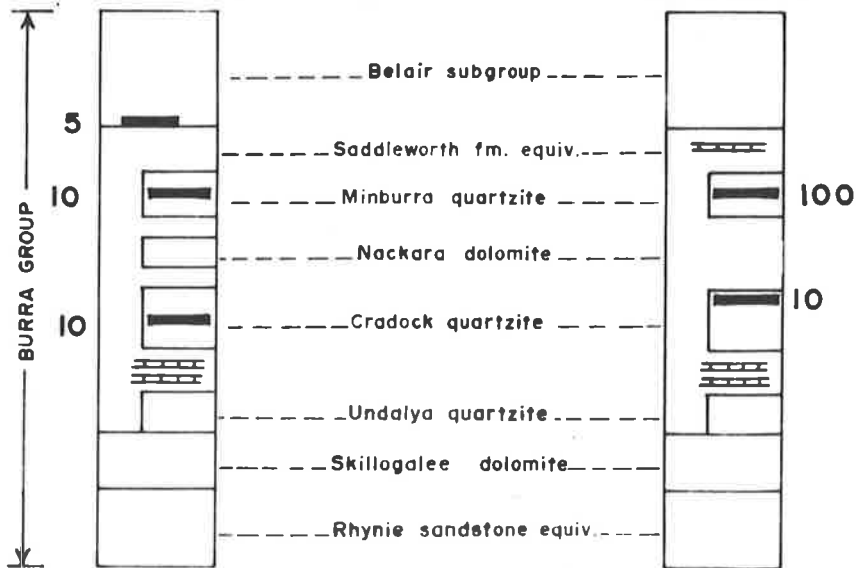
AREA B

AREA A



AREA B

AREA A



(Stratigraphic Column and Rock Relation Diagram after S.A. Dept. of Mines 1:250,000 Orroroo sheet.)

Figure 4.1 : (a) The upper diagram shows the results of reading a vertical field fluxgate magnetometer at the same stations on two different days. The lower diagram shows the differences between the two sets of data. The envelope of the differences is 10-20 gammas wide and is attributed to reading errors.

(b) Vertical field profile across the Lower Tapley Hill magnetic bed.

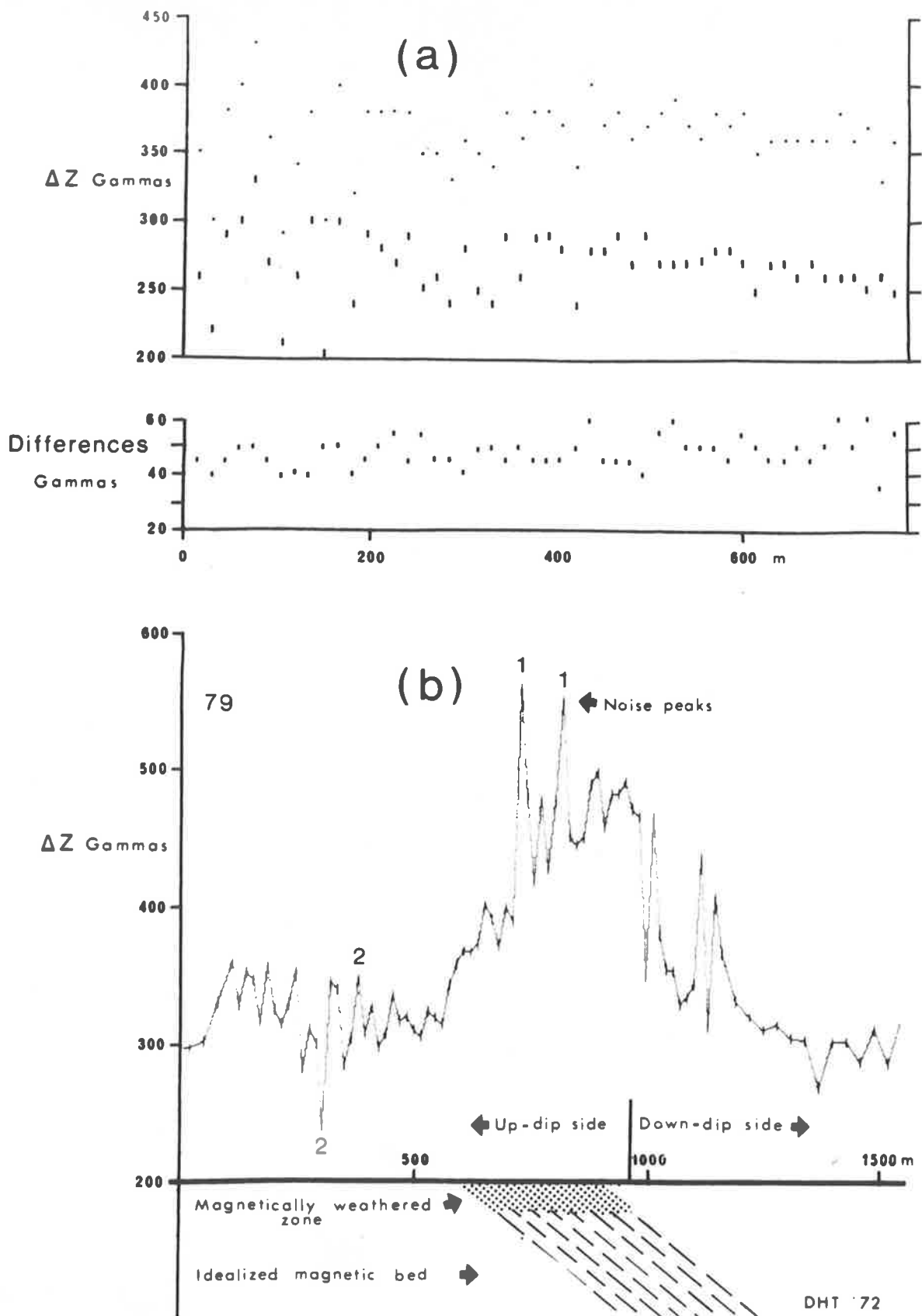


Fig. 4-1

Figure 4.2 : Stratigraphic column for the lower part of the Tapley Hill Formation in the Waukaringa area.

The Lower Tapley Hill magnetic bed is interpreted to lie between the two arrows.

Source of data - field work in the Waukaringa area.

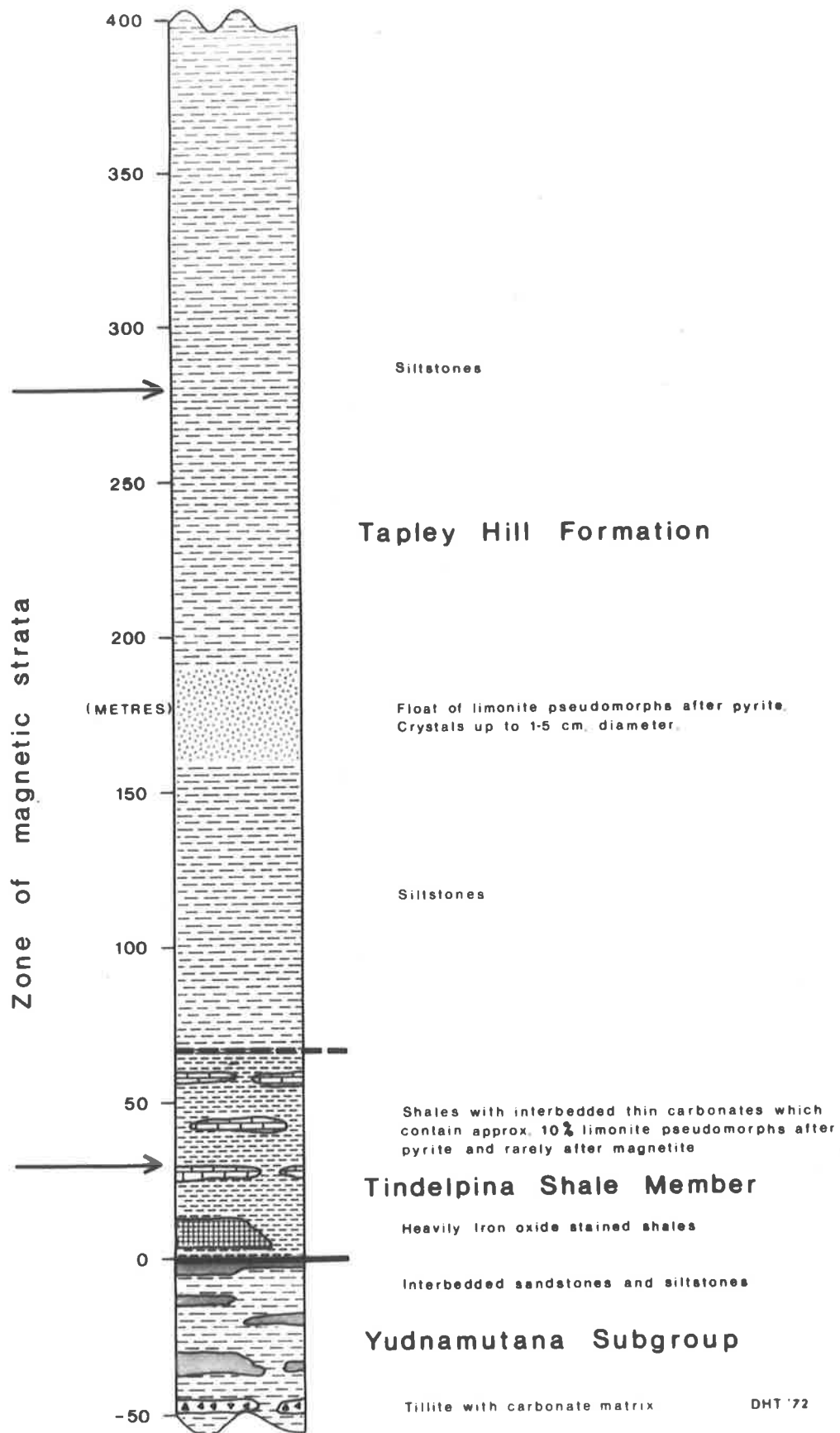
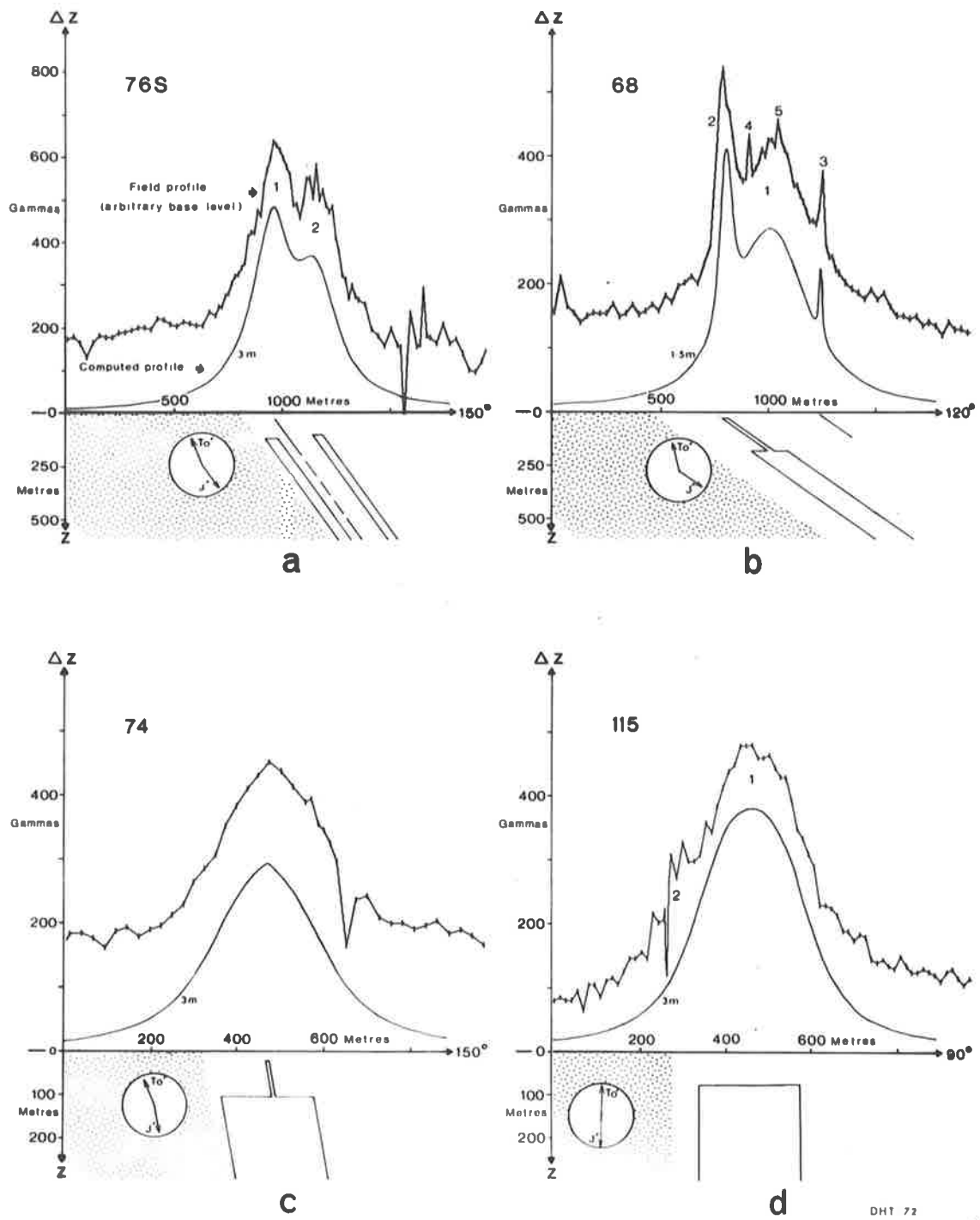


Fig. 4-2

Figure 4.3 : Four interpreted vertical field magnetometer profiles across the Lower Tapley Hill magnetic bed. (The locations of the profiles are shown on Figure 4.4(c)).

The field profiles are drawn on an arbitrary base level. The directions indicated on the right hand side of the profiles are measured east of geographic north. Note that the amplitude and distance scales on the diagrams are different. Data points on the field profiles are indicated by vertical lines; the grid intervals for computation of the theoretical profiles are indicated in metres. The Yudnamutana Subgroup (Appila Tillite) is shown as the shaded formation on the geological cross sections. The inset clocks show the effective direction of the earth's field ( $T'$ ) at the localities, and the direction of the effective magnetization ( $J'$ ) in the models for which the theoretical anomalies were computed.



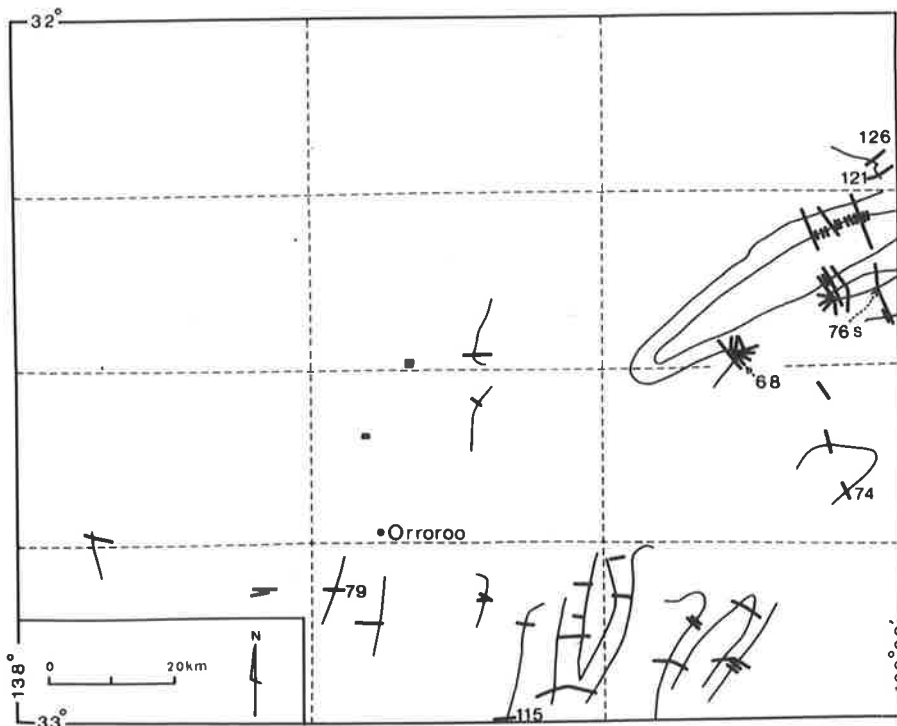
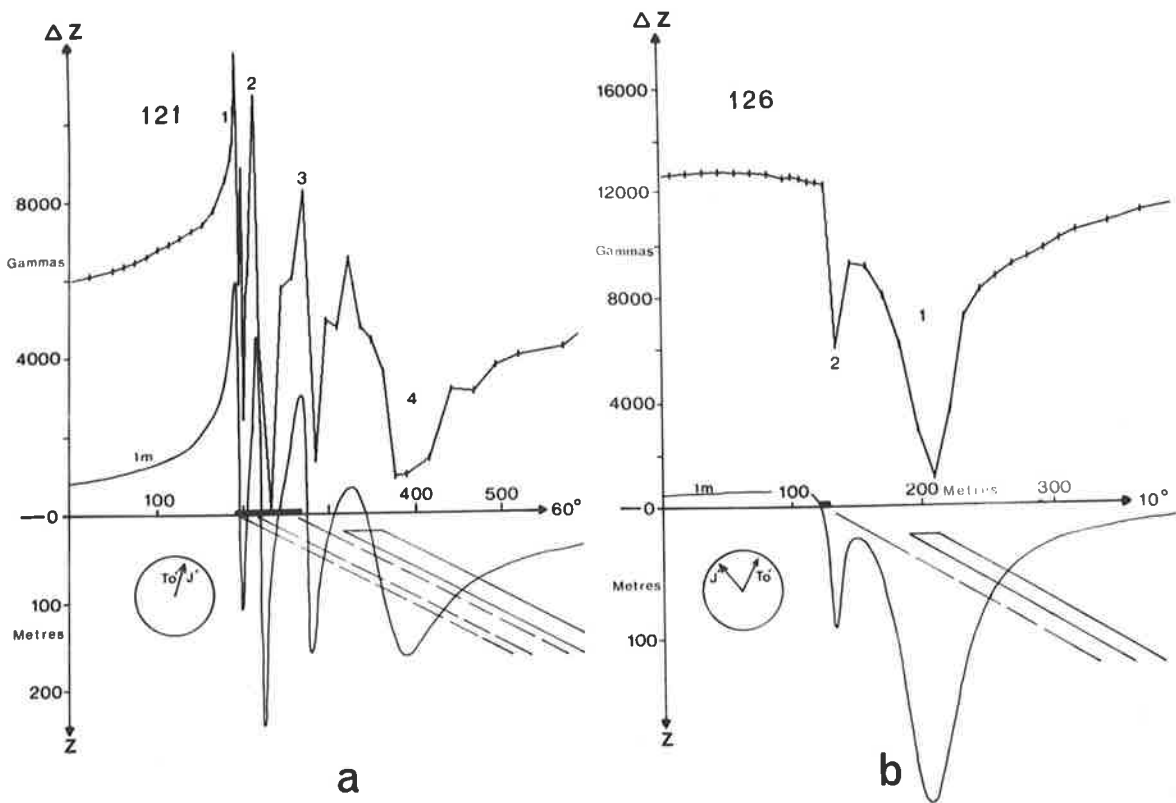
DHT 72

Fig. 4-3

Figure 4.4 : (a) & (b) Two interpreted vertical field magnetometer profiles across the Holowilena Ironstone (Yudnamutana Subgroup). (c) shows the localities of the profiles on Figures 4.3 and 4.4 on ORROROO.

The field profiles are drawn on an arbitrary base level. The directions indicated on the right hand side are measured east of geographic north. Note that the amplitude and distance scales are different. Data points on the field profiles are indicated by vertical lines; the grid intervals for computation of the theoretical profiles are indicated in metres. The zones of outcrop of ironstone beds are indicated on the cross sections by thick black lines; in these zones individual ironstone beds are about 1 m thick and are separated from each other by siltstones. The inset clocks show the effective direction of the earth's field ( $T'$ ) at the localities, and the direction of the effective magnetization ( $J'$ ) in the models for which the theoretical anomalies were computed.





DHT 72

Fig. 4-4

Figure 5.1 : Total field aeromagnetic anomalies over the lower (pocket) part of the Tapley Hill Formation (Lower Tapley Hill magnetic bed) in the Adelaide Geosyncline.

Source of data - geology from SADM geological maps; magnetic anomalies for ORROROO from a study of aeromagnetic flight charts, magnetic anomalies for other areas from SADM contour maps of total magnetic intensity.

Figure 5.2 : Areas of characteristic total field magnetic anomalies over the Lower Tapley Hill magnetic bed in the Adelaide Geosyncline.

The characteristics are as follows:

Characteristic 1 - anomalies over S, SE and E dipping beds are negative; anomalies over N, NW or W dipping beds are positive; the amplitudes of negative anomalies exceed those of positive anomalies.

Characteristic 2 - anomalies over S and E dipping beds and N and W dipping beds are negative; the amplitudes of anomalies over S and E dipping beds exceed those over N and W dipping beds.

Characteristic 3 - anomalies over E and W dipping beds are positive; the amplitude of anomalies over W dipping beds are higher than over E dipping beds.

The locations of two anticlinal structures near Waukaringa, where detailed vertical field ground magnetometer traverses were put in, are arrowed (C and D).

Source of data - Figure 5.1.

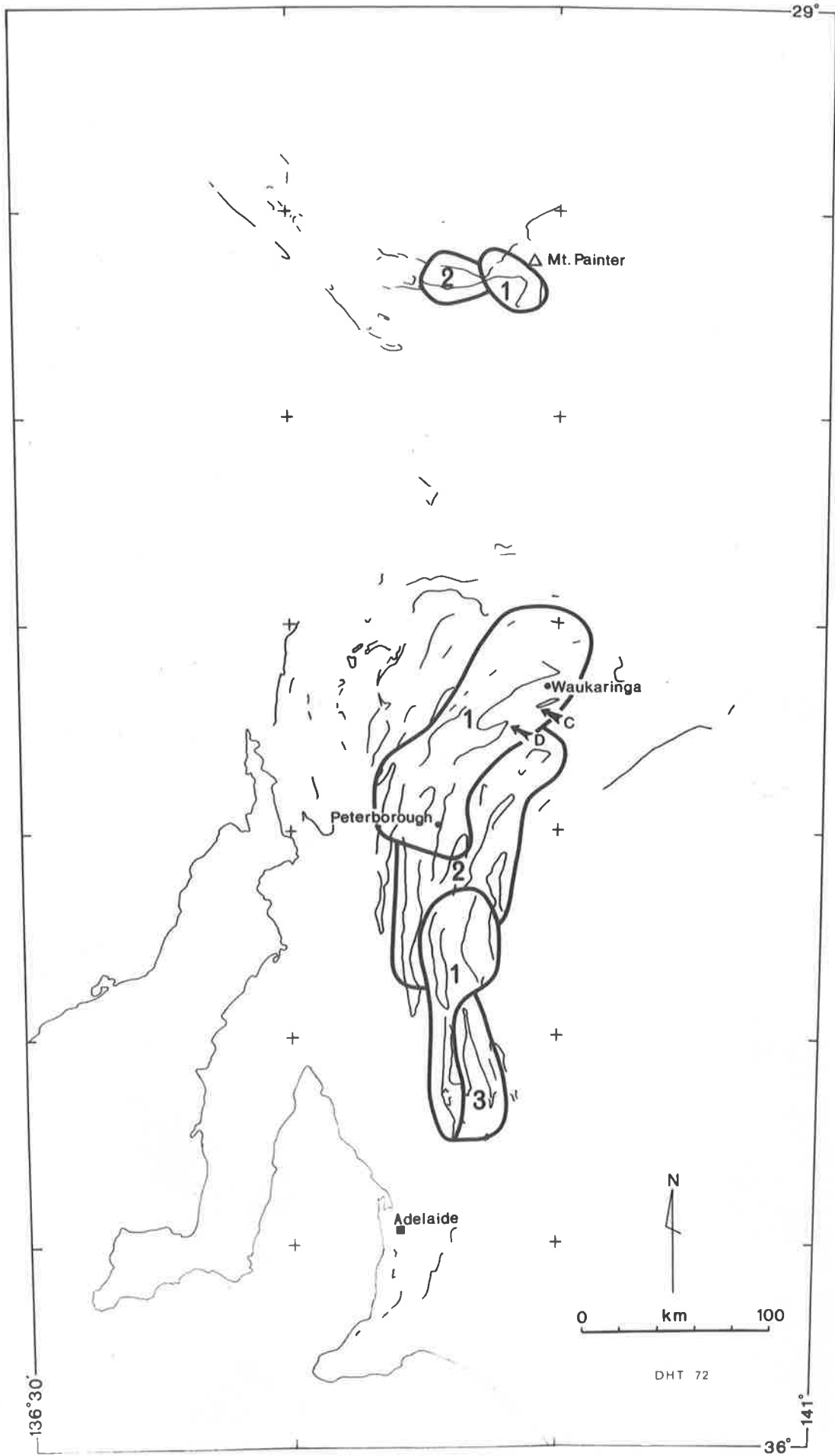


Fig. 5-2

Figure 5.3 : Vertical field ground magnetometer profiles over the anticlinal structures C and D near Waukaringa.

The unit shaded with small circles is the Yudnamutana Subgroup (Appila Tillite). The grey shaded unit corresponds with the Lower Tapley Hill magnetic bed at a depth of 100-200 m below the surface. Note the change of anomaly sign around structures.

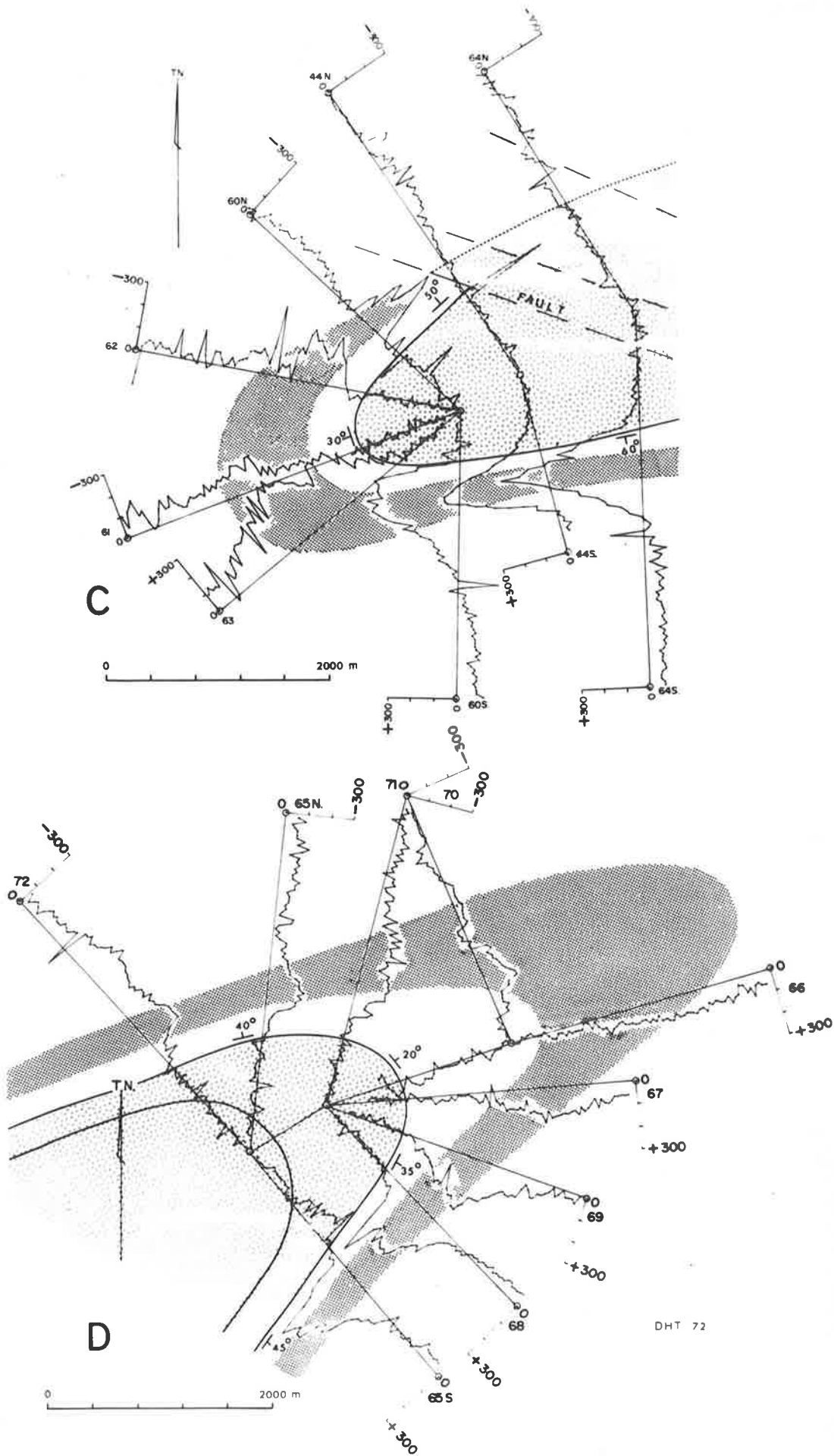


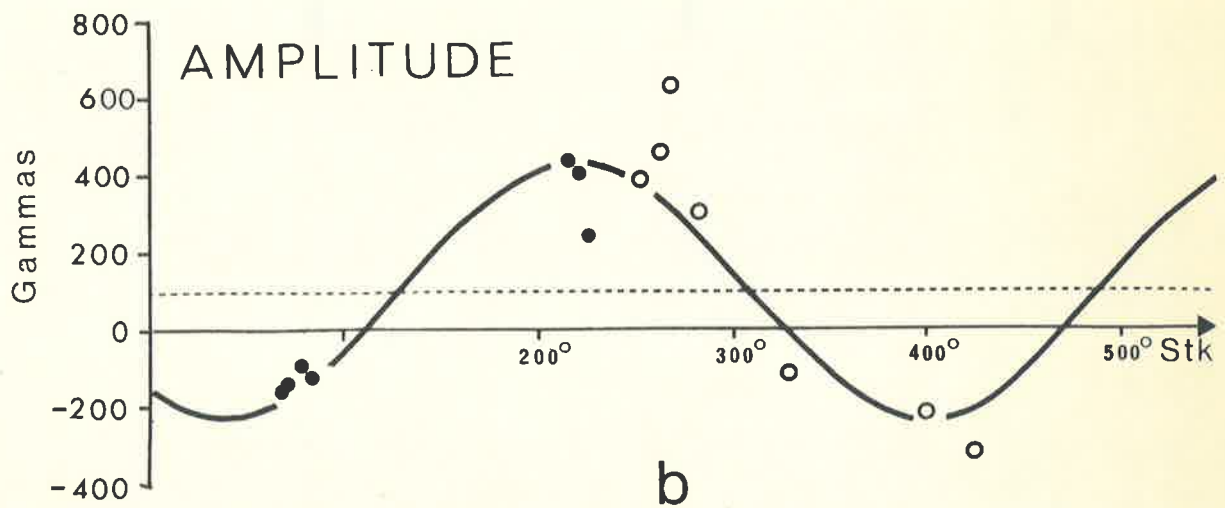
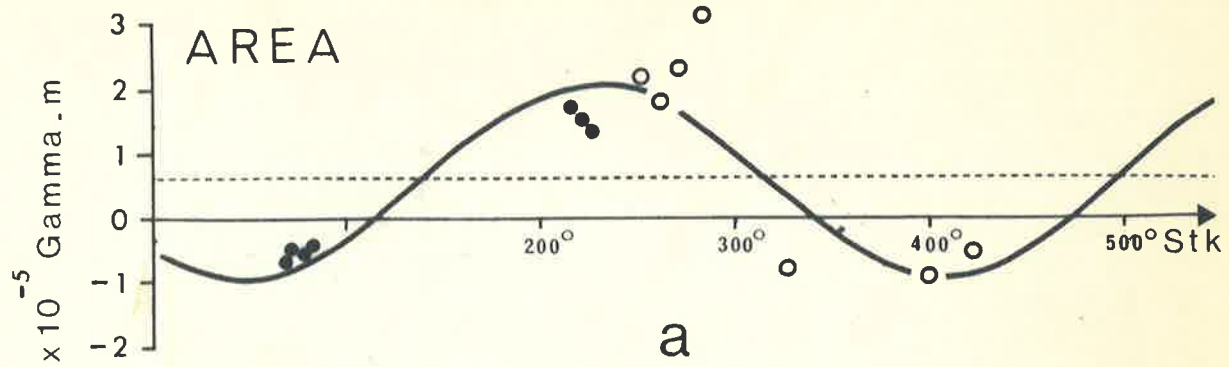
Fig. 5-3

Figure 5.4 : Amplitudes and areas under anomalies attributable to the Lower Tapley Hill magnetic bed, plotted against strike direction.

Solid points are for data from Area D, circles are for data from Area C.

The convention for strike is as follows:

when standing directly over the interpreted position of the Lower Tapley Hill magnetic bed, facing down dip, the strike is measured east of north to the direction of the right hand. On the figure, strikes have been plotted beyond  $360^{\circ}$  to group the data from each area. The dashed line gives the zero level for the sinusoids fitted to the data. See text of Chapter 5 for further discussion.



DHT '72

Fig. 5 - 4



Figure 6.1 : Magnetic features on ORROROC which are not caused by magnetic beds within the Adelaide System sediments.

Legend - geology

- A Cainozoic sediments
- B Adelaidean sediments
- C Diapiric breccia

Legend - magnetics

- D Linear magnetic feature (maximum amplitude shown in gammas)
- E Localized magnetic feature (amplitude in gammas)
- F Group of magnetic anomalies (average amplitude in gammas)
- G Non-magnetic zone

Diapirs with strong associated aeromagnetic anomalies are shown thus: Baratta (100). Arrowed localities 1 and 2 are discussed in the text of Chapter 6. Magnetic features recognized previously by Bennett (1968) are indicated with a B; features recognized by Tipper and Finney (1966) are indicated with a T.

Source of data - study of aeromagnetic flight charts and 1:47,520 scale geological maps of ORROROC.

Fig. 6-1

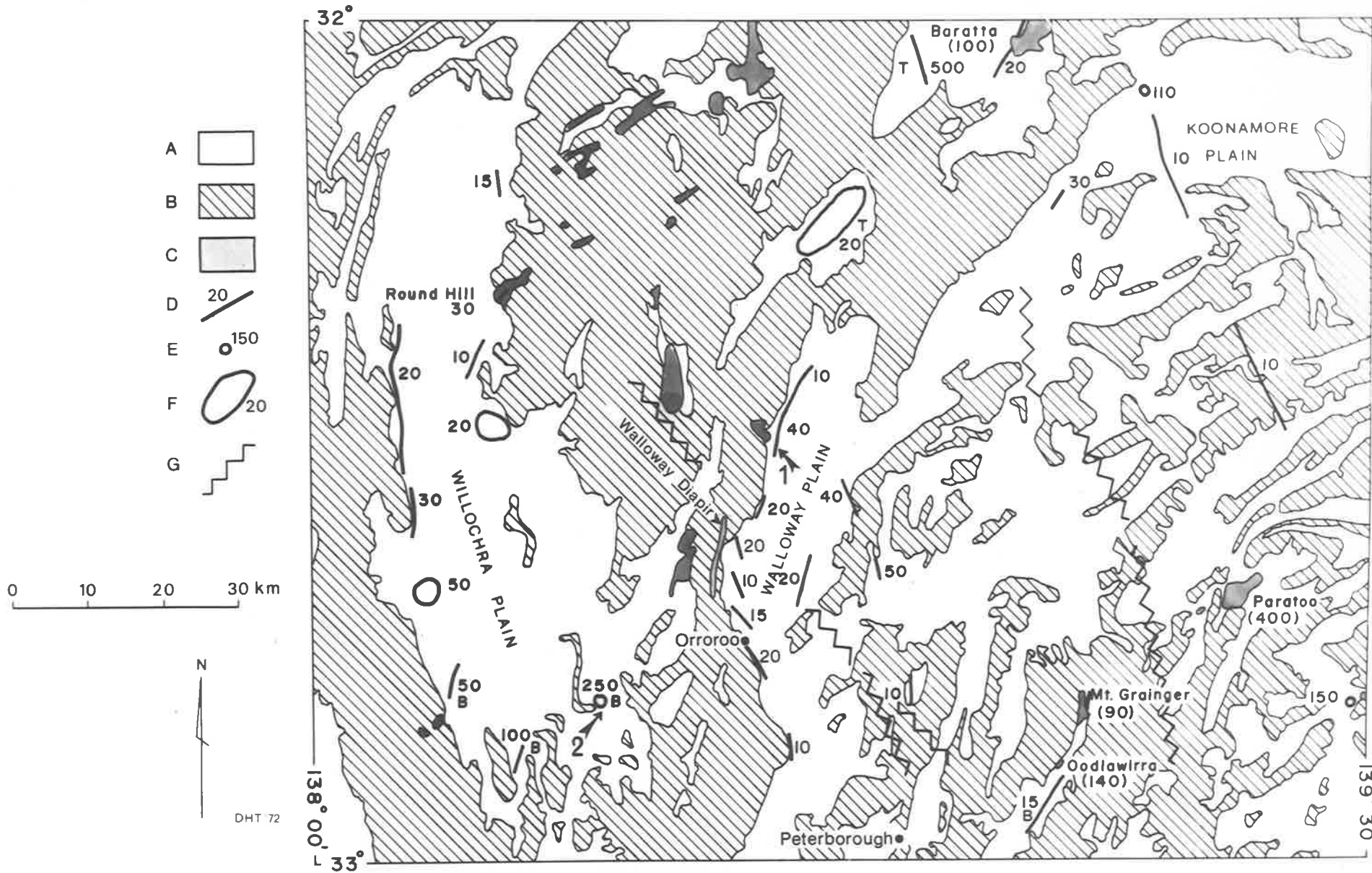


Figure 6.2 : Interpreted linear cross cutting magnetic features near the town of Orroroo, which are unlikely to be caused by magnetic beds within Adelaide System sediments. Linear features attributable to the Lower Tapley Hill magnetic bed are also shown.

Legend - geology

Unshaded unit - Quaternary sediments  
Grey unit - Tapley Hill Formation  
Circled unit - Yudnamutana Subgroup (Appila Tillite)

Legend - topography

Narrow dashed lines - roads  
Heavy dashed line - railway line

Legend - magnetics

The peaks of anomalies are indicated by arrows (amplitudes in gammas). Linear features are indicated by heavy lines.

Source of data - aeromagnetic flight charts and 1:47,520 scale geological maps.

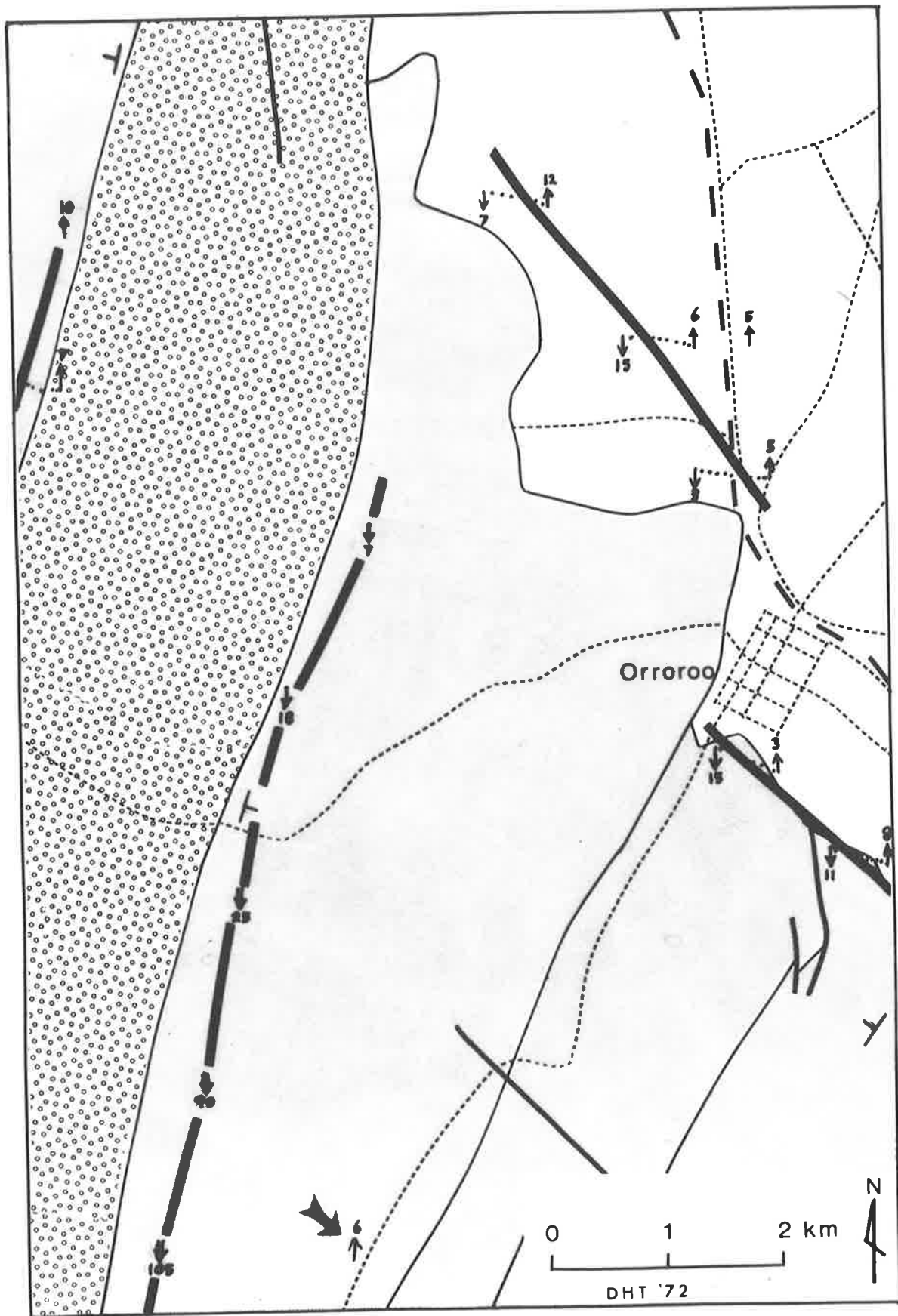


Fig. 6-2

Figure 6.3 : Positions and amplitudes (gammas) of aeromagnetic anomalies over areas of diapiric breccia on ORROROO.

The areas of breccia are numbered for reference in the text of Chapter 6.

Source of data - aeromagnetic flight charts and 1:47,520 scale geological maps.

Fig. 6-3

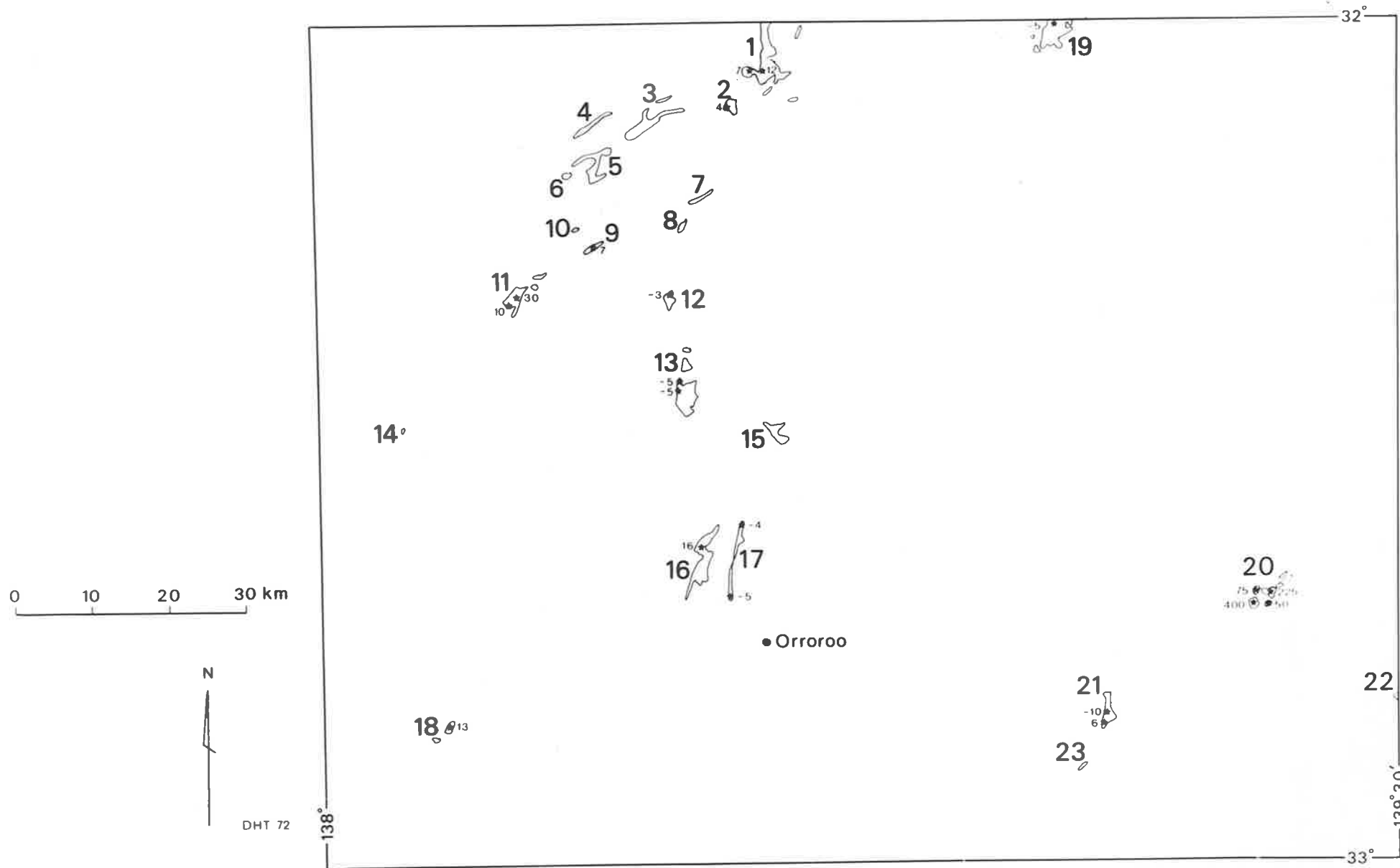


Figure 6.4 : Interpretation of magnetic anomalies near Hesso, attributed to a member of the Eyre Peninsula dyke swarm.

Legend

1. Cainozoic sediments
2. Flat lying Adelaide System sediments
3. Geological boundary
4. Creek
5. Road
6. Railway line
7. Zone of magnetic material indicated by interpretation of aeromagnetics
8. Ground magnetometer traverse
9. Magnetic dyke indicated by interpretation of vertical field ground profiles

Source of data - SADM geological maps and aeromagnetic contour maps; field work in the area.

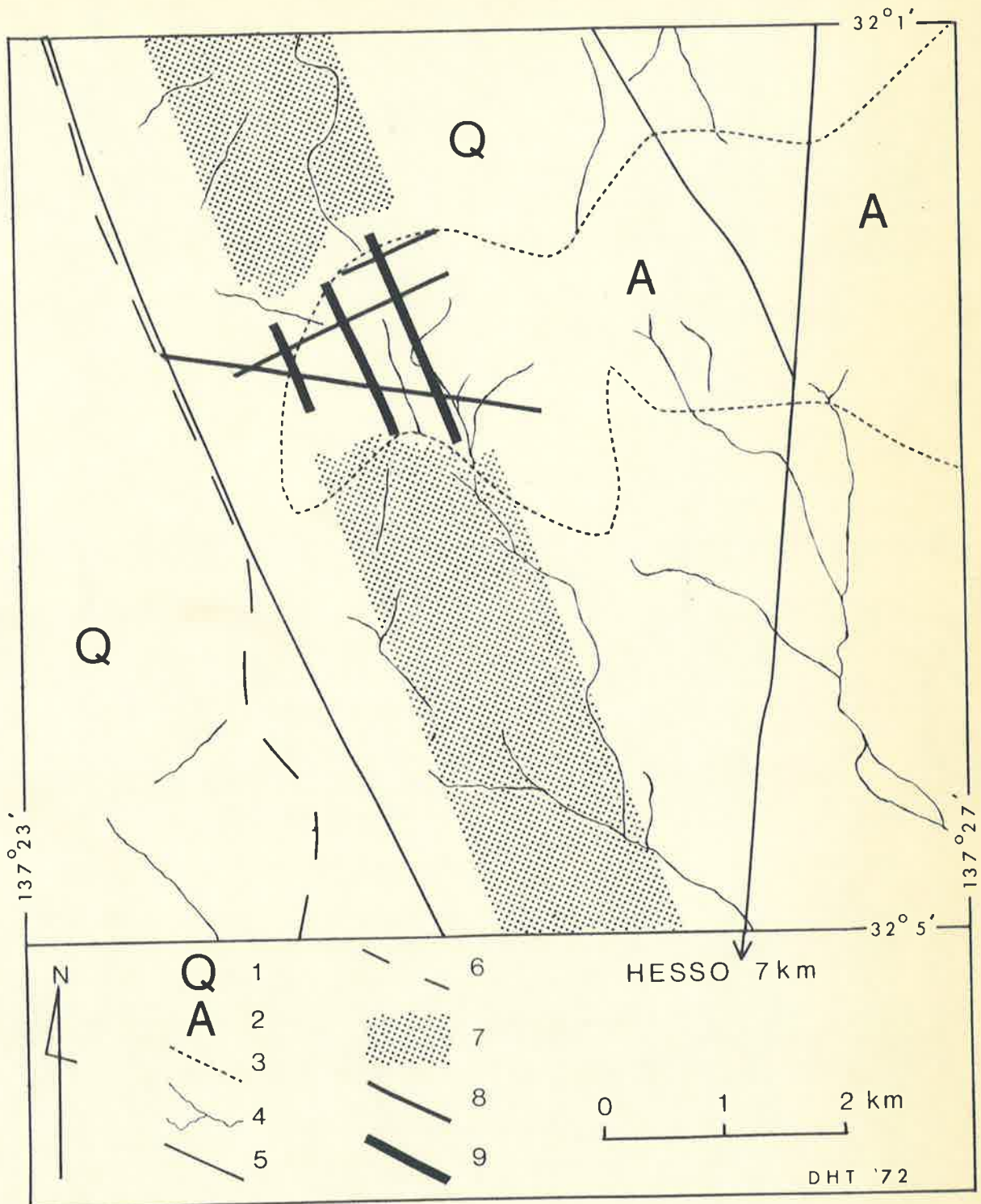


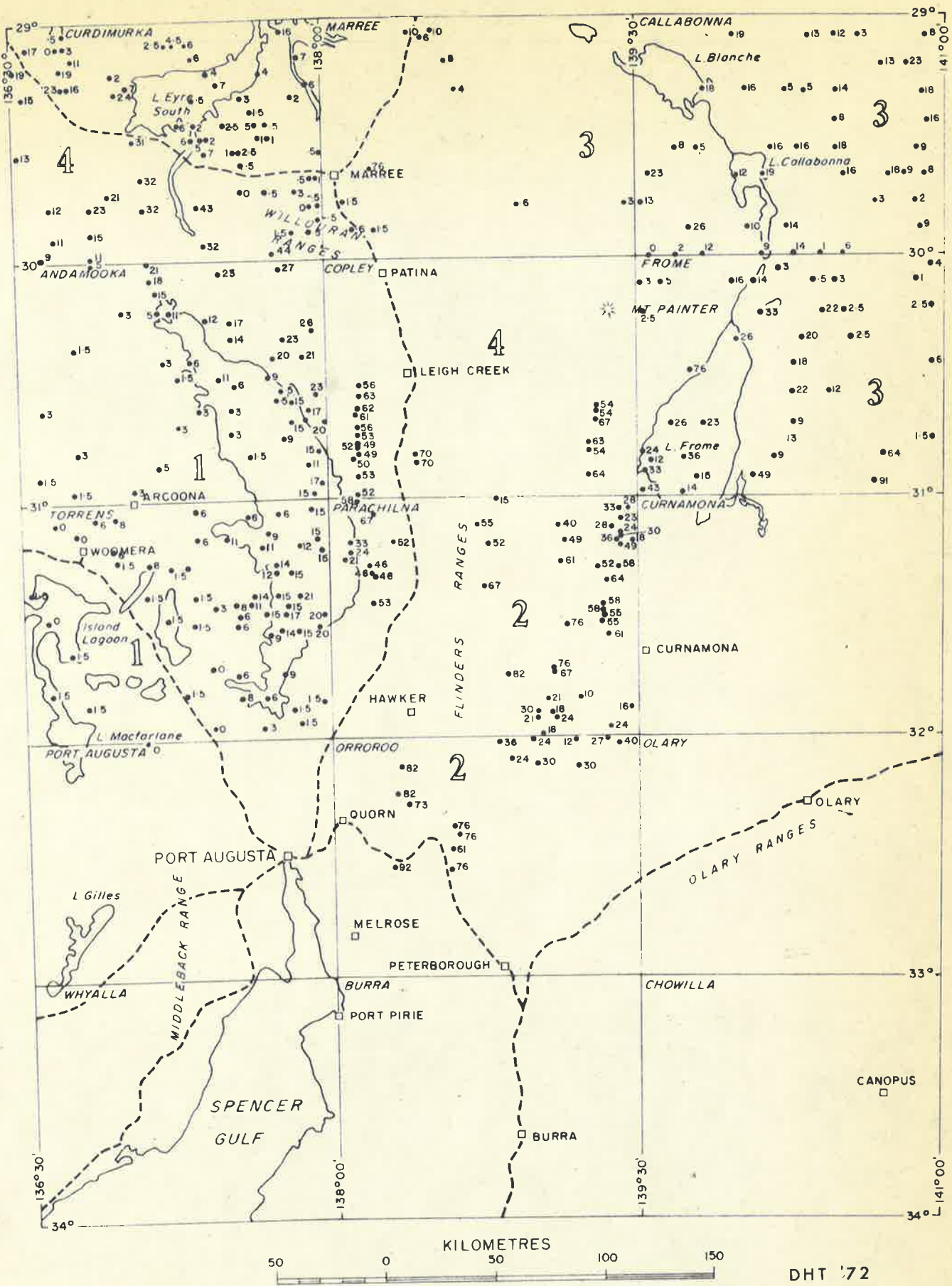
Fig. 6 - 4



Figure 7.1 : Interpreted depths to magnetic sources in the northern part of the Adelaide Geosyncline.

Depth estimates are shown in hundreds of metres.

Source of data - BMR Records (depths originally scaled in feet).



DEPTHS SHOWN ARE IN HUNDREDS OF METRES  
 ESTIMATES FROM BMR RECORDS : 1 1964/31  
 2 1966/126  
 3 1965/1  
 4 1966/224

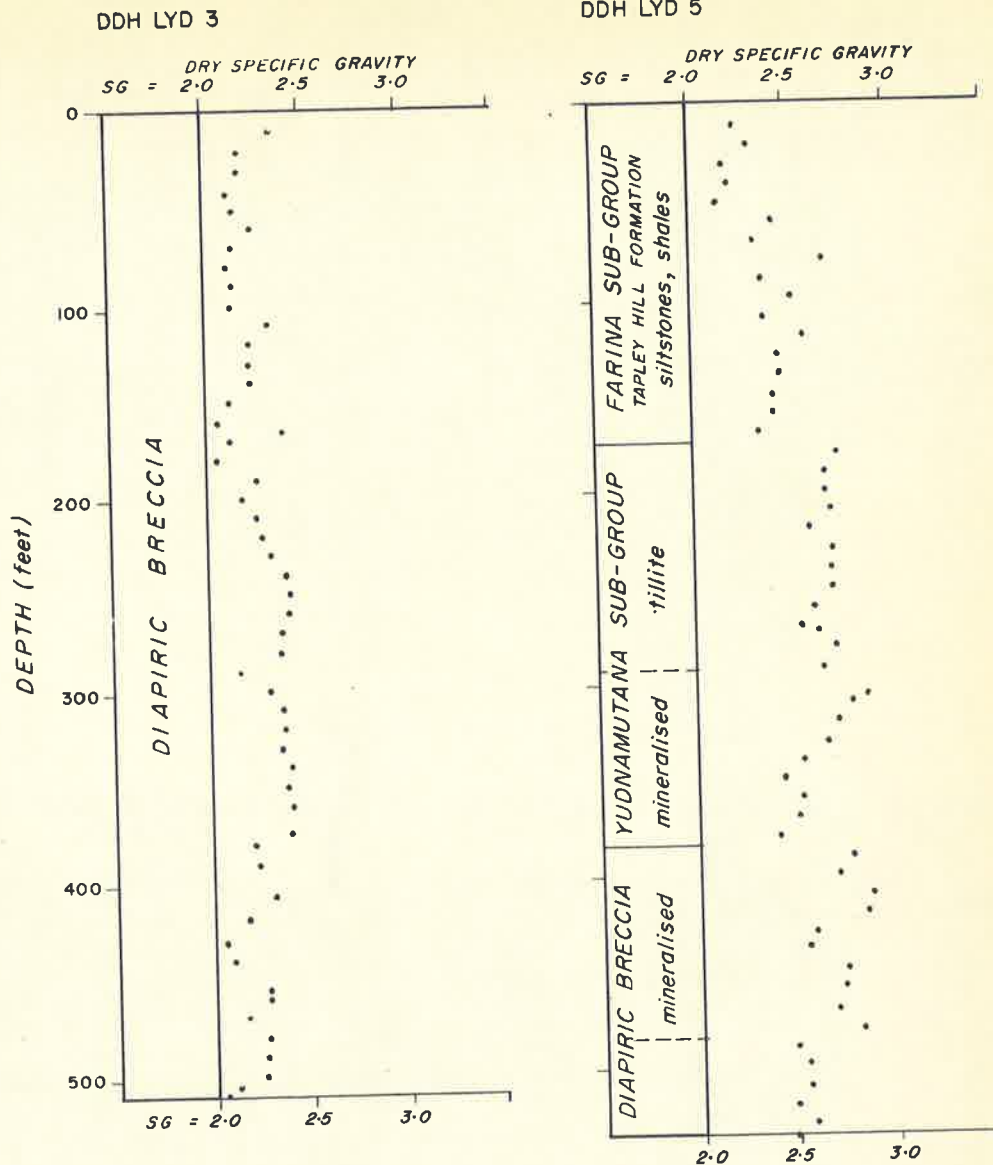
DHT '72

INTERPRETED DEPTH TO MAGNETIC SOURCES

Fig. 7-1

Figure 8.1 : Dry specific gravity logs for drill core from the  
Lyndhurst Diapir.

Source of data - SADM general drilling program, 1966.



Core sampled at 10ft intervals. Specimens of approximately 40g.  
Specific gravity by Archimedes method.

After South Australian Department of Mines general drilling programme 1966

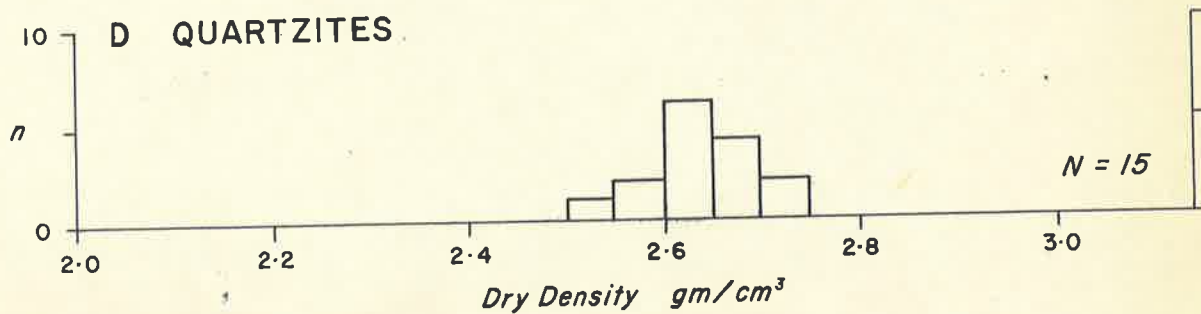
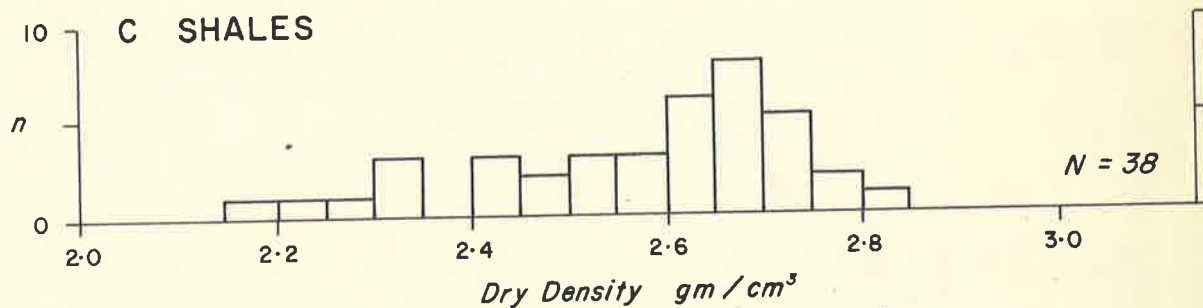
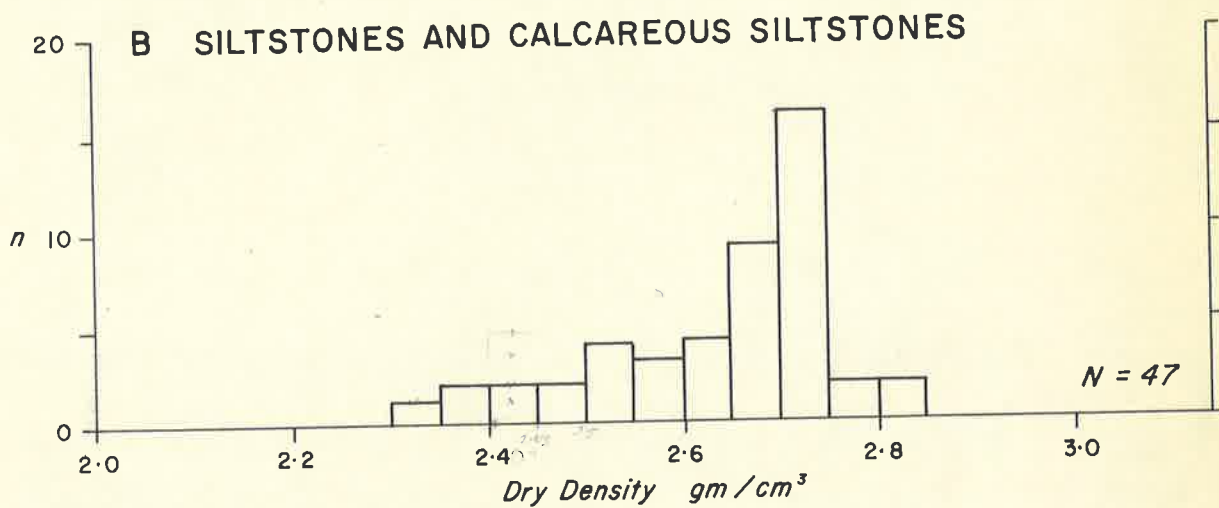
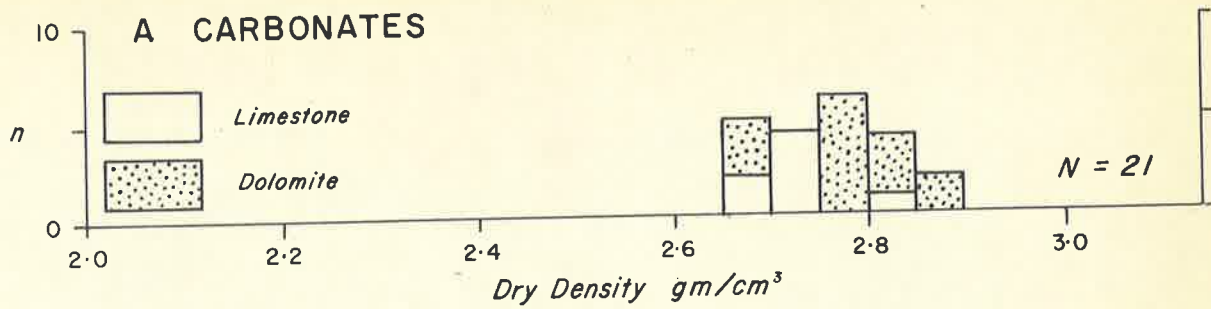
## LYNDHURST DIAPIR

### DRY SPECIFIC GRAVITY LOGS

DHT '72

Fig. 8-1

Figure 8.2 : Frequency histograms of dry density measurements  
on Adelaide System sediments.



DENSITY OF ADELAIDEAN SEDIMENTS

DHT '72

Fig. 8 - 2

Figure 8.3 : Density profiles across the Adelaide Geosyncline.  
(pocket)

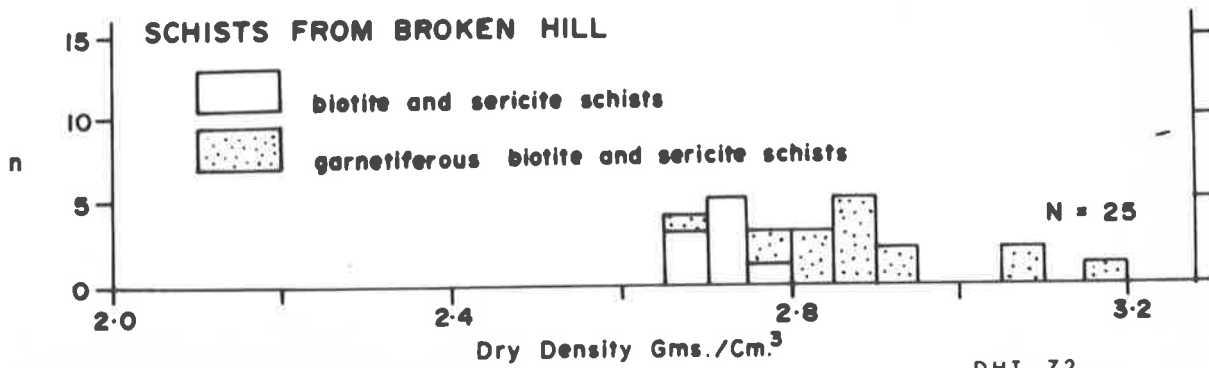
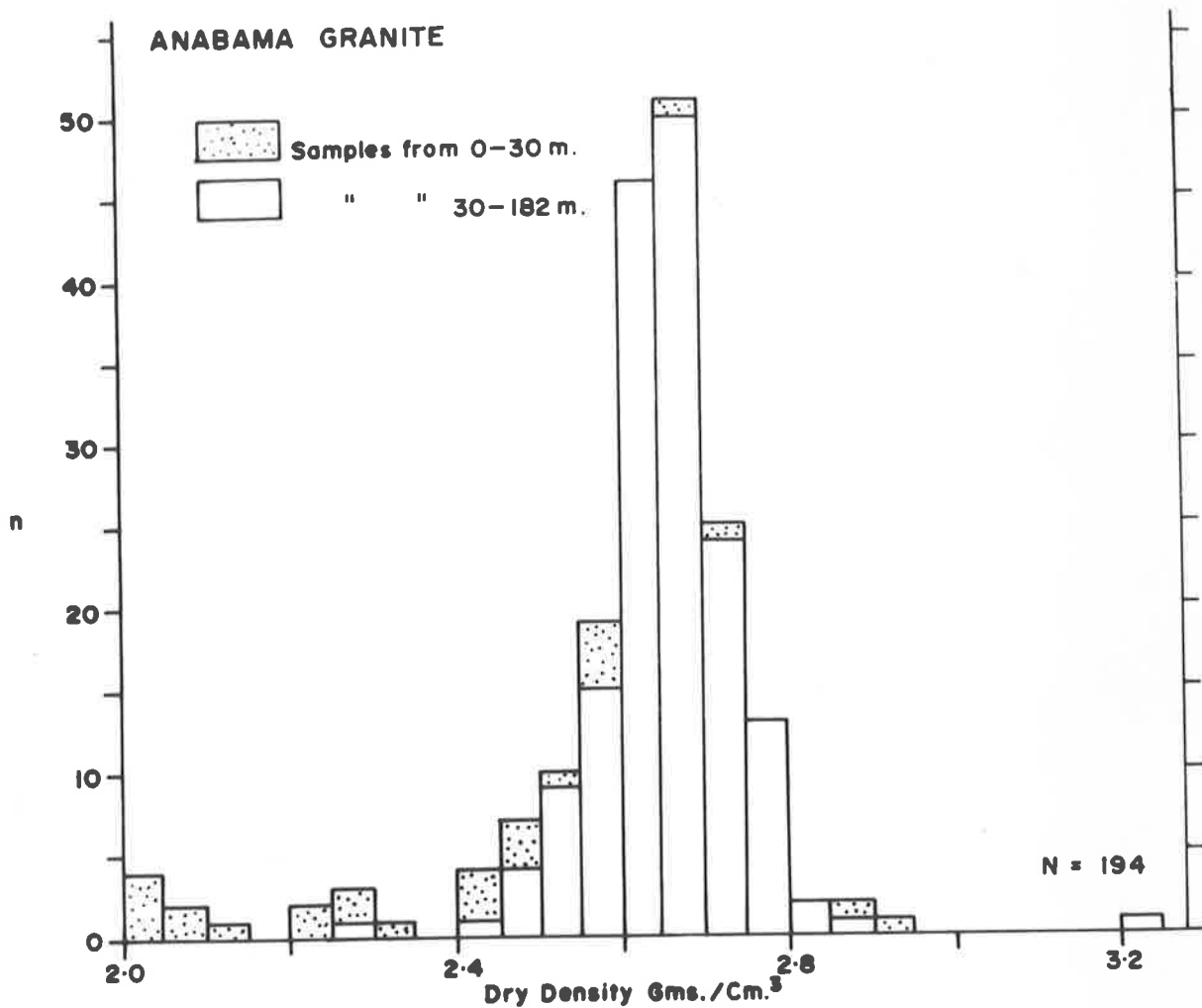
The Bouguer densities used for the calculation of Bouguer anomalies are shown on Profile A. The dashed line below each group of density profiles shows the topography as recorded at the gravity stations.

Source of data - original elevations and Bouguer anomaly values from BMR maps (Bouguer density  $2.67 \text{ g/cm}^3$ ).

Figure 8.4 : Frequency histograms of dry density measurements on drill core from the Anabama Granite, and schists in the Broken Hill area.

Source of data - original measurements on schists provided by Broken Hill South Pty. Ltd.

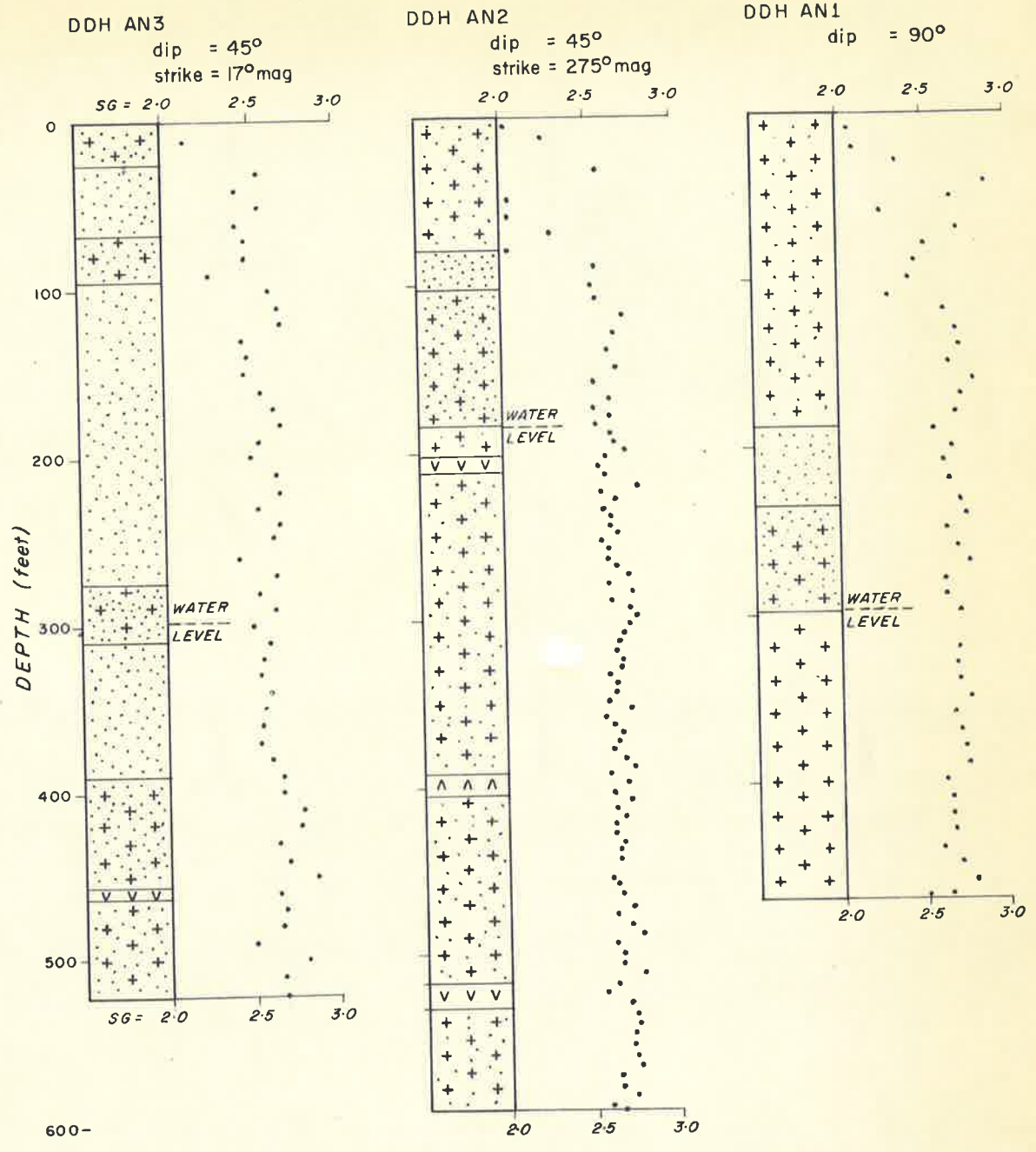




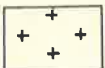

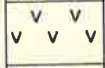
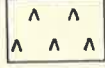
DHT 72

Fig. 8 - 4

Figure 8.5 : Dry specific gravity logs for drill core from the  
Anabama Granite



LEGEND

-  Granite
-  Greisen
-  Feldspar porphyry
-  Quartz biotite porphyry

*Lithology generalized after A.J.Hosking(1970)*  
*Specific gravity by Archimedes method. Measurements by D.H.Tucker using regular samples of split core (weight approximately 150 grammes)*

ANABAMA GRANITE  
 ANABAMA HILL SA

DHT '72

DRY SPECIFIC GRAVITY LOGS

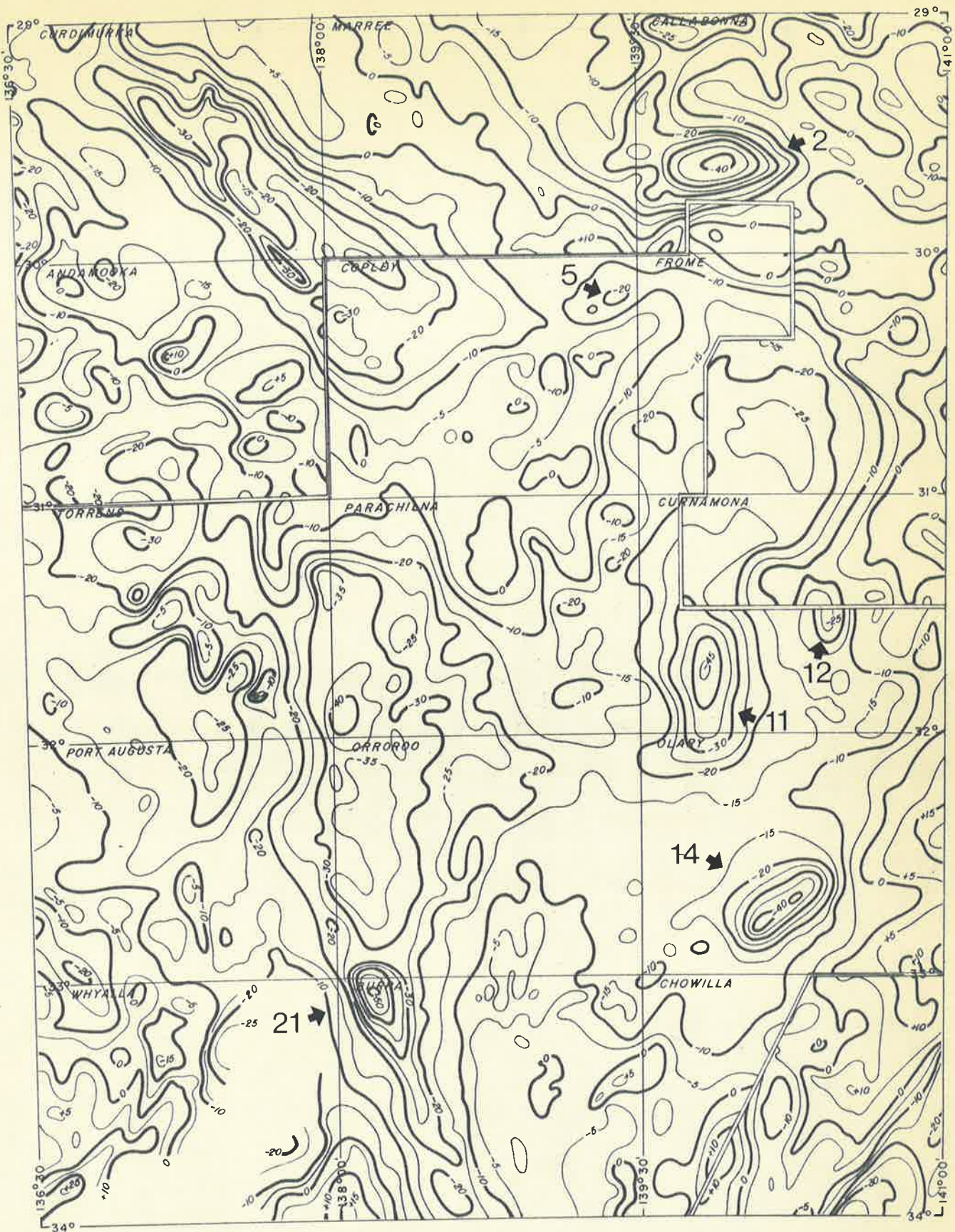
Fig.-8-5

Figure 9.1 : Bouguer anomalies over the northern part of the Adelaide Geosyncline.

The contour interval is 5 milligals. Anomalies arrowed and numbered are discussed in the text of Chapter 9.

Source of map - BMR.





KILOMETRES



DHT '72

BOUGUER DENSITY in  $g/cm^3$

1.9	
2.67	
2.2	

BOUGUER ANOMALIES

Fig. 9-1

Figure 9.2 : Bouguer anomaly profiles and generalized geological cross sections in areas of granitic rocks on the eastern side of the Adelaide Geosyncline.

The dots are Bouguer anomaly values recorded on adjacent lines of gravity stations. Models were determined to account for the dashed Bouguer anomaly profiles. On diagram B, Profile 2 was used for model studies. In the area of Profile 2, material at the surface consists of Cainozoic sediments. Profile 1 for anomalies on a single line along latitude  $32^{\circ}$  corresponds with the generalized geological cross section.

Source of data - BMR 1:250,000 maps of Bouguer anomalies. The plotted points on sections A and C are for data reduced with a Bouguer density of  $2.67 \text{ g/cm}^3$ ; on diagram B the data were reduced with a Bouguer density of  $2.2 \text{ g/cm}^3$ .

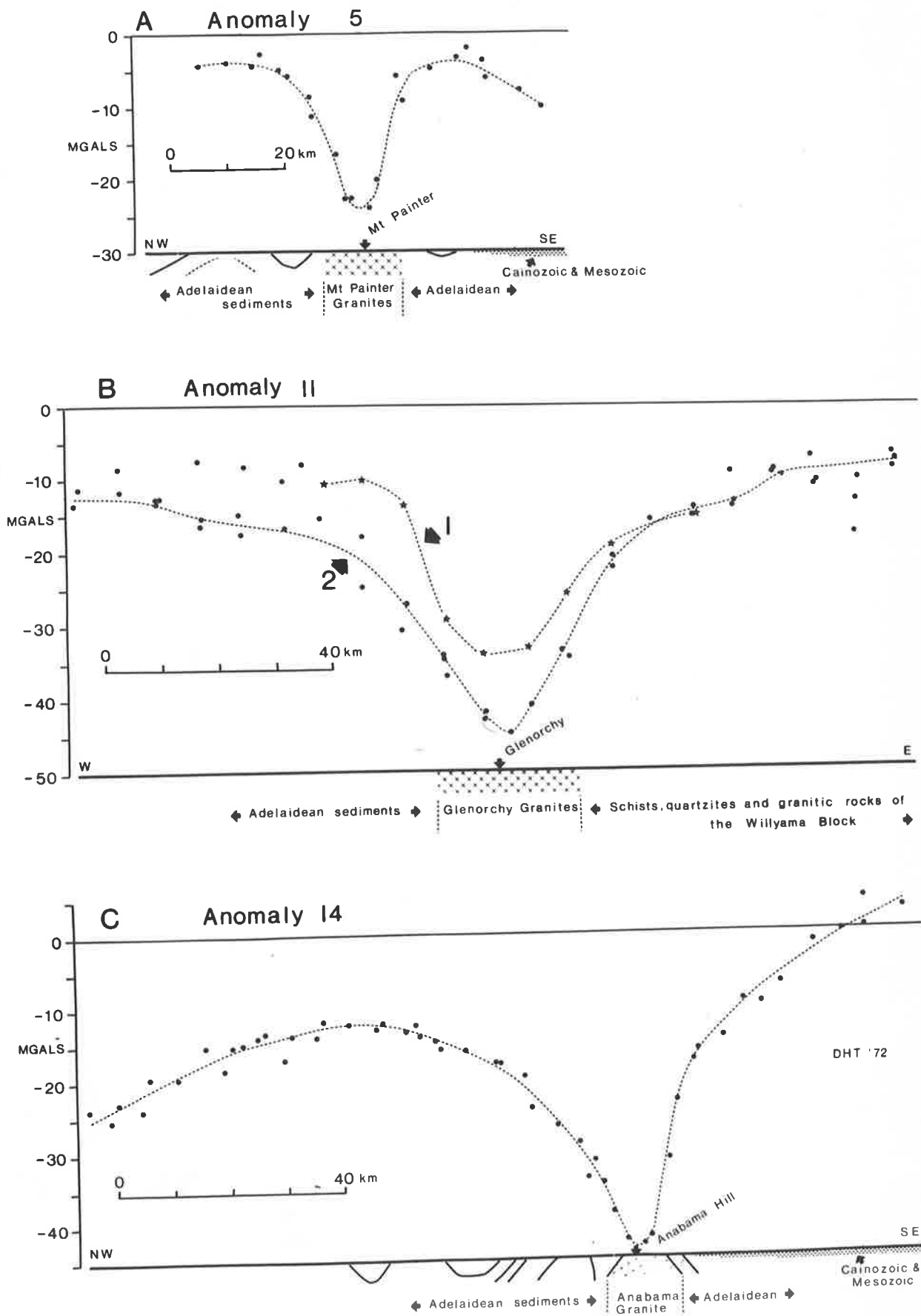


Fig. 9 - 2

Figure 9.3 : Geology and geophysics for the area of the Anabama Granite  
(Bouguer Anomaly 14).

The drill holes shown on the figure were located on Anabama Hill. Anabama Hill is the index point for the geophysical models shown on Figures 9.4 and 9.5. The distance scales on Figures 9.3, 9.4 and 9.5 are the same.

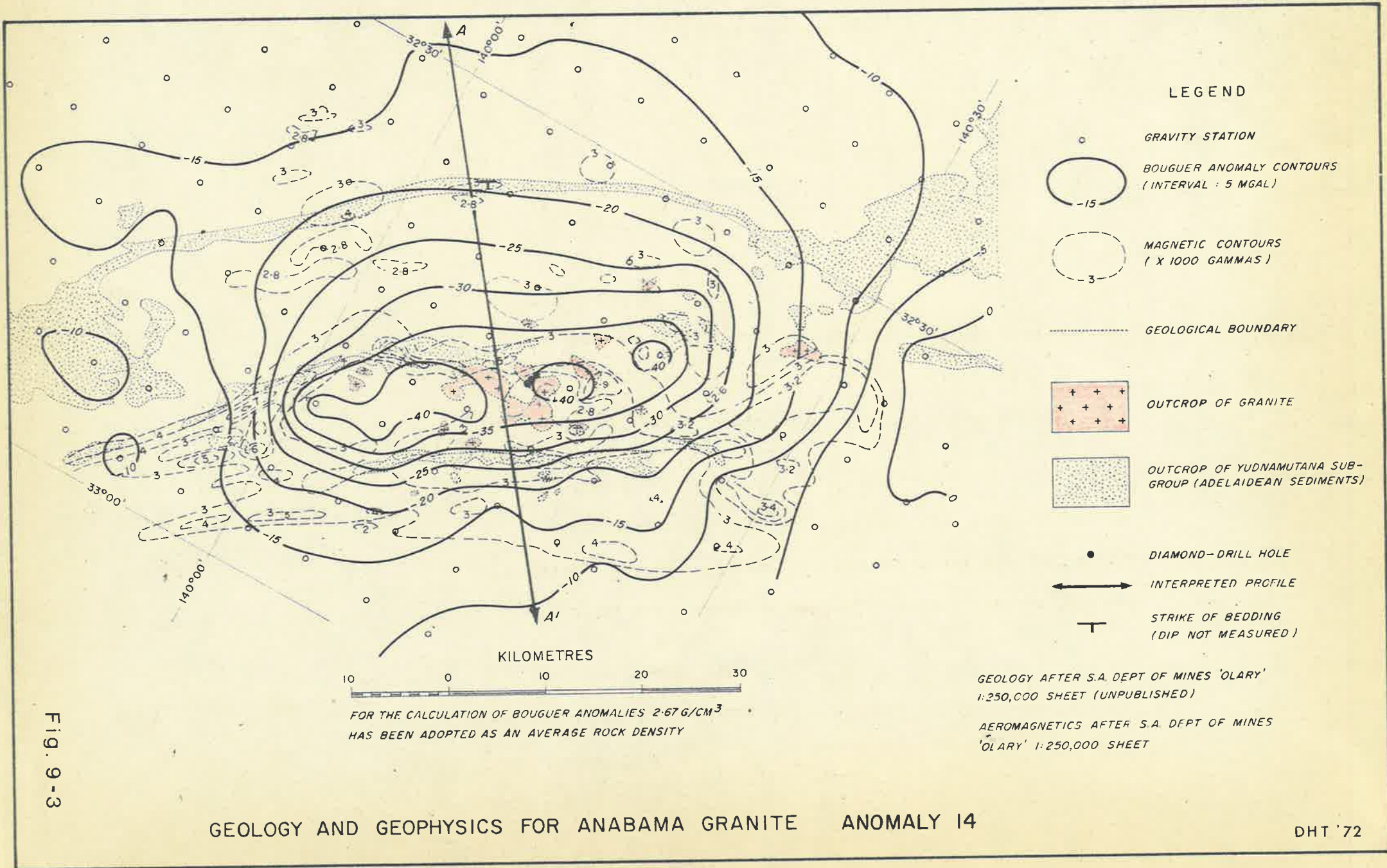
Source of data - geology and magnetics - see figure;

Bouguer anomaly contours from the BMR map of OLARY.



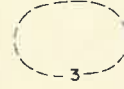
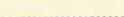


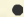


The Bouguer density used for reduction of the data was

2.67 g/cm<sup>3</sup>.





LEGEND

-  GRAVITY STATION
-  BOUGUER ANOMALY CONTOURS  
(INTERVAL : 5 MGAL)
-  MAGNETIC CONTOURS  
( X 1000 GAMMAS )
-  GEOLOGICAL BOUNDARY
-  OUTCROP OF GRANITE
-  OUTCROP OF YUDNAMUTANA SUB-GROUP  
(ADELAIDEAN SEDIMENTS)
-  DIAMOND-DRILL HOLE
-  INTERPRETED PROFILE
-  STRIKE OF BEDDING  
(DIP NOT MEASURED)

GEOLOGY AFTER S.A. DEPT OF MINES 'OLARY'  
1:250,000 SHEET (UNPUBLISHED)

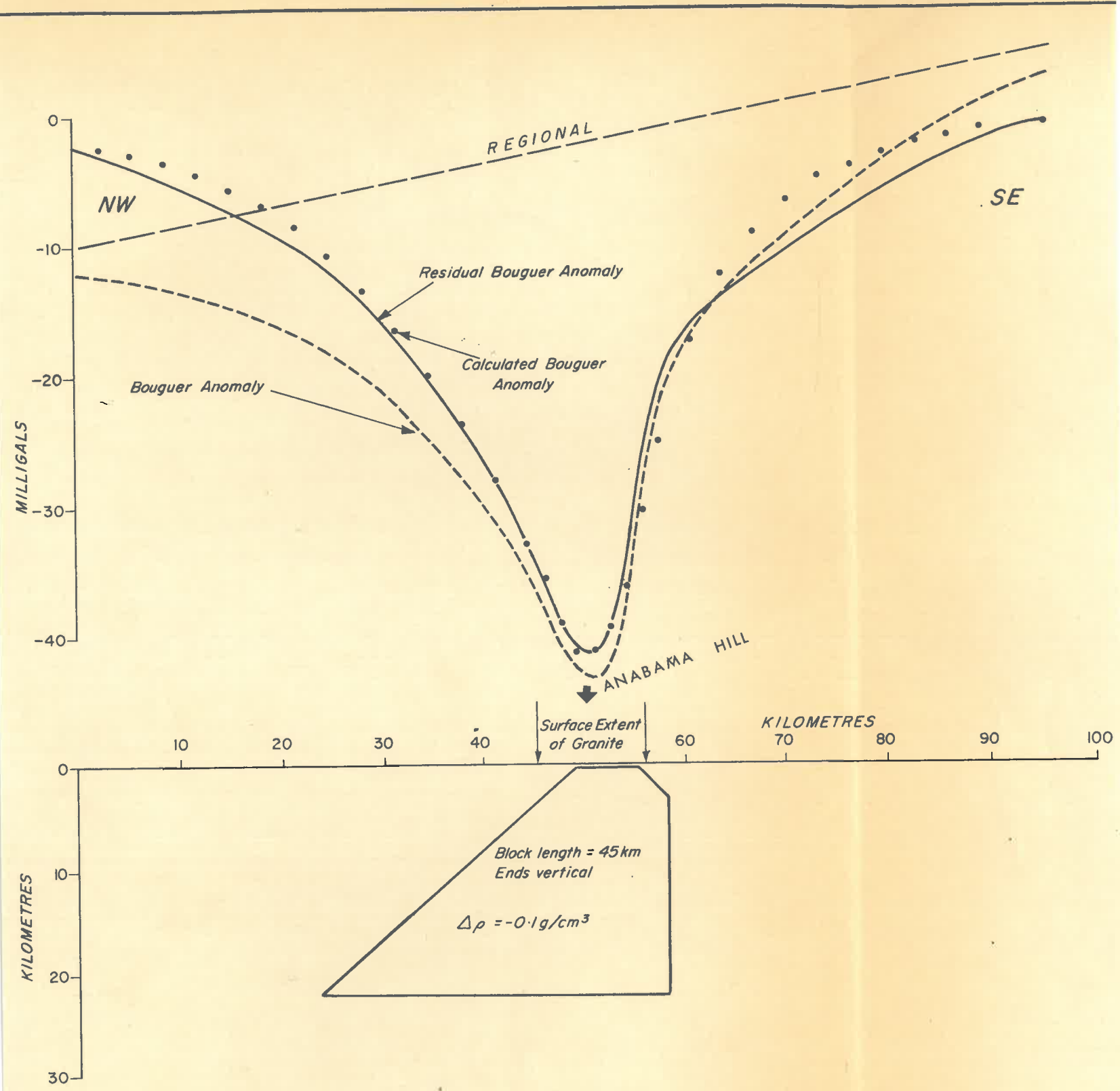
AEROMAGNETICS AFTER S.A. DEPT OF MINES  
'OLARY' 1:250,000 SHEET

KILOMETRES  
10 0 10 20 30

FOR THE CALCULATION OF BOUGUER ANOMALIES 2.67 G/CM<sup>3</sup>  
HAS BEEN ADOPTED AS AN AVERAGE ROCK DENSITY

Fig. 9-3

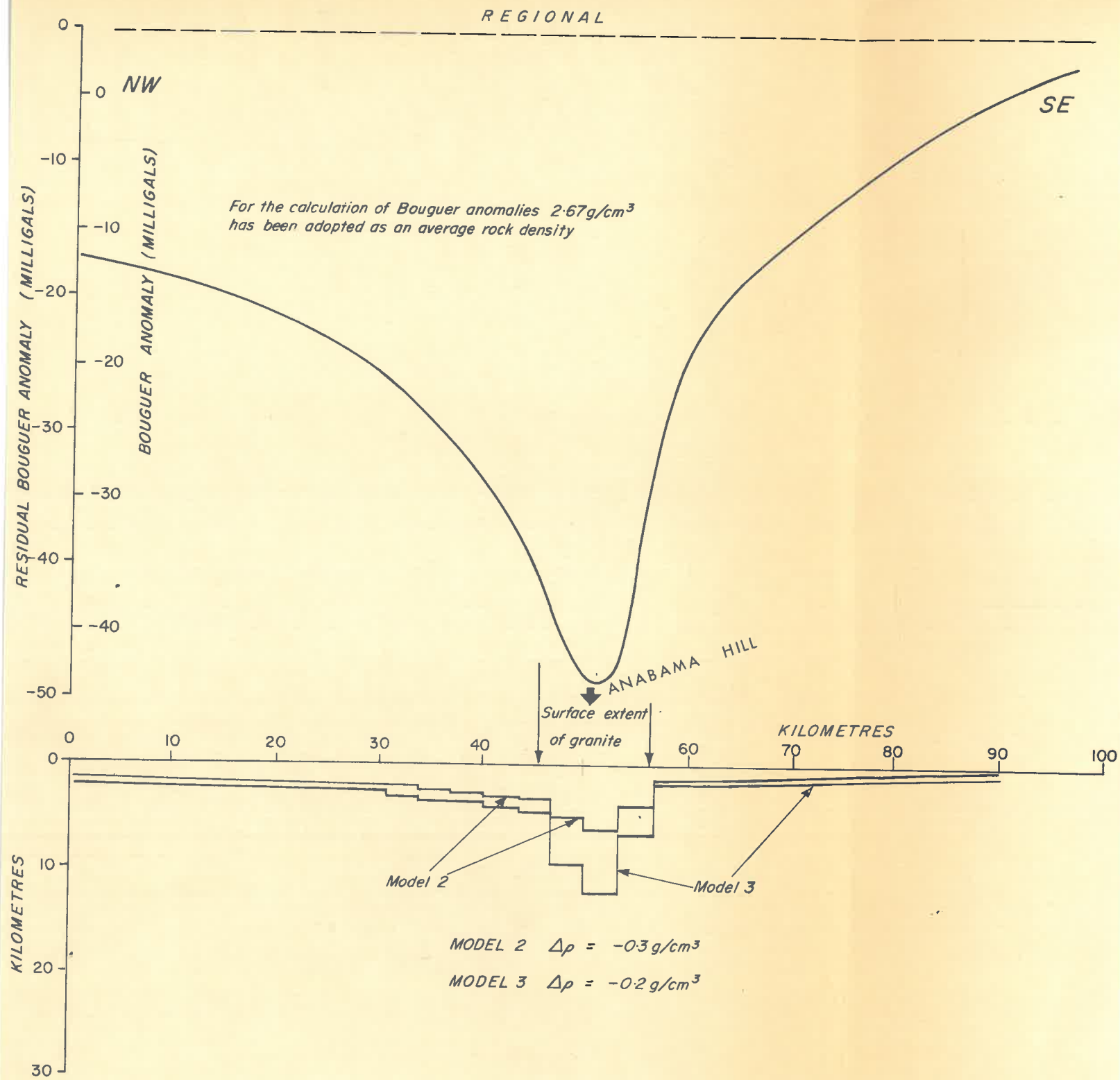
GEOLOGY AND GEOPHYSICS FOR ANABAMA GRANITE ANOMALY 14



GEOPHYSICAL MODEL 1 FOR ANOMALY 14

DHT'72

Fig. 9-4



GEOPHYSICAL MODELS 2 & 3 FOR ANOMALY 14

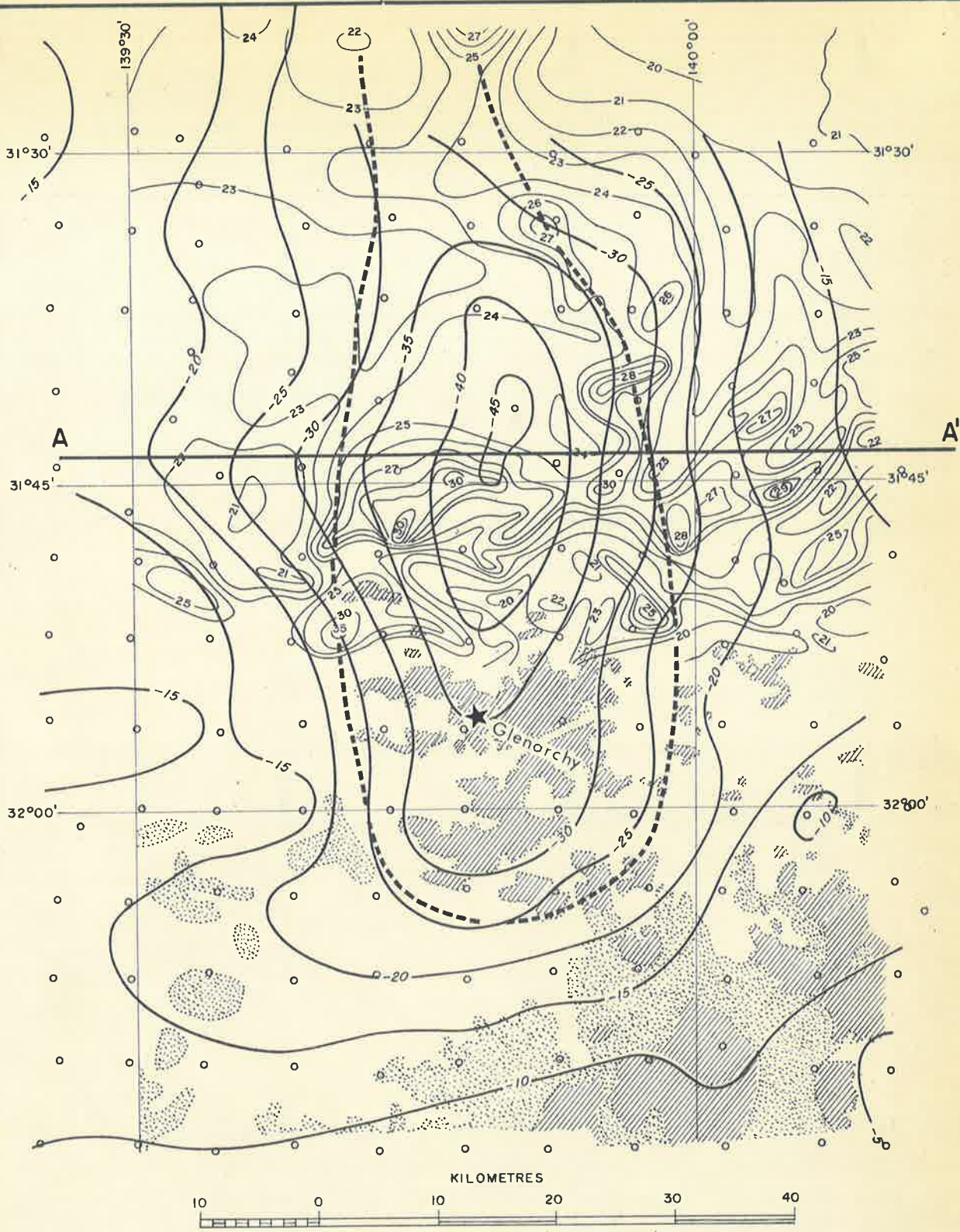
Fig. 9-5




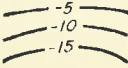


Figure 9.6 : Geology and geophysics for the Gleniorchy area  
(Bouguer Anomaly 11).

Models determined to account for the gravity anomaly  
are shown on Figures 9.7 and 9.8; these are for a  
profile along AA'.

Source of data - geology and magnetics - see figure;  
Bouguer anomaly contours from BMR maps of CURNAMONA  
and FROME. The Bouguer density used for reduction  
of the data for computation of the map was  $2.67 \text{ g/cm}^3$ .





-  RECENT SEDIMENTS
-  ADELAIDEAN SEDIMENTS
-  WILLYAMA COMPLEX
-  BOUGUER GRAVITY CONTOURS
-  AEROMAGNETIC CONTOURS  
( X100 GAMMAS)
-  GRAVITY STATIONS

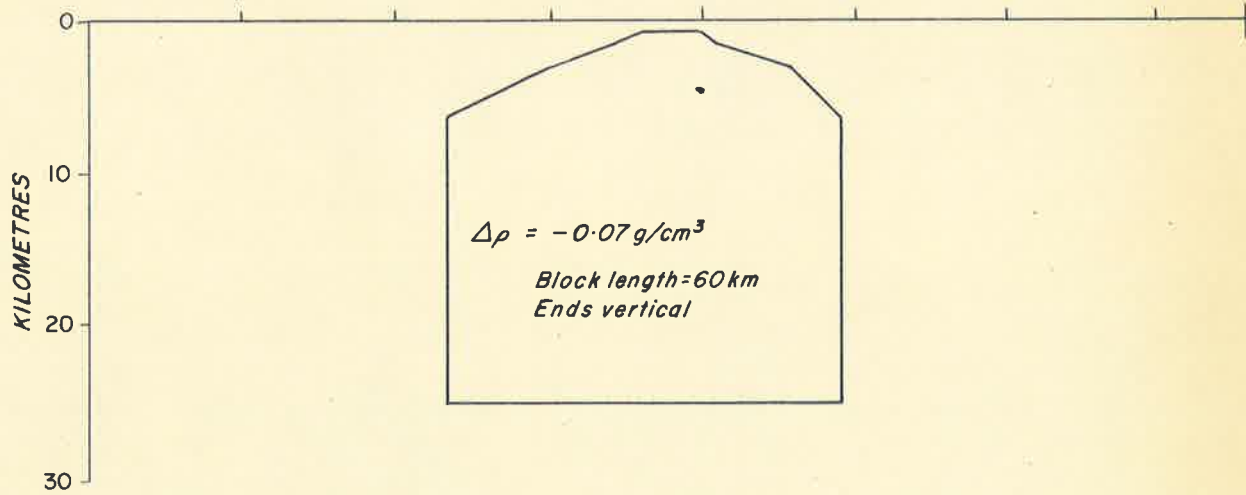
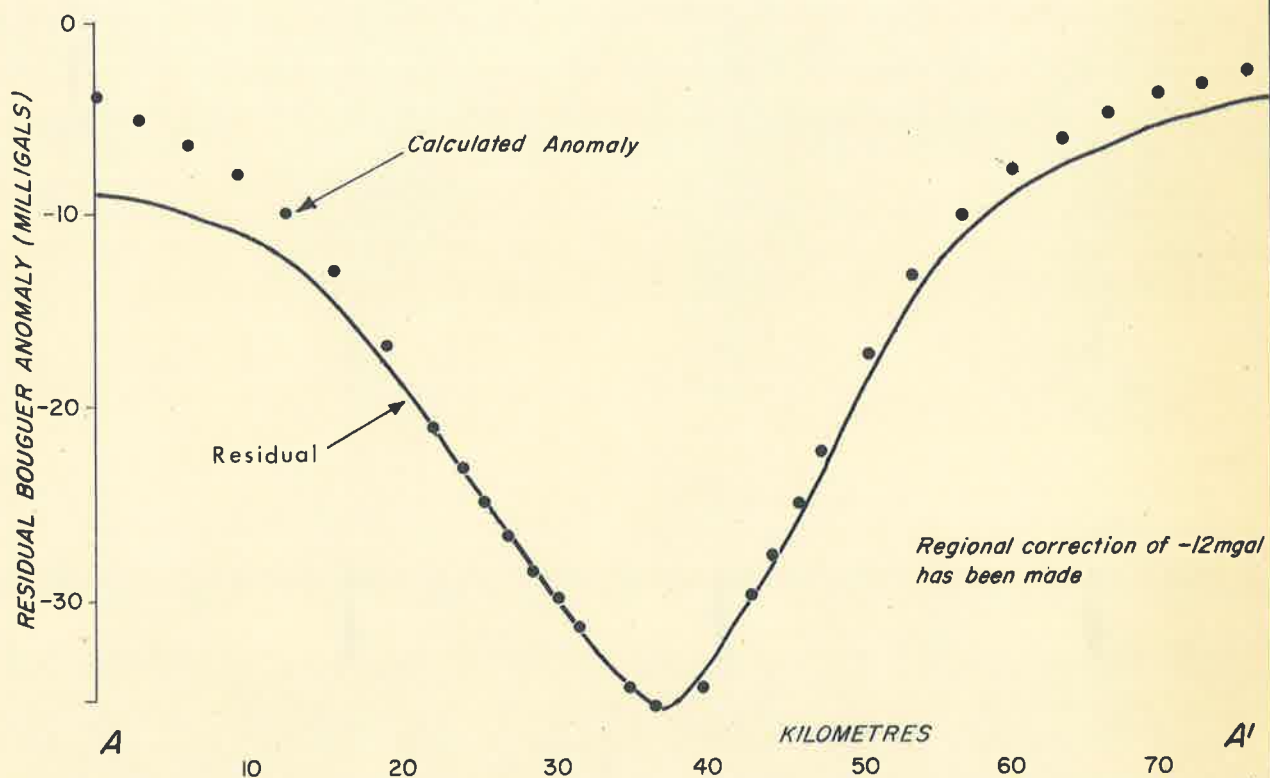
----- BOUNDARY OF LOW DENSITY  
 BLOCK AS INDICATED BY  
 GEOLOGY AND GEOPHYSICS

GEOLOGY GENERALIZED FROM SA DEPT OF MINES PRELIMINARY  
 1:250,000 SHEETS; CURNAMONA AND OLARY.

AEROMAGNETIC CONTOURS FROM SA DEPT OF MINES  
 1:250,000 CONTOUR MAP OF CURNAMONA

**GEOLOGICAL AND GEOPHYSICAL  
 SKETCH MAP OF AREA COVERING  
 ANOMALY 11**

Fig. 9-6



MODEL 1 ANOMALY 11

DHT '72

Fig. 9-7

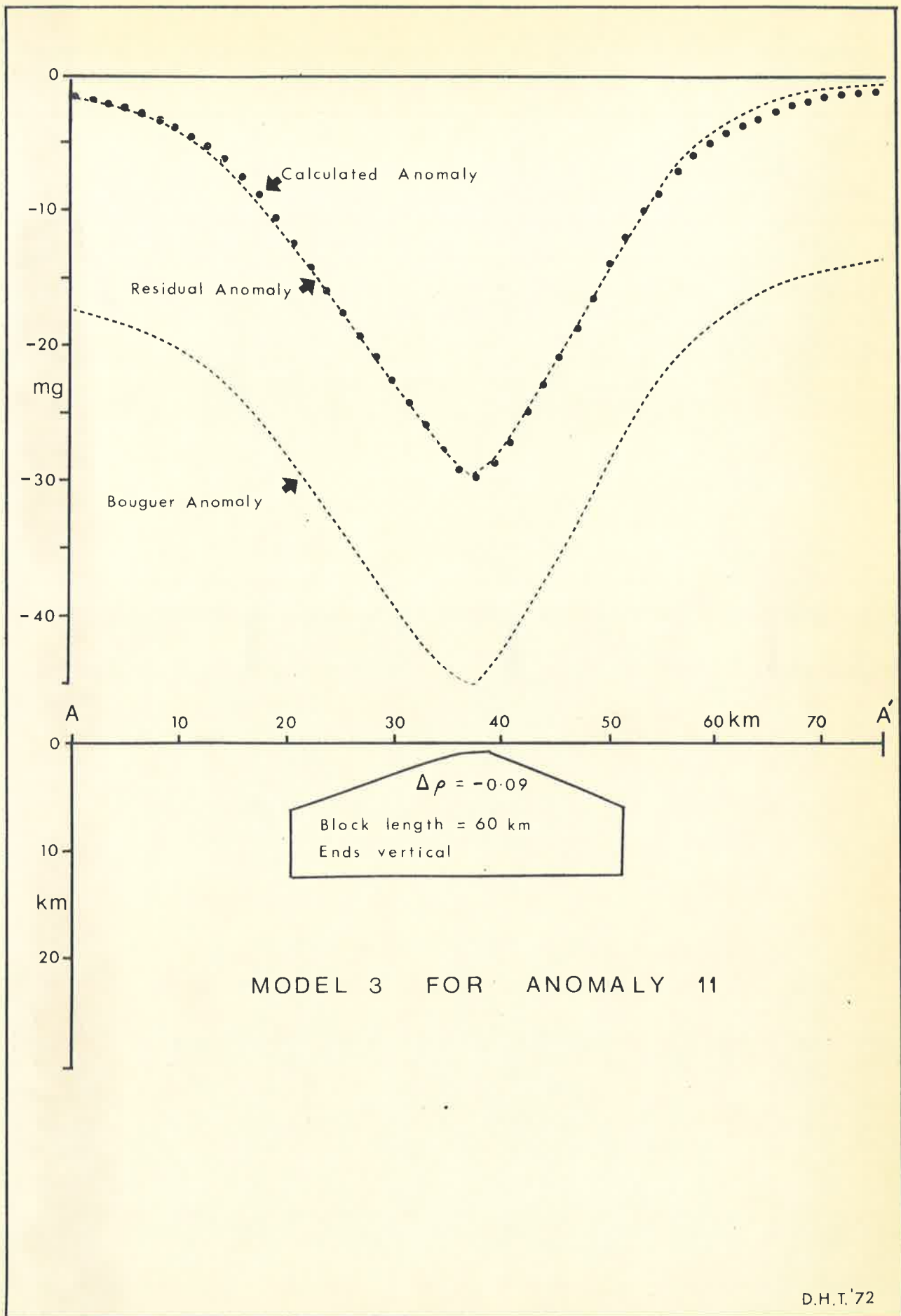
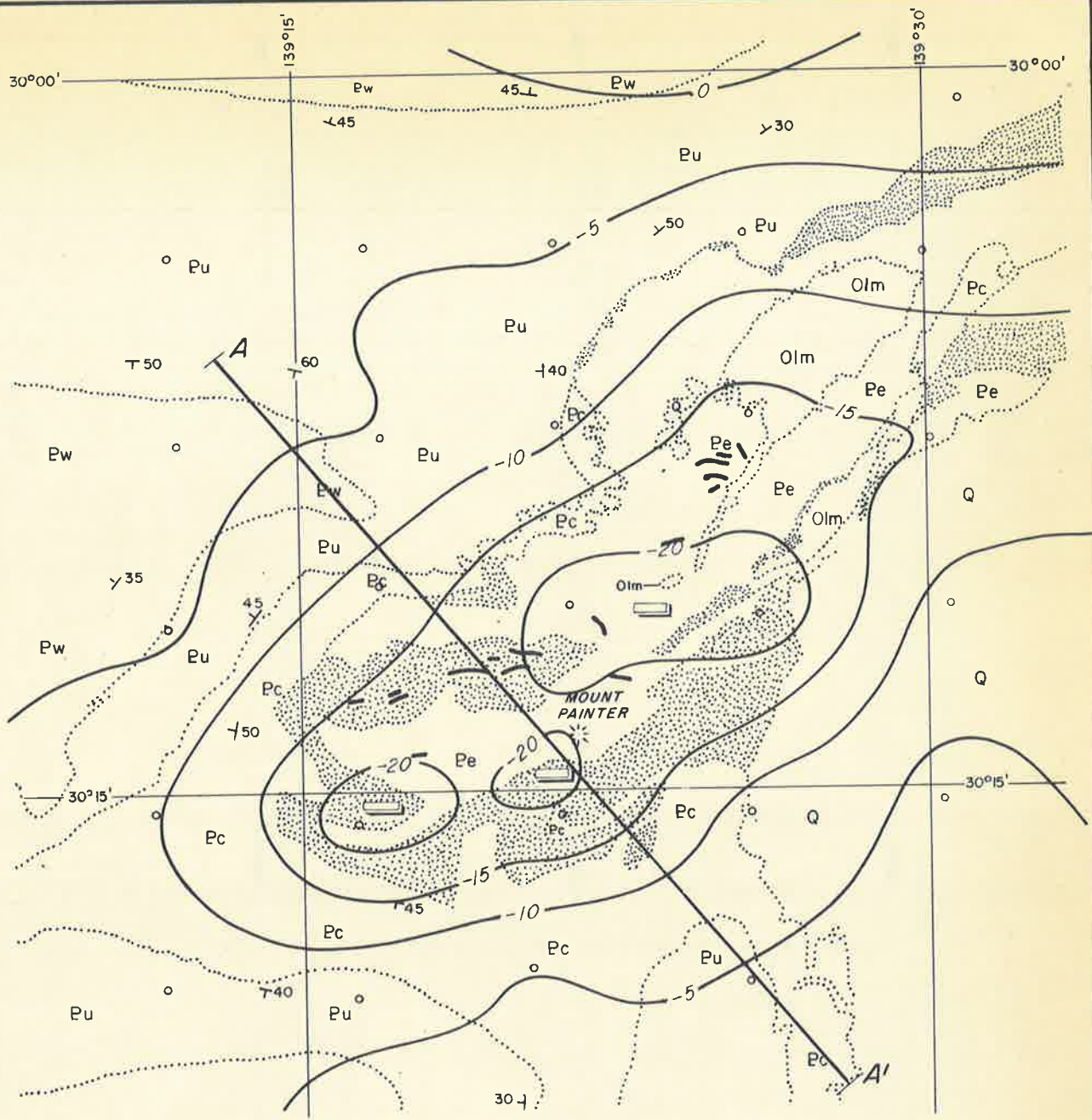


Fig. 9-8

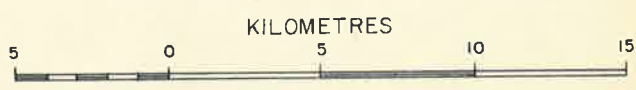
Figure 9.9 : Geology and geophysics for the Mt. Painter area  
(Bouguer Anomaly 5).

Source of data - geology - see figure; Bouguer  
anomaly contours from the BMR maps of COPLEY and  
FROME.





..... Geological boundary



(-20) Bouguer anomaly contour (mgal)

▭ Gravity 'low'

Olm Mudnawatana granite and pegmatite

○ Gravity station

Pw Wilpena group

⊥ Strike & dip of bedding

Pu Umberatana group

Geology generalised after SA Department of Mines Mt Painter provisional 2m = 1" map and Copley preliminary 1:250,000 sheet

Pc Burra group and Callanna beds

For the calculation of Bouguer anomalies  $2.67 \text{ g/cm}^3$  has been adopted as an average rock density

Older granite suite

Pe Radium Creek metamorphics

**GEOLOGICAL AND GEOPHYSICAL SKETCH MAP OF AREA COVERING ANOMALY 5**

Fig. 9-9

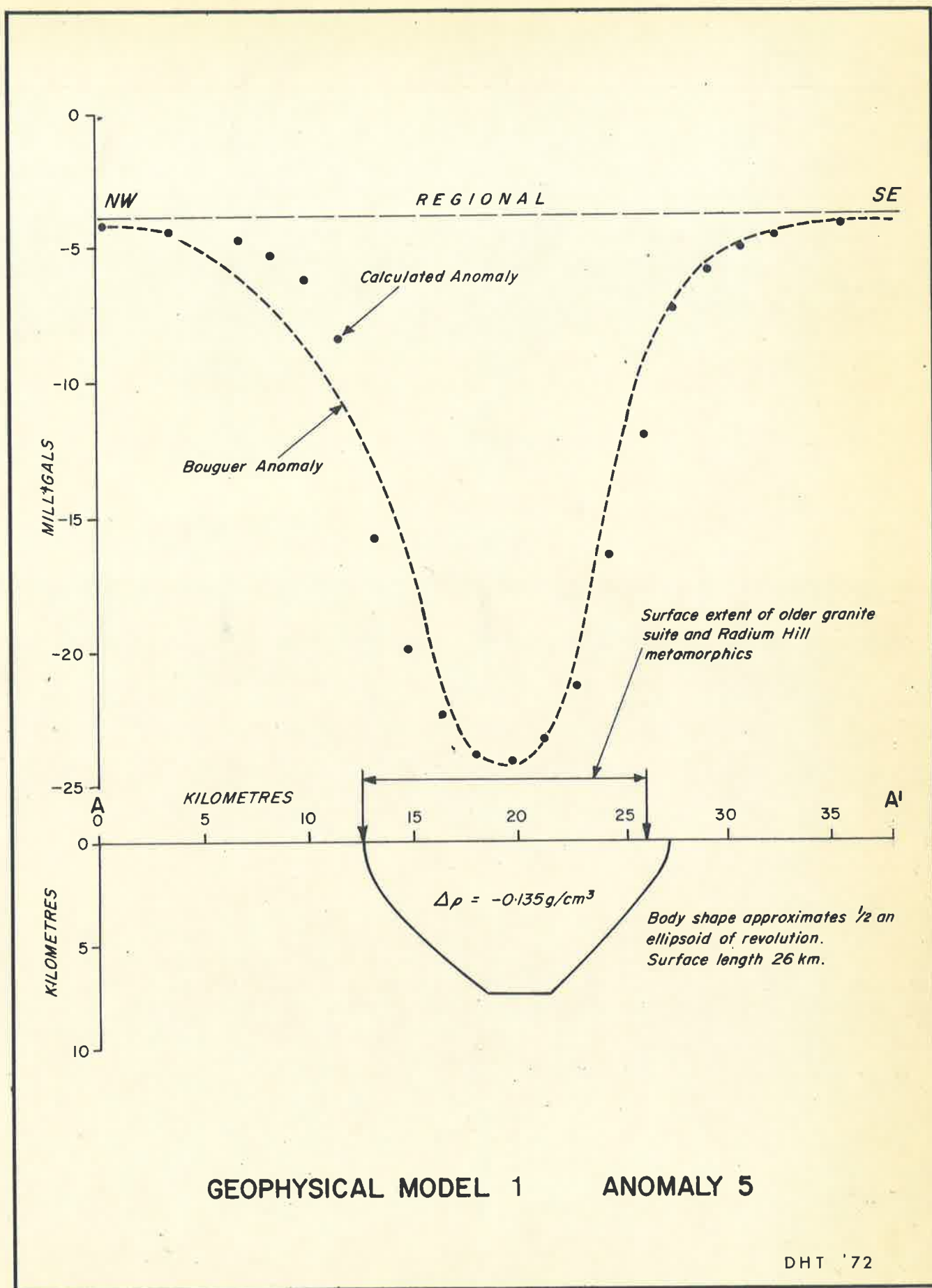
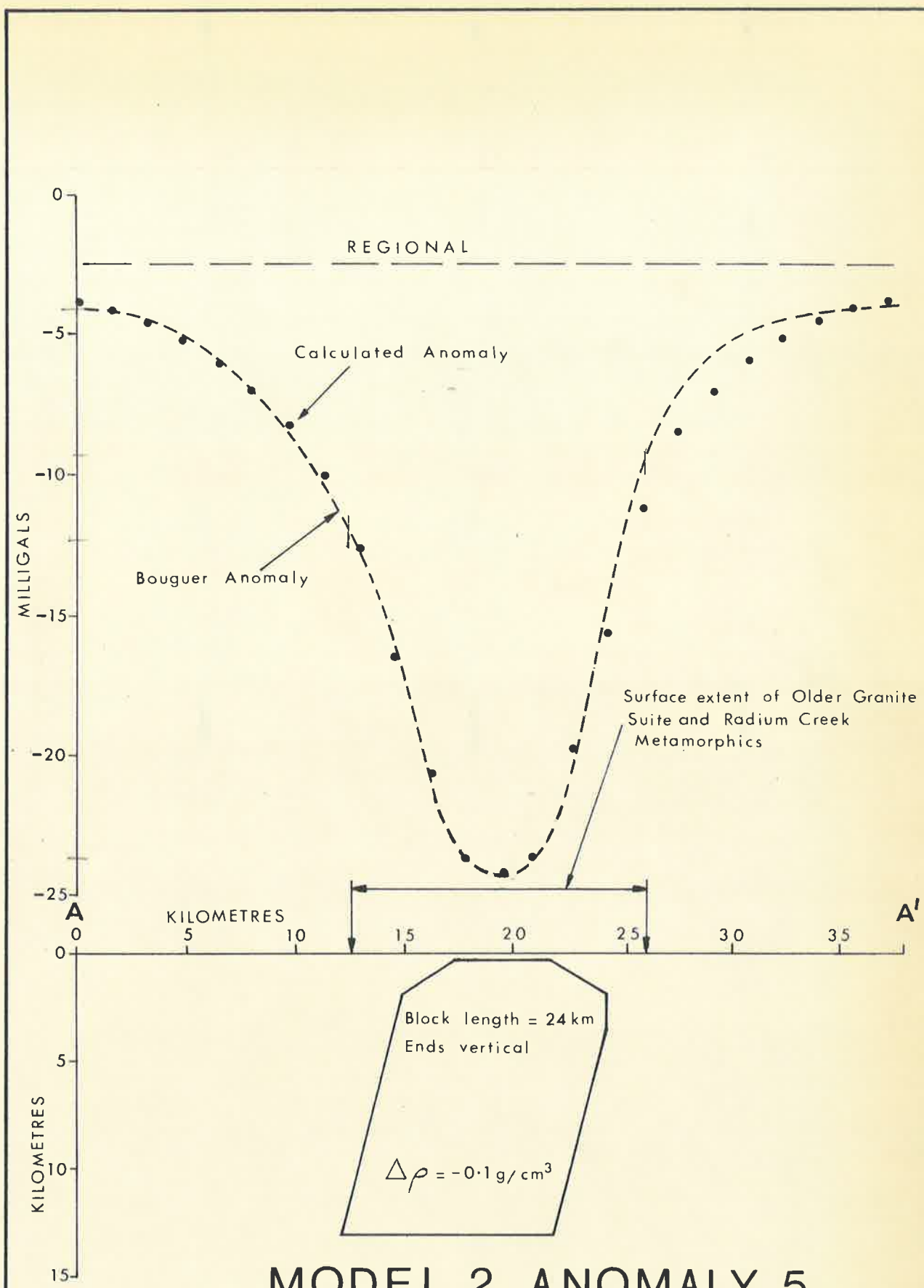


Fig. 9-10

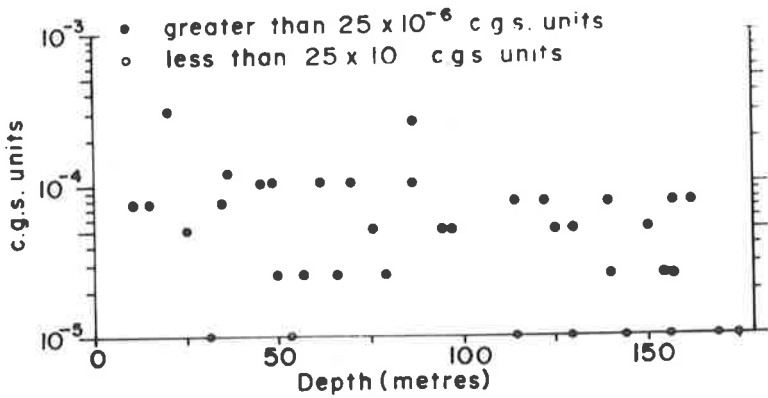


# MODEL 2 ANOMALY 5

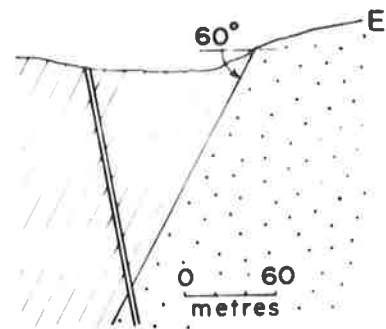
Fig. 9 - 11

Figure A2.1 : Volume magnetic susceptibility measurements on  
the Tindelpina Shale Member

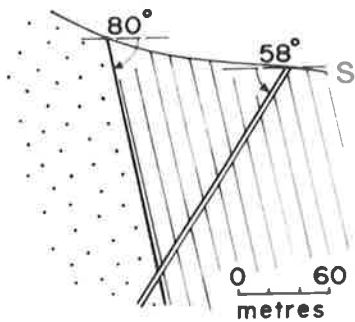
SPRING CREEK MINE  
DDH 1/29



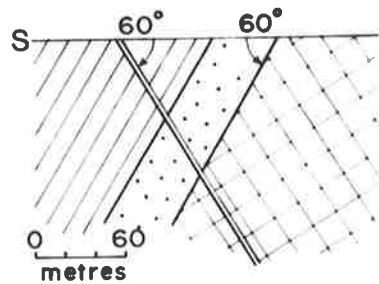
SPRING CREEK MINE  
DDH 1/29



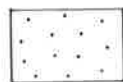
PAULL CONSOLIDATED  
DDH PC2



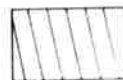
WHITE LEAD  
DDH DLY5



LEGEND



Yudnamutana sub-group



Tindelpina shale member



Diapiric breccia

DHT 72

Fig. A2-1

Figure A2.2 : Volume magnetic susceptibility measurements on the  
Appila Tillite - Ajax Mine Area (ORROROO).

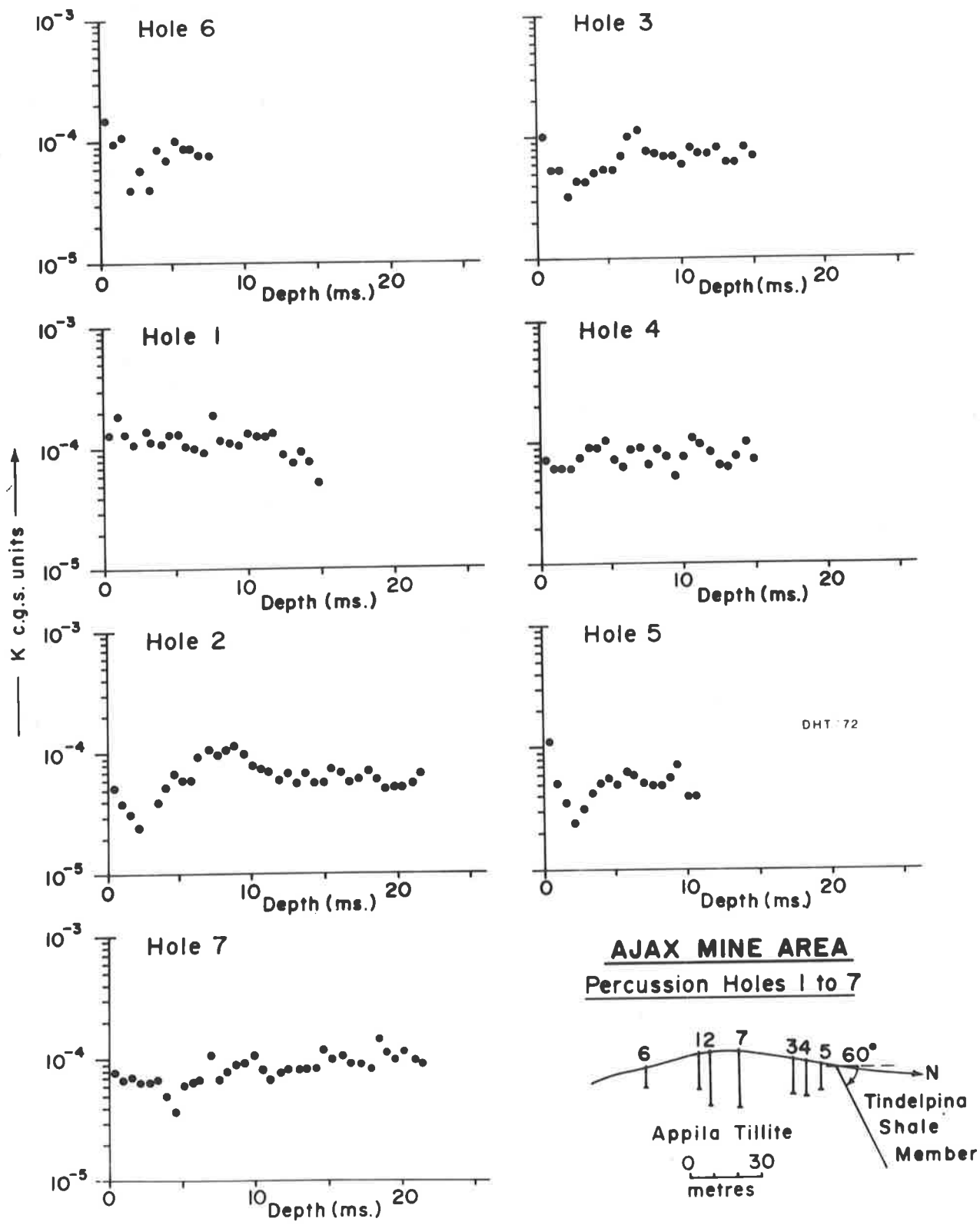
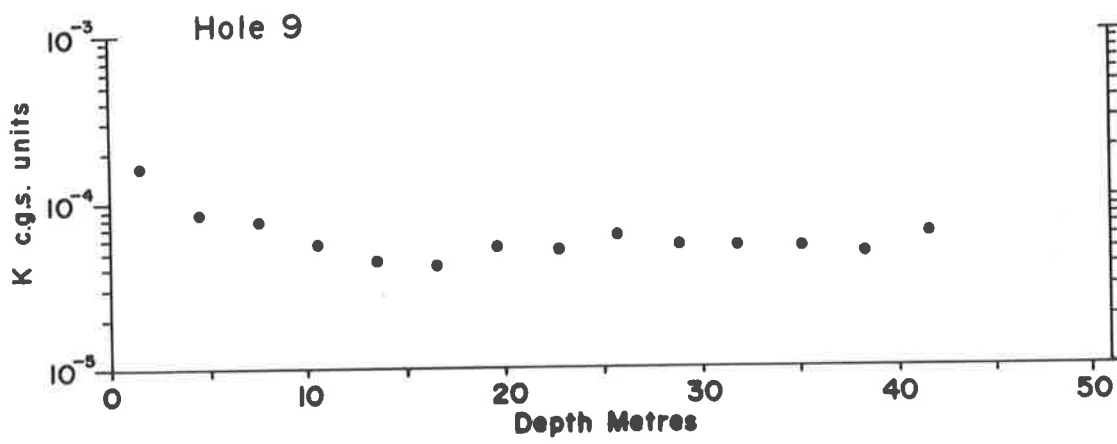
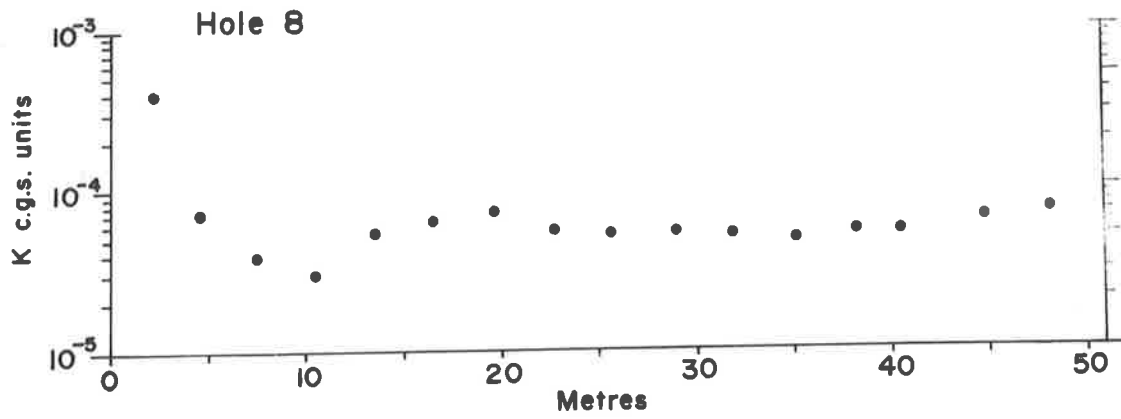


Fig. A 2-2

Figure A2.3 : Volume magnetic susceptibility measurements on the Tapley Hill Formation and Tarcowie Siltstone - Waukaringa Area.





**WAUKARINGA AREA**

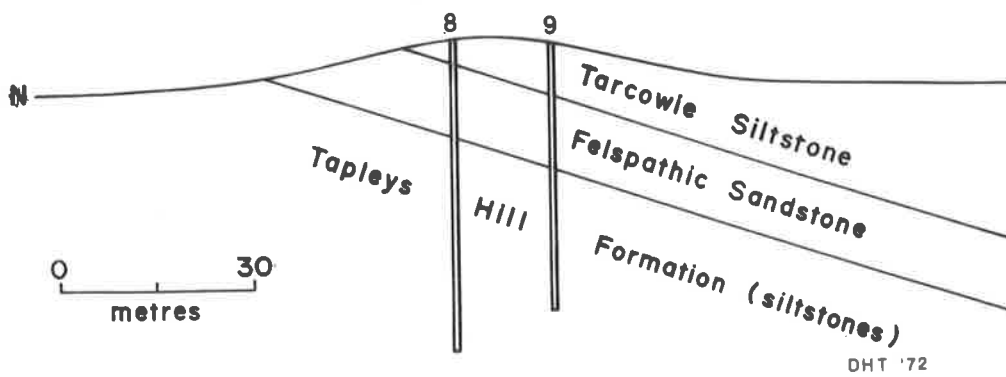
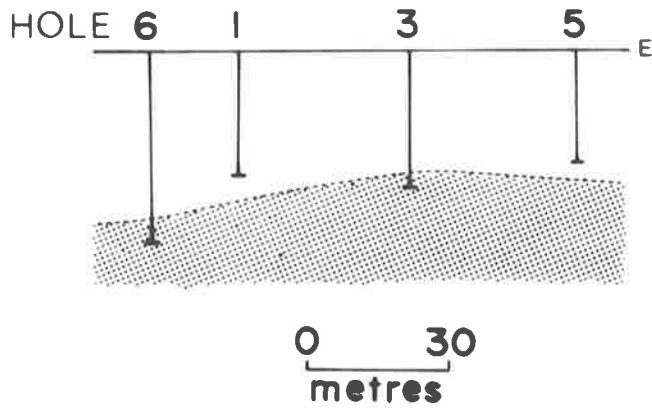


Fig. A 2-3

Figure A2.4 : Volume magnetic susceptibility measurements on Quaternary sediments of the Walloway Plain.

The shaded unit on the cross section is interpreted to be Adelaide System sediments.



DHT 72

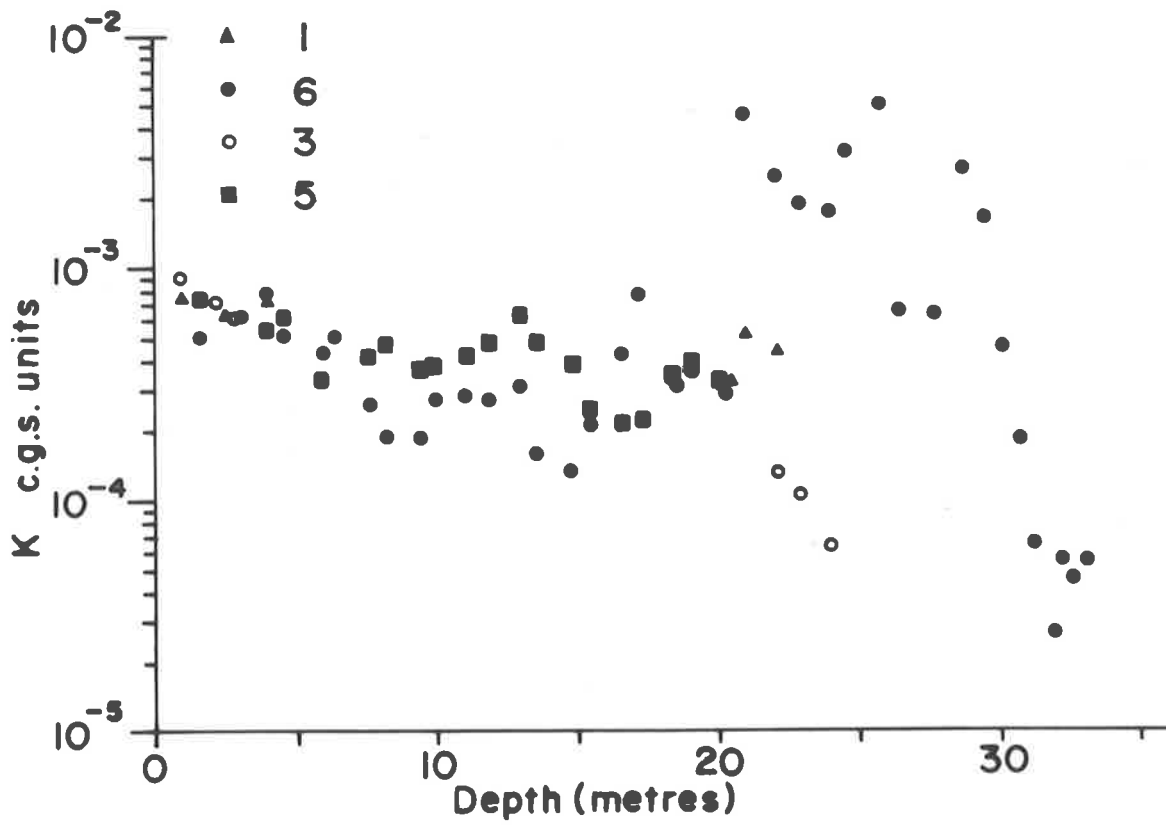


Fig. A2-4

Figure A2.5 : Histograms of volume magnetic susceptibility measurements on surface samples of Adelaide System sediments.

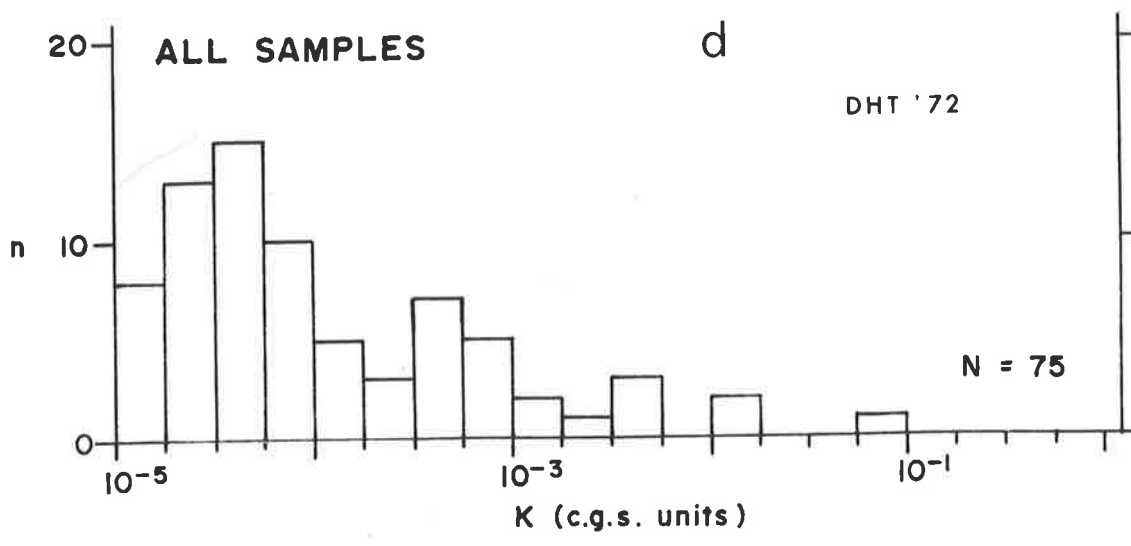
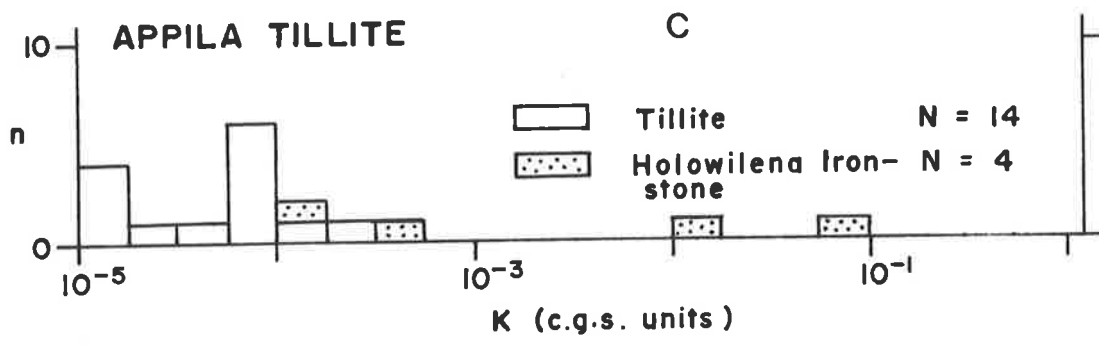
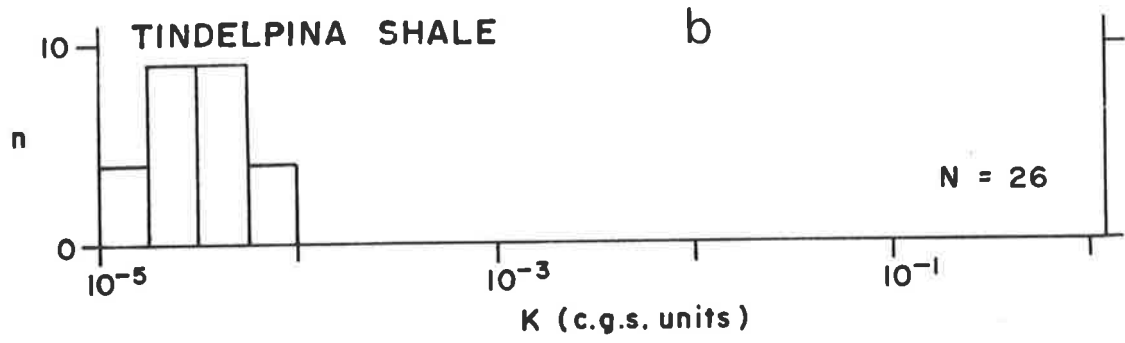
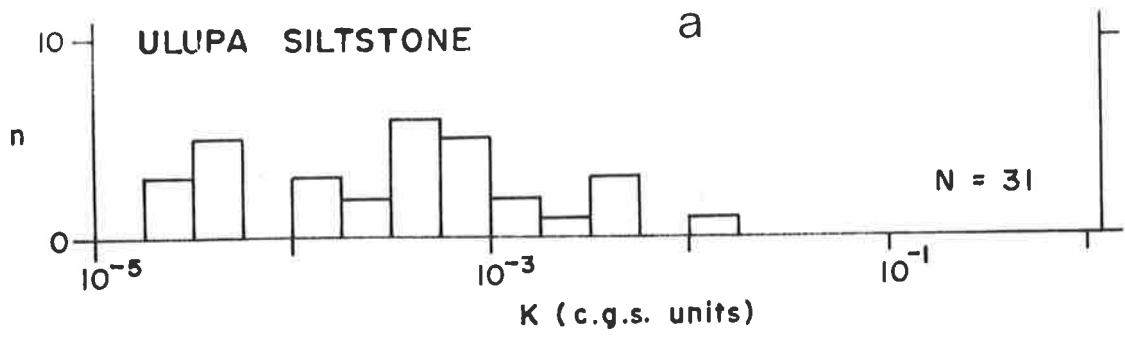


Fig. A2-5

Figure A6.1 : Theoretical vertical field magnetic anomalies and an illustration of the method of determining the effective direction of magnetization in magnetic beds. See text of Appendix A6 for discussion.

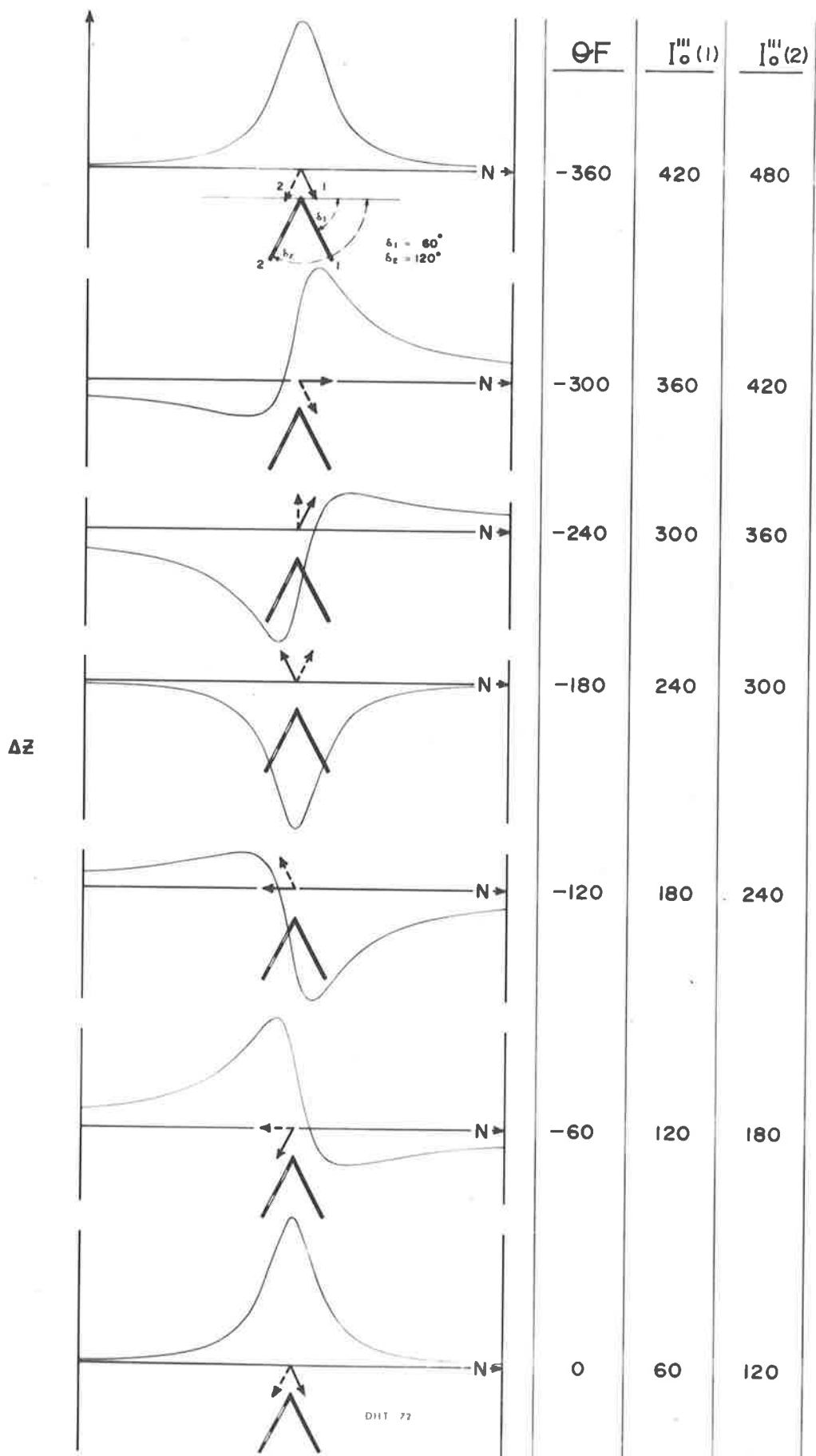


FIG. A6-1